NTNU

Norwegian University of
Science and Technology

New Techniques for Estimating Sediment Load for the Catchment of Banja HPP

Sigurd Sørås

Civil and Environmental Engineering
Submission date: June 2017
Supervisor: Nils Rüther, IBM
Co-supervisor: Hanne Nøvik, Multiconsult
Massimo Guerrero, University of Bologna
Siri Stokseth, Statkraft

Norwegian University of Science and Technology
Department of Civil and Environmental Engineering

MSc Thesis in Hydraulic Engineering

Candidate: Sigurd Sørås

New Techniques for Estimating Sediment Load for the Catchment of Banja HPP

1. Background

It is widely recognized that sedimentation poses a significant threat to the longevity, usefulness, and sustainable operations of both storage reservoirs and ROR projects. Over time, as sediment builds up in reservoirs, it results in the loss of storage space, which, in turn, negatively affects hydropower generation, reduces the reliability of water supply and flood management services, and degrades aquatic habitat. The current estimate of total reservoir storage worldwide is around 7,000 km3 (ICOLD, 2011). This storage is used for water supply, irrigation, power generation and flood control. Concern about loss of reservoir capacity due to sedimentation was raised by Mahmood (1987) and has recently been expressed in many studies and publications. It is estimated that more than 0.5 percent of the total reservoir storage volume in the world is lost annually because of sedimentation (White, 2001). This translates into the need to add some 45 km3 of storage per year worldwide. Costs would be on the order of US$13 billion per year and the associated environmental and social impacts significant.
There are many sediment management strategies to mitigate this problem. However, often the data is not sufficient or reliable to make sustainable strategies.
Therefore, it is of extreme importance to monitor sediment reaching the reservoir. The present study investigates the possibility to monitor suspended load concentration from advanced, continuous logging system in order to establish a concentration rating curve for a hydro power plant in the Devoll river catchment in Albania. If proven to be successful, this system can be used for many other cases in order to improve the data base for planning and designing sediment strategies. In addition, the thesis will attempt to quantify soil loss and sediment yield in the Devoll catchment by satellite-based remote sensing techniques.

2. Main questions for the thesis

The thesis shall cover, but not necessarily be limited to the following main questions:

- Short overview of sediment related challenges for hydro power
- Using single frequency ADCP for measurement of suspended sediment concentrations (SSC), state of the art and some short and illustrative examples.
- Case specific work: Relate the concentration measurements to the discharge and establish a rating curve for SSC
- Estimate soil loss and sediment yield by InSAR deformation data.
- Discuss the results concerning the total sediment yield derived from previous studies.

3. Supervision, data and information input, reporting

Dr. Nils Ruther will supervise the thesis work and make relevant information available. Discussion with colleagues and other research staff at NTNU is recommended. In addition, the thesis is co-supervised by Hanne Nøvik (Multiconsult), Massimo Guerrero (University of Bologna) and Siri Stokseth (Statkraft)

The data needed is provided by the supervisors.

4. Format and reference statements

- It shall be typed using a word processing system on a computer.
- Table of content, list of Figure and tables and a list of reference shall be included.
- The candidate is requested to include a signed statement that the work presented in his own.

Department of Civil and Environmental Engineering, NTNU

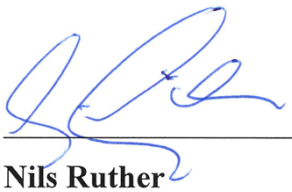

Nils Ruther

Associate professor

References:

ICOLD (2011), World Register of Dams, International Comission on Large Dams, Paris, France.

Mahmood, K.. 1987. Reservoir sedimentation : impact, extent, and mitigation. World Bank technical paper ; no. WTP 71. Washington, D.C. : The World Bank.

White, R., 2001. Evacuation of sediments from reservoirs. Thomas Telford, London

Abstract

Storing water in artificial reservoirs is a common method for ensuring constant water supply for among others irrigation, electricity and drinking water. The construction of such artificial storages will disturb the natural processes in the river, leading to possible unwanted accumulation of eroded mass, sediments, in the reservoir. Sedimentation can cause great challenges, and must be held at a minimum. Despite this, many reservoirs are today facing big problems due to the designer ignoring or underestimating the problem. This could have been avoided by better and more cost efficient predictions for sediment yield used in the design process.

This thesis investigates state of the art methods to estimate sediment yield in the upstream parts of the Devoll river catchment in Albania. The study will firstly attempt to quantify the sediment yield with data derived by ADCP (Acoustic Doppler Current Profiler) for large periods of 2016. By measuring backscattered echo-intensity, the suspended sediment concentration (SSC) can be calculated, and used to determine sediment yield if discharge is known. The thesis will also assess the possibility to quantify soil loss and sediment yield by the remote sensing technique InSAR (Interferometric synthetic aperture radar). By converting vertical deformation values to volume change in the catchment, the soil loss can be calculated. Applying this information in context with a sediment delivery ratio (SDR) will result in the sediment yield for the observed period.

The study showed promising results for both methods. The excessive erosion in the catchment clearly leads to large annual sediment yields in the Devoll river. The InSAR results correlated well with the expectation of monthly erosion in Albania, and showed a high sediment yield estimation for parts of the Devoll catchment. The continuous logging of the ADCP gave important insight into the nature of the sediment transport in Devoll, indicating that the highest concentrations and transport of sediments were occurring mainly in the wake of high flood peaks. Both ADCP and InSAR techniques of estimating erosion and sediment situations will be of value for the future.

Sammendrag

Lagring av vann i magasiner er en universell metode for å sikre konstant vannforsyning både til jordbruk, elektrisitetsproduksjon og til drikkevann. Bygging av dammer er et tiltak for å tilrettelegge for lagring, men vil også føre til en hindring i det naturlige elveløpet som kan føre til uønsket opphopning av erodert masse, sedimenter, i magasinet. Sedimentering kan forårsake store utfordringer, og det er i dag mange magasiner som utsatt for problemer på grunn av at effekten av sedimenter har blitt oversett eller underestimert. Dette kunne vært unngått ved hjelp av bedre og mer kostnadseffektive målemetoder.

Denne avhandlingen vil ta i bruk moderne metoder for å estimere sedimenttransport fra de øvre delene av nedbørsfeltet til elven Devoll i Albania. Studien vil først forsøke å kvantifisere sedimenttransport med data utledet fra ADCP (Acoustic Doppler Current Profiler) for store deler av 2016. Ved å måle ekkointensitet kan den suspenderte sedimentkonsentrasjonen beregnes og sedimenttransport kan regnes ut med hjelp av vannføringsdata. Oppgaven vil også vurdere muligheten til å kvantifisere erosjon og sedimenttransport ved hjelp av satellittbasert InSAR (Interferometric synthetic aperture radar). Ved å konvertere vertikale deformasjonsverdier til volumendring i nedbørsfeltet, kan erosjonen beregnes. Erosjonen kan gi et estimat på sedimenttransport ved hjelp av SDR (sediment delivery ratio).

Studien viste lovende resultater for begge metodene. Den massive erosjonen i nedbørsfeltet fører til store sedimentproblemer i Devoll-elven. InSAR-resultatene korrelerte godt med forventet månedlig erosjon i Albania, og viste et høyt estimat for årlig sedimenttransport i 2015. Den kontinuerlige logging av ADCP ga god innsikt hvordan sedimenter blir transportert i Devoll. Det ble avdekket at de største konsentrasjonene oppstår hovedsakelig i etterkant av store flommer. Bruk av både ADCP og InSAR for å estimere erosjon og sedimenttransport vil være av stor verdi for kommende prosjekter.

Preface

This master's thesis is conducted at the Department of Civil and Environmental Engineering at the Norwegian University of Science and Technology (NTNU), Trondheim. The thesis investigates the possibility for advanced surveying methods to quantify the extreme sediment situation in the Devoll river in Albania, and is the work performed by the author during the spring 2017.

The project has granted me great insight into the complex science of sediments, acoustic measuring techniques and satellite surveying. Sustainability is a topic with broad and current interest, and the design of sustainable hydraulic structures is essential to uphold value for coming generations. Improved sediment measuring and remote sensing will without doubt be valuable to improve longevity for many projects in the future. I am very thankful for the knowledge gained around the topic this semester. I am also grateful for the opportunity to learn valuable previously unfamiliar tools such as GIS and MATLAB. As part my work I was able to partake in an educational study trip to Bologna, Italy as an introduction to acoustic measuring of sediments. I also received the opportunity to travel to Albania for a first-hand look at the Devoll River, which was priceless for understanding the high erosivity in the catchment that can be hard to imagine with a Norwegian reference basis.

The project would not have been possible to accomplish without many people, but first and foremost I would like to thank my supervisors Nils Ruther and Hanne Nøvik for exceptional guidance. The discussions have been a great inspiration for my work, and has helped me overcome many challenges. I would also like to thank Massimo Guerrero for taking the time to host my stay in Bologna. A special thanks to Rui Jorge Ferreira Aleixo for the phenomenal help he has provided to understand the sometimes baffling theory of estimating sediment concentrations with acoustic devices, but also for taking the time to provide help for simple MATLAB problems. I would like to thank Siri Stokseth for allowing me to use the Devoll river and its catchment as a case study, and Frano Cetinic and his help with understanding InSAR.

Trondheim, June 2017

Sigurd Sørås

Table of Contents

List of Figures

List of Tables

1 Introduction

The demand for steady water supply in the world is constantly increasing. One of the solutions to cover this need is storage of water in artificial reservoirs, and subsequently harnessing it for utility purposes. Today water is a limited resource, and with global warming it will become even more inconsistently distributed throughout the planet. Optimizing reservoirs to handle the local situations will be of great importance to uphold the many benefits that persistent water supply gives.

As the natural equilibrium of the river is disturbed by dams built to store water, many challenges will appear. In rivers with high concentrations of eroded material, referred to as sediments, the particle transport will be obstructed leading to unwanted trapping. A high sediment content in the reservoir can significantly reduce the lifetime, flood-handling abilities and electricity production of the man-made construction. Designing hydraulic structures that can prevent or reduce unwanted accumulation of sediments will result in a constant and predictable volume for water storage, as well as acquiring a significantly reduced wear and tear on turbines and other technical equipment.

However, historically there has been a trend to neglect the importance of designing to prevent sediment build-up. Today it is estimated that the annual rate of global loss of reservoir capacity is between 0.5-1% (Mahmood, 1987, White, 2010) as a consequence of this misjudgement. The constant loss of reservoir volume leads to reduction in both monetary and sociologic values, and also challenges some hydropower plants on their status regarding sustainability. In 1987 the United Nations proposed through the Brundtland Commission that “Sustainable development is development that meets the needs of the present without compromising the ability of future generations to meet their own needs” (Brundtland, 1987, p. 41). As a part of the 2030 Agenda for Sustainable Development, 17 goals were introduced to end poverty, protect the planet and ensure prosperity for all (UN General Assembly, 2015). Reservoirs that are not sufficiently able to handle sedimentation contradicts the definition of sustainability, as they will eventually fill up and no longer uphold their designed purpose. Correctly designed reservoirs will meet several of the 17 goals introduced in the 2030 agenda, where the most important contributions will be towards hunger and clean energy.

Reasons related to the underestimation of the sedimentation problem can often be found in the uncertainty and complexity in sediment measurements, as the sediment transport in a river is an intricate, site-specific phenomenon that can be difficult and expensive to quantify. Disregarding this, measurements of sediment in rivers planned for various development have been performed for decades. The technology and methodology used contains many uncertainties, and is demanding, expensive manual labour. Due to errors caused by measuring techniques, surveys regarding mapping of the sediment situation of rivers often contain large errors, or has in many cases been completely overlooked resulting in large sedimentation problems in many of today's reservoirs. Because of the continuous loss of reservoir volume, as well as the increase in demand for electricity and water storage, more dams and management methods will have to be built in the future. To ensure sustainability and longevity for these projects disposed for high sediment yields, better and lower priced sediment measurement techniques should be introduced.

1.1 Objectives

In this thesis the overall objective will be to assess advanced methods to determine sediment yield in the Devoll river in Albania. The catchment is heavily influenced by erosion, and the river is often referred to as the most turbid river in Europe (Pano and Frasheri, n.d.), which results in an interesting case study for state of the art sediment survey methods. Two different methods to quantify sediment yield and erosion in a catchment will be discussed. The first being the use of advanced acoustic devices placed in the river to monitor continuous sediment concentrations. Establishing a concentration time-series for a river is valuable information in the determination of the suspended sediment yield, as well as uncovering the different processes of sediment transport. The sediment concentrations will be assessed in context with discharge to quantify suspended sediment yield, as well as to establish a relationship between the discharge and suspended sediment with a rating curve.

The second method will investigate the possibility to assess data related to ground deformation gained by satellites to quantify sediment yield. The continuous logging of satellites of the Devoll catchment has been carried out for several years. In this thesis, an attempt will be carried out to use this data to quantify soil loss, and later relate the soil loss to an estimate of sediment yield.

2 Background

2.1 Sediments

2.1.1 Origin of Sediments

Forces of nature is constantly changing the surface of the Earth. Tectonic activity is mainly responsible for new land mass, whereas wind, water, glaciers etc. is actively working as a counteracting force. These counteracting forces result in the deterioration of the surface of the planet, referred to as erosion, where the loosening of soil specifically is called soil erosion (Broz et al., 2003). The driving forces responsible for soil erosion in a catchment is raindrop impact and runoff. Falling raindrops in a heavy rainfall is a tremendous source of kinetic energy that will strike the soil on the ground and subsequently detach soil particles that will be transported throughout the catchment by flowing water (Wischmeier and Smith, 1958). The eroded particles transported by water are referred to as fluvial sediment particles. (Lysne et al., 2003)

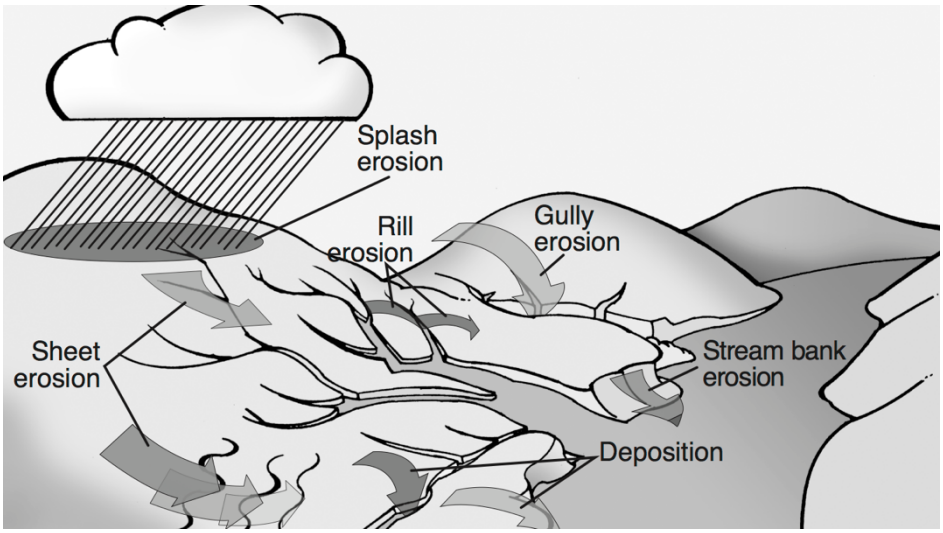

Figure 2.1 Soil erosion processes in a catchment with low vegetation (Broz et al., 2003)

The process of mechanical erosion of soil in the illustrated catchment (Figure 2.1) is initiated by a heavy rainfall that detaches soil particles from the ground. After reaching the ground the rainwater will travel downstream and the flowing water on the surface (overland flow) will cause further erosion by both sheet, rill and gully erosion. As the water is accumulated in rivers and streams, the erosion process will continue on the bed and banks. Erosion in the catchment is referred to as external erosion, whereas erosion in the river caused by concentrated flowing

water is referred to as internal erosion (Broz et al., 2003, Lysne et al., 2003). After the soil particles are loosened they will be transported with the water due to the shear forces in the water body. Depending on the size of the particles as well as the velocity and turbulence in the water, the sediment particles will either be transported or deposited by the flowing water, as further described in 2.1.2.

There are several factors influencing the rate of erosion in a watershed. For instance, in areas influenced by humans such as cultivated land, sheet and rill erosion is the predominant reason for wear of the landscape. A small impact on the fragile equilibrium in the terrain that has been developed over the course of time, will sometimes cause big erosion and sediment problems. An example of such destabilization is removing the natural vegetation (i.e. deforestation for cultivation purposes) that will lead to destabilization of areas that were previously not prone to soil erosion. A general remark is that dry, low-vegetated areas will have a much higher degree of erosion than wet, vegetated areas at rainfall-events (Morris and Jiahua, 1998). For mountainous regions, mass wasting from landslides can cause most of the sediment that is produced. Water can destabilize areas with steep and unstable slopes, and a heavy rainfall or a vigorous snow-melt can trigger landslides etc. that can cause large volumes of sediment. Erosion due to land-slides is far harder to predict than the continuous erosion from i.e. sheet and rill erosion. The sediment production caused by landslides is divided into phases, where the first phase is the actual landslide going into the river, and the second phase is the continuous erosion caused by rainfall on destabilized scars left behind the slide (Morris and Jiahua, 1998).

The occurrence of sediments will vary both locally and at a global scale. Mountainous areas, Mediterranean, semi-arid climate regions and the humid tropics are all associated with a high sediment yield (total quantity of sediments, often described in tons/year*km^2). Areas that have a desert climate, as well as low relief, glaciated regions are considered as areas with low sediment yield (Walling and Webb, 1996). Information about sediment yield must however also be assessed along the total precipitation in the observed area. Areas with a moderately low total sediment yield, can in combination with a low annual discharge cause challenges. The relative scarce amount of water will contain large concentrations of sediments. Regions where this is the case are described as semi-arid and arid areas where storing water is of tremendous importance. Storage of water containing high concentrations of sediments, both for electricity, irrigation and consumption purposes, will cause large problems (further discussed in 2.1.2) (Jacobsen, 1997).

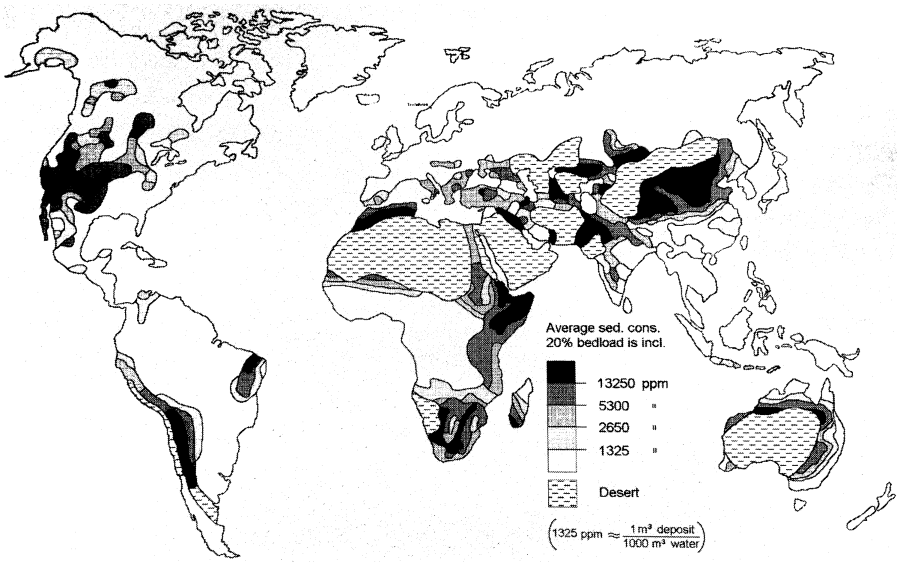

Figure 2.2 Global pattern of sediment concentration (Jacobsen, 1997)

2.1.2 Sediment Transport and Deposition

When the eroded particles are transported, either by water or by wind, they are defined as sediment particles. Particle transport in a river is mainly distinguished by two different transport modes: bed-load or suspended load, where bed load is the particles that move along the river bed, and suspended load is the particles that mainly are carried in suspension in the water column. The particle size of the sediments varies depending on the attributes of the river. A general remark is that bed-load is characterized by a coarser particle size distribution than suspended load. As sediments are a product of the erosion that occurs in different areas of the catchment, they can also be defined by origin. Bed material load describes particles that have been eroded from the river bed (internal erosion), and wash load defines fine sediments that have no contact at all with the river bed, and is often a product from erosion in the watershed slopes (external erosion). As a general rule, the suspended load in a river is often assumed to describe around 75% of the sediment yield in a river, but this can fluctuate depending on the observed site (Lysne et al., 2003).

The driving force for sediment transport is the shear stress and turbulence in the water column. In other words, the sediment transport capacity will increase significantly as the velocity in the river increases. This is why large floods with fast flowing water often correlate with high sediment loads. The annual sediment transport, however, varies much more than the annual discharge. The ratio between 100-year flood (Q_{100}) and two-year flood (Q_2) can be around 5-

10, but the ratio between the 100-year and the two-year annual sediment yield may be 100 or more. Floods will carry substantially more sediments than normal flow situations, but the quantification of the relationship between flow and sediment yield has to be done separately for each study, and is a time-consuming effort (Guerrero et al., 2016a, Lysne et al., 2003).

Sediment particles that are transported by forces in the water will eventually deposit as the water velocity is reduced. This deposition is referred to as sedimentation, and is a natural outcome of erosion and sediment transport. Sedimentation occurs in areas where the shear-stress and turbulence in the water is reduced. In a catchment this will happen when the river reaches a deeper body of water, such as a lake or reservoir, but also in locations where the water velocity decreases due to change in river geometry, such as in slopes or bends. Particles will deposit according to size and weight, where larger particles will be unsuspended first as these require more energy to hold in suspension (Lysne et al., 2003). Fluctuating discharge of the river will also affect the sedimentation situation of a river. With increasing flow, deposition-zones can become areas with high enough water velocity to re-suspend sediments that have been deposited in deltas and river banks during lower discharges. This also partly explains why flood periods will carry far more sediments than the normal flow (Devoll Hydropower and Støle, 2010).

When designing hydraulic structures in catchments with high sediment yield, the issues regarding deposition and sediment particles in the water has to be taken into account. Although the structure is designed to store water, it will also prevent transported material from travelling further downstream. An uncontrolled accumulation of particles can lead to a significant reduction of storage capacity and eventually filling up the reservoir, questioning the sustainability of the project in general (Tigrek and Aras, 2012). The deposition creates challenges for the stability of the dam-structure because of unpredicted loads, as well as reducing flood-handling abilities. Sediments in the water will also affect the mechanical components in the reservoir, such as the functionality and wear of outlets and turbines (Lysne et al., 2003). To reduce the problems related to sedimentation, counter measures have been introduced, but the design of these measures rely on data describing the sediment situation of the river.

2.1.3 Measuring and Predicting Sediment Yield

Measurements of the sediment values are important both in the preliminary and design phases of a project, but also when operating mechanical equipment related to the hydraulic structure. For hydropower plants, knowing the optimal flow and sediment situations in which to shut down production can be a determining factor for power plant economy. However, measuring sediments in a river is a difficult task. As for most cases when quantifying processes in nature, the data set must be systematically collected over time to give a representative description of the situation. As mentioned in 2.1.2, the annual sediment yield differs much more than i.e. the annual discharge. The sediment yield varies not only from year to year, but also greatly from season to season. High concentrations of sediments can for instance occur in small off-season floods. As a matter of fact, the unpredictability of sediment transport and uncertainty in measurement-methods is often the reason why lifetime of reservoirs and technical equipment sometimes are overestimated (Lysne et al., 2003).

Including suspended sediment concentrations (SSC) and discharge data, some additional information should be known for the sediment situation of a river. The particle size distribution, bed-load transport and composition of sediment load (material, mineral, organic content as well as density) are all parameters that will affect the hydraulic structure (Lysne et al., 2003). To quantify these parameters, standard measuring devices should be used. A wide array of sediment samplers exists, where the main difference is what type of sediment they measure (suspended or bed load) as well as how (direct or indirect). Typically, the sediment measuring devices are instruments that are lowered into the water column or placed on the river bed. Direct suspended sediment samples are generally bottles or pumps located in the river at a fixed position that allow the water containing the sediment particles to enter with an undisturbed velocity and flow pattern. Bed samplers are generally appliances that are positioned on the bed of the river, allowing the transported material to be accumulated in a sampling container over a given time period (Edwards et al., 1988). By obtaining measurements that cover both time and fluctuating discharge, estimates for the site specific sediment situation can be developed.

Directly measuring sediment transport is a difficult, time consuming, and expensive way to obtain the required statistical variance in the sediment data set. Therefore, indirect methods have been developed to quantify the sediments in the river. Indirectly estimating sediment yield can give great spatial insight at a far lower cost than direct methods. Techniques vary from use of electronic instruments (i.e. Acoustic devices as discussed in 2.2) to empirical approximations

such as the Universal Soil Loss Equation (USLE) in combination with a Sediment Delivery Ratio (SDR). USLE is an equation developed by the Soil Conservation Service of the U.S. Department of Agriculture (USDA) in 1958 from more than 10,000 test plots in the U.S. The equation is one of the most common methods for estimating soil erosion due to raindrop impact and surface runoff. USLE is based on six empirical factors: rainfall intensity, runoff intensity, soil erodibility, slope length and steepness, cover management and support practice (Morris and Jiahua, 1998). USLE was updated in 1997 by USDA, introducing the revised version (RUSLE), where the parameters for USLE were updated to give a wider usage (Morris and Jiahua, 1998). Because sediments are a product of erosion, the erosion rate of a catchment derived from RUSLE, or other similar models, can be used to predict sediment transport by finding a relationship between the weathering and sediment production.

2.1.4 Sediment Delivery Ratio

Eroded material will be deposited and re-suspended multiple times within a catchment before it reaches the basin outlet. Because of this, the observed sediment yield at a cross section will not have the same magnitude as the gross erosion. In most cases, only a fraction of the sediment eroded in a catchment will eventually find its way to the bottom outlet. Several attempts have been made to estimate the sediment delivery from a watershed as a function of erosion, introducing the sediment delivery ratio as a parameter used to describe the ratio between the eroded mass and sediment yield (Walling, 1983).

$$SDR = \frac{Y}{E} \tag{1}$$

SDR is the sediment delivery ratio, Y is the sediment yield and E is the erosion. Knowing the SDR of a catchment can be a valuable tool to predict the behaviour of an ungauged catchment in combination with models that quantify gross erosion, such as the (R)USLE method. The most common empirical equations to describe the relationship between erosion and sediment yield are based on the basin area (A), where SDR will decrease as the area increases. (Vanoni, 1975, Walling, 1983)

$$SDR_w = 0.4724 \times A^{-0.125} \tag{2}$$

This method does not specifically take into attention the influence of local conditions in the catchment. The formula is derived through observations of numerous watersheds, assuming

that the area sufficiently will describe the topographic influence on sediment transport. However, in most cases the complex nature of sediment transport cannot solely be described on basis of the area of the catchment (de Vente et al., 2007). Many other variables affect the rate of sediment delivery, and with this in mind, other empirical relationships have been derived. The parameters that primarily have been used in these empirical equations are catchment area, land slope and land cover (Kothyari and Jain, 1997, Walling, 1983). To determine the sediment delivery from designated grid cells within a catchment, equation 3 was developed as part of the sediment delivery distributed (SEDD) model (Ferro, 1997, Ferro and Minacapilli, 1995, Ferro and Porto, 2000). The hypothesis of this relationship was based on an assumption that the SDR in a grid cell is a function of the travel time of overland flow within a cell. Travel time is a function dependent on the topographic and land cover characteristics in the cell, proving its relationship with sediment delivery as discussed in the previous paragraph. The information around SDR in a grid cell within a catchment is interesting to assess when calculating sediment yield with i.e. GIS (Geographic Information Systems) tools. (Jain and Kothyari, 2000)

$$SDR_i = \exp(-\beta t_i) \tag{3}$$

Equation 3 consists of the parameters β which is the basin-specific parameter and t_i which is the travel time (hr) for cell i to the nearest channel grid down the drainage path. To determine the travel time within the cell, the velocity and the length of the flow path has to be calculated. With GIS tools, the flow between cells in a given topography can be determined and the overland flow length (l_i) to the nearest channel is thus known (Jain and Kothyari, 2000). As mentioned, the overland flow velocity is a function of slope and land use. A DEM (Digital Elevation Model) will contain the information required to determine the slope angle s_i of the grid cell, whereas the area specific land-use map can give information on the land-use parameter a_i (Haan et al., 1994). t_i can be calculated with the following equations:

$$t_i = \sum_{i=1}^{N_p} \frac{l_i}{v_i} \tag{4}$$

$$v_i = a_i {s_i}^{0.5} \tag{5}$$

The basin specific parameter, β, is a constant for a given catchment. It depends primarily on watershed morphological data (Ferro, 1997). It can be estimated with an inverse modelling

approach, with basis on a value for the sediment delivery rate for the whole catchment and a weighted average as shown in equation 6 (Ferro, 1997). This sediment delivery value for the entire catchment (SDR_w) can be obtained by either field measurements, or by estimations such as equation 1 (Fernandez et al., 2003).

$$SDR_w = \frac{\sum_{i=1}^{N} \exp(-\beta t_i)\, {l_i}^{0.5} {s_i}^2 a_i}{\sum_{i=1}^{N} {l_i}^{0.5} {s_i}^2 a_i} \tag{6}$$

2.2 Measuring Sediment Concentrations with ADCP

To obtain a sufficient spatiotemporal coverage, research has been performed on determining sediment concentrations through indirect methods. One of these indirect methods use the data collected from one or several Acoustic Doppler Current Profilers (ADCPs) to determine concentrations of sediments in the water. One of the advantages of this method is the possibility to station the devices in the field to continuously collect data at a set time-interval. This gives an unmatched coverage of time, and is valuable information in the assessment of the nature of the river and its catchment.

2.2.1 The Sonar Equation

The ADCP is an instrument widely utilized in the field of hydraulics. Originally it is designed to create three-dimensional velocity profiles in a body of moving water by the Doppler shift principle. The device works by transmitting high frequency pings into the water, and subsequently measuring the frequency of the echoes produced by the pings hitting suspended particles. The Doppler shift principle states that the sound echoed from a particle moving relative to a receiver will be shifted relative to the original transmitted frequency. If the instrument frequency is known, the measured echo can be assessed to determine the velocity of the particle. A particle moving towards the instrument will cause a backscattered echo with a higher frequency than that of the instrument. The opposite situation will be caused by a particle moving away from the device. (Kostaschuk et al., 2005)

In the field of sediment measuring, the ADCP has also been shown to be useful. In contradiction to measuring the frequency of the echo, as is done for velocity profiling, the device can also measure the backscattered intensity of the signal. This intensity can be used to determine the sediment concentration in the river by applying the sonar equation (Thorne and Hanes, 2002):

$$I = {p_0}^2 {r_0}^2 \cdot \frac{{k_t}^2 * {k_s}^2 \cdot M_s}{r^2 \psi^2} \cdot e^{-4(\alpha_w + \alpha_s)r} \quad (7)$$

where the measured intensity I is dependent on the backscattering coefficient ${k_s}^2$ and the mass concentration M_s, as well as the water viscosity and suspended sediment attenuation coefficient α_w and α_s, respectively. p_0 is the reference pressure at unit distance r_0. k_t is an instrument constant that describes the acoustic system settings (i.e. amplifier gain, transmit power and pulse length). Geometrical spreading and near field correction are described by r^2 and ψ^2. The backscattering strength (${k_s}^2 M_s$) and the attenuation coefficient are both dependent on range (r). For the estimation of suspended sediments in the water, attenuation should be integrated along the path of the beam from the ADCP to the furthest backscatter distance, r_{max} (Guerrero et al., 2016b). The sonar equation has a logarithmic form function. This also includes the backscattering strength that is ten times the natural logarithm of ${\theta_s}^2$. The attenuation coefficients are converted by the factor of $20\log(e)$. The reason for this is that the echo intensity E recorded by the ADCP is proportional to the received sound intensity in the dB scale. This is shown in equation 8 (Guerrero et al., 2016b, Guerrero et al., 2017, Guerrero et al., 2016a).

$$I_{dB} = 10log\left(10^{\frac{k_c \cdot E}{10}} - 10^{\frac{k_c \cdot E_0}{10}}\right) = C + 10\log\left({k_s}^2 \cdot M_s\right) - 20log(r\psi) - 20\log(e) \cdot 2(\alpha_w + \alpha_s) \cdot r \quad (8)$$

Equation 8 also includes k_c, which is a coefficient that converts the intensity counts to dB, and E_0, that describes the environmental noise in the river. C is a constant which represents the instrument constants that are reported as p_0, r_0, and k_t in the sonar equation (equation 7). (Guerrero et al., 2016b)

2.2.2 Acoustic parameters

For calibration of the sonar equation to determine sediment yield, the different parameters in the sonar equation is interesting to assess. If the relationship between the intensity and the parameters exists for known situations, it can be used to determine the parameters where only a time-series of intensity is known. To find these parameters, suspended sediment samples must be taken at known time periods, and processed by the equations in the following subchapter.

Backscattering strength ${\theta_s}^2$, is dependent on mass concentration and the backscattering coefficient. ${K_s}^2$ is affected by the particle size distribution (PSD) as well as the density of the particles ρ_s (Thorne and Hanes, 2002, Guerrero et al., 2016b).

$$\langle {\theta_s}^2 \rangle = \langle {K_s}^2 \rangle \cdot M_s = \frac{3\langle f \rangle^2 \cdot M_s}{16\pi\rho_s \langle a \rangle} \tag{9}$$

Equation 9 consists of parameters f, which is the form factor of the PSD, a that describes the particle mean radius. As the suspended sediment concentration is heterogeneous, and not well sorted (mono-sized) the parameters $f, a, {k_s}^2$, and ${\theta_s}^2$ must be assessed by a mean value. Hence the brackets in equation 9. The mean values for these parameters can be determined by the following equations: (Thorne and Hanes, 2002, Guerrero et al., 2016b)

$$\langle a \rangle = \int a \cdot p(a) da \tag{10}$$

$$f = \frac{x^2 \cdot \left(1 - 0.35 \cdot e^{-\frac{x-1.5^2}{0.7}}\right) \cdot \left(1 + 0.5 \cdot e^{-\frac{x-1.8^2}{2.2}}\right)}{1 + 0.9 \cdot x^2} \tag{11}$$

$$\langle f \rangle = \left(\frac{\int a \cdot p(a) da \cdot \int a^2 \cdot f^2 \cdot p(a) da}{\int a^3 \cdot p(a) da}\right)^{0.5} \tag{12}$$

The form factor of the particles is estimated experimentally, and the empirical form factor function (equation 11) is given (Thorne and Hanes, 2002). The equation was derived by fitting measurements of backscatter to a homogeneous particle size distribution. x is the product of k and a, where k is the wave number [rad*m^{-1}]. In a river, the PSD is rarely homogeneous, so to give a mean form factor for a heterogeneous PSD, equation 12 must be applied (Guerrero et al., 2016b).

The backscattered intensity is also affected by the attenuation of sound caused by the suspended sediments and the water. As the sound waves travels along the beam path, various factors will affect the dissipation, and the sum of all these factors will describe the total losses. The movement of the water under the oscillating pressure field, or water viscosity, is determined as α_w. The contribution of sediments to sound attenuation is described by viscous dissipation caused by motion between water and particles (α_{sv}) and the scattering of sound caused by particles (α_{ss}) (Hanes, 2012). The two attenuation coefficients that are a result of sediment

particles are added up to form the suspended sediment attenuation coefficient α_s. The given coefficients are different for specific situations regarding mass concentration, PSD and the range. The viscous attenuation coefficient is dominant for fine clay-silt particles, whereas for sand it becomes negligible and the attenuation can be described by the scattering attenuation coefficient. (Guerrero et al., 2016b, Hanes, 2012)

The attenuation coefficient α_{ss} is related to the total scattering cross-section χ. To determine the coefficient α_{ss} the following equations can be applied. χ is calculated by a semi-empirical equation derived from best fitting of total scattering cross-section from tests with homogeneous PSDs. Once again the equations must be assessed for a heterogeneous size distribution resulting in equation 14. (Thorne and Meral, 2008, Guerrero et al., 2016b)

$$\chi = \frac{0.29 \cdot x^4}{0.95 + 1.28 \cdot x^2 + 0.25 \cdot x^4} \tag{13}$$

$$\langle \alpha_{ss} \rangle = \langle \zeta_{ss} \rangle \cdot M_s = \frac{3 \cdot M_s}{4 \cdot \rho_s} \cdot \frac{\int a^2 \cdot \chi \cdot p(a) da}{\int a^3 \cdot p(a) da} \tag{14}$$

The viscous attenuation coefficient α_{sv} can be derived through equations 15-18 (Urick, 1948). The coefficient must also be adjusted for a heterogeneous PSD. This is done in equation 19 reported by Guerrero et al. (2016b).

$$\Upsilon = \sqrt{\frac{\pi \cdot F}{v}} \tag{15}$$

$$s = \frac{9}{2 \cdot \Upsilon \cdot d} \cdot \left(1 + \frac{2}{\Upsilon \cdot d}\right) \tag{16}$$

$$T = \frac{1}{2} + \frac{9}{2 \cdot \Upsilon \cdot d} \tag{17}$$

$$\zeta_{sv} = \frac{\alpha_{sv}}{M_s} = \frac{k}{2\rho_s} (\sigma - 1)^2 \left(\frac{s}{s^2 + (\sigma + T)^2}\right) \tag{18}$$

$$\langle \alpha_{sv} \rangle = \langle \zeta_{sv} \rangle \cdot M_s = M_s \cdot \frac{\int a^3 \cdot \zeta_{sv} \cdot p(a) da}{\int a^3 \cdot p(a) da} \tag{19}$$

2.2.3 Inverse method and Sediment Yield Estimations

To determine the sediment concentrations by a continuous logging system, there has been research showing that the relationship between the attenuation α_s and the backscatter intensity ${k_s}^2$ can be used. Rearranging equation 8 to get the backscatter coefficients on the left hand side, as well as integrating the two-way attenuation due to the heterogeneous suspended sediment along the path between the transducer to the particle actual distance, R, results in equation 20. R is the ranging distance of the ADCP. This is a more generally applicable equation than the previous presented versions of the sonar equations. (Guerrero et al., 2017)

$$10log\big(k_s(R)^2 \cdot M_s(R)\big) - 20\log(e) \cdot 2\int \big(\zeta_{ss}(r) + \zeta_{sv}(r)\big) \cdot M_s(r) \cdot dr = I_{dB} - C + 20\log(R\psi) + 20\log(e) \cdot 2\alpha_w R) \tag{20}$$

An indirect method will determine the sediment concentration in equation 20. By assessing the relationship of the parameters on the left hand side of the equation with results from sampling, the data series for concentration can be determined by a calibration process (Guerrero et al., 2017). The process of calibrating is further described in the chapter 3.2.2.

2.2.4 Use of multiple ADCPs

The use of multiple ADCPs to monitor the different concentration situations in a river has proven to be useful. The acoustic parameters change in different situations. Viscous attenuation α_{sv} is dominant for small particles (i.e. silt) while measured with a low frequency. For larger particles the sound scattering attenuation α_{ss} is dominant for higher measuring frequencies. By neglecting the non-dominant attenuation parameter, the different grain sizes in the cross-section can be determined, with several ADCPs transmitting at different frequencies (i.e. 600 and 1200 kHz). This was done in a qualitative study in the Devoll river performed by Guerrero et al. (2016a), where the results indicated that the clay-silt (wash load) concentrations were less dependent on the water level than the sand suspended from the river bed, and an indication was made that there was a lag of fine particle sediment transport compared to water discharge. In this thesis only one ADCP (600 kHz) will be used to quantify the whole range of PSD in the water column.

2.3 Satellite Measurements

For a long time, satellites in space have been available for a number of purposes. Satellites have been essential for the advancement in fields such as in i.e. navigation, communication, meteorology and geodesy. The recent years has seen a leap in technology used for Earth observations, which has enabled the possibility to survey large areas at a much lower workload than has been traditional. The following chapter will describe one of the methods to detect deformation on the surface of the Earth with satellite measurements.

2.3.1 InSAR

Interferometric synthetic aperture radar (InSAR) is a remote measurement method that is designed to detect relative movement over time. The technology is based on data collected by synthetic aperture radars (SARs), and is widely accepted as a valuable tool to construct digital elevation models, as well as to assess the change in landscape over time. The SAR radars used in this study are placed on satellites that have a near polar-orbit. This means that they travel on a path from pole to pole on their orbit around the Earth which enables them to investigate large areas of land. The radars emit a series of electromagnetic pulses that are reflected when hitting solid objects on the surface. To calculate the distance between the satellite and the ground, the SAR measures the time and amplitude in the reflected microwave echo, and assigns it with a location in a measurement image. By combining two SAR images the phase differences between the electromagnetic waves is calculated, and the relative deformation between the images can be produced in potential sub-millimetre scale. This processing is referred to as InSAR, and is recognized as a precise tool in deformation studies (Smith, 2002, Cetinic and Lauknes, 2016).

Because the SAR satellites travel in a near polar orbit, and measures the Earth at an angle perpendicular to its path, it can provide useful information for varying topography. As the Earth rotates around its own axis at the same time as the satellite travels either from the north to the south (descending orbit), or from the south to the north (ascending orbit), it can measure the same location from two angles. This is a great advantage when measuring landscapes with varying topography, where steep hills can cause radar shadows. A slope that faces an unfavourable direction in terms of SAR measuring at i.e. an ascending orbit, can be favourable

in the descending orbit. Figure 2.3 describes the geometrical advantages of polar orbit. (Cetinic and Lauknes, 2016)

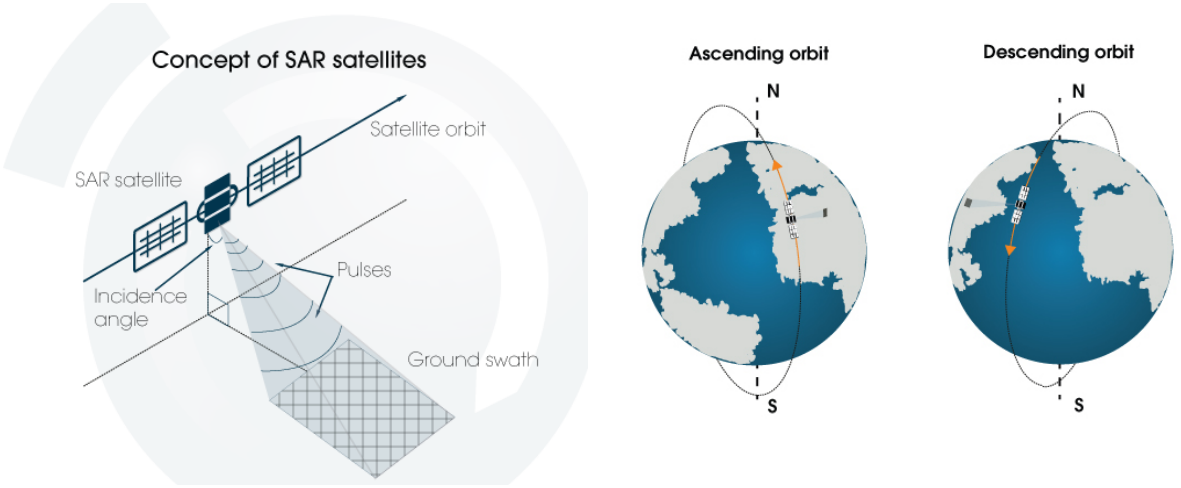

(a) (b)

Figure 2.3 Measuring geometry of InSAR satellites. (a) describes the measurement angle perpendicular to the orbit, (b) describes how the ascending and descending orbits will cover the same location from two different angles (Cetinic and Lauknes, 2016)

By obtaining a time series of InSAR calculations produced by the continuous scanning of the radar orbiting Earth, the relative change of the landscape can be documented. The SAR produces a series of electromagnetic pulses with a known wavelength that are reflected off hard surfaces on the ground. If the surface has been deformed between two measurements, the phase of the two images will be different. This phase difference can be processed by InSAR methods to give a value for this deformation. To describe the deformation of a natural surface, the method referred to as SBAS-InSAR is best suited. This is because the method studies an average deformation in a given cell. The average value is used to reduce the uncertainties that occur when measuring surfaces that does not have a "persistent scatter" of waves that large stable objects will give. To produce a time-series with SBAS at least 12-15 measurements of the same pixel have to be carried out, and as further observations are done the accuracy of the method will increase. As a matter of fact, studies have shown that with sufficient InSAR measurements, it is possible to obtain the same accuracy as GPS or beyond into the sub-millimetre level (Cetinic and Lauknes, 2016).

2.3.2 Using InSAR to predict Erosion and Sediment Yield

Using deformation studies to assess areas with high rates of erosion can give great insight of attributes in a catchment. If the deformation that takes place is due to weathering, it can describe volumetric change in the topography, resulting in an estimation of soil loss. As the masses that are eroded from the catchment are carried away by water as sediments, InSAR derived estimates of soil erosion can be used to predict sediment yield. Previous remote sensing methods have shown promising results by using both LiDAR (Light Detection and Ranging) (Corsini et al., 2009) and other geodesy surveying tools, but at a far smaller scale. If satellite based tools with high enough precision can be proven to give similar results, they can be a useful tool to determine soil loss and sediment yield. This information will be of important value when designing hydraulic structures. A feasibility study performed prior to this thesis showed promising results when assessing sediment yield from InSAR measurements. The conclusion, however, claimed that the method must be further developed. (Sørås, 2016)

Because the SAR radar is directed at an angle not perpendicular towards the Earth, the deformation that is recorded in InSAR processing must be carefully assessed. The InSAR tool is designed for observing the velocity of deformation in critical slopes and objects, but when assessing the actual values the processing method produces some care must be taken. The SAR radar measures the landscape in a Line of Sight (LOS) between the ground and the measured pixel at an angle to the vertical component. This means that the recorded deformation also will be relative to the vertical component. In studies of erosion, this can cause some inaccuracy, as the different topography of various pixels will cause volumetric changes that does not necessarily reflect that of reality. To provide the actual vertical deformation that is occurring in the measured pixel, some additional processing has to be performed. By combining the image from the ascending as well as descending orbit, the vertical displacement can be calculated by decomposing the displacement vectors. This decomposed value will sufficiently describe the displacement in both the horizontal and vertical axis (Cetinic and Lauknes, 2016).

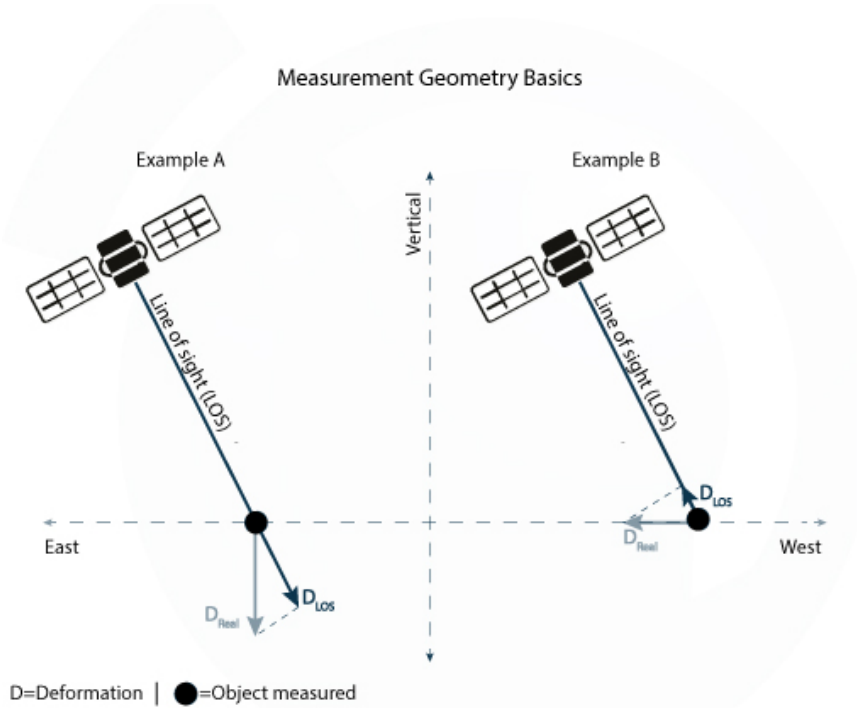

Figure 2.4 Decomposing measured deformation values (Cetinic and Lauknes, 2016)

2.3.3 InSAR limitations

Several factors will affect the interferometric measurement. To be able to combine two SAR-images, high correlation and coherence is needed. High coherence is related to low system noise, volume scattering and temporal changes. This means that excessive degree of weathering, vegetation, random change in dielectric properties (i.e. soil moisture) all affect the correlation between two images (Pacheco-Martínez et al., 2015). For the Devoll catchment, the most important parameter is the high weathering taking place. The data used in this thesis is derived from the Sentinel I & II satellites. The radars measure the site approximately every 12 days. To uphold the coherence in a InSAR derived deformation time-series, the deformation cannot surpass ½ of the wavelength of the SAR radar between the 12-day interval. For the produced data set, this implies that the deformation must not exceed 25mm between every satellite measurement (Cetinic, 2016). This is a shortcoming, as probable mass wasting events can remain undocumented. Because of coherence thresholds, highly vegetated areas will also be filtered out, leaving ungauged areas in the observed plot. For soil erosion studies, this will most likely have little impact, as areas with dense vegetation generally are associated with low erosivity.

3 Methodology

3.1 Study Area

This study focuses on the Devoll river and its catchment. The following subchapter is provided to give an insight of the general research location, as well as to enlighten the issues the Devoll project experiences around sediments. This is important information in the further understanding of results derived in this thesis.

3.1.1 The Devoll River and Catchment

Albania is a small country (28,748 km^2) in southern Europe located on the coast of the Mediterranean. It borders to Greece, Kosovo, Montenegro and Macedonia as well as the Adriatic Sea in the west. Geographically the country is dominated by mountainous regions, with an area of more than 75% being hills and mountains. This is also reflected in the mean altitude 708 masl. (Shundi, 2006).

Figure 3.1 Devoll catchment (Devoll Hydropower and Norconsult, 2011)

The Devoll river is located South-East of the capital in Albania, Tirana, and the catchment of the river is as the rest of the country characterized by varying topography. It covers an area of approximately 3,140 km^2 with steep hills and valleys with low vegetation illustrated in Figure 3.1. Since the catchment is of such magnitude, the climate and hydrology describing the 196 km long river is also varying. The highest rates of precipitation fall over the mountainous areas in the middle of the catchment. The flow regime is characterized by snowmelt in the upstream part, while precipitation dominates the lower regions. As to peak events during the year, the flow maximums are usually located in March/April and November/December, whereas high flood values span from September to April (Pano and Frasheri, n.d.). Albania is divided into different climate zones, but the year in general can be described as having cold and wet winters and dry, warm summers (Shundi, 2006). This is also the case for the Devoll catchment.

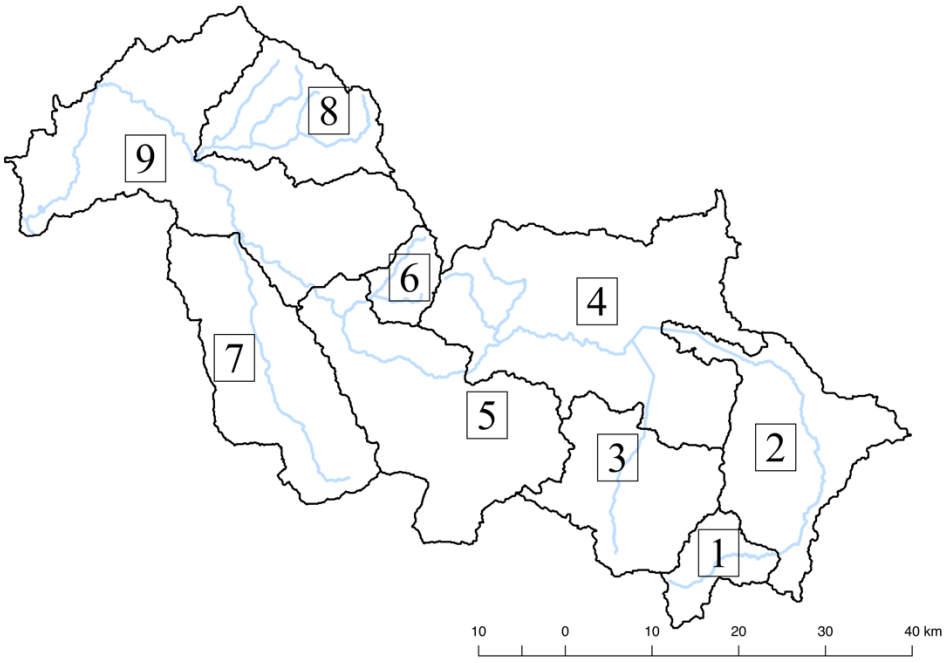

Figure 3.2 Devoll sub-catchments

To further describe the attributes around the Devoll river, the basin has been divided into sub-catchments as shown in Figure 3.2. The sub-catchments that drains into the Kokel gauging station (1-6 in Figure 3.2) are of interest for this thesis, and the attributes of these are summed up in Table 3-1. The sediment contribution of these sub-catchments will be further described in 3.1.4.

Table 3-1 Sub-catchments draining into Kokel gauging station (Omelan, 2015)

Basin #	Sub-catchment	Area [km^2]
1	Miras	89.39
2	Shequeras	341.13
3	Turhan	272.75
4	Gjinkikas	653.97
5	Poshtme	63.04
6	Kokel	459.37

3.1.2 Devoll Hydropower Project

The population in Albania of 3.1 million is experiencing a growth, and the general living conditions are improving (Shundi, 2006). This results in an increase in energy demand that is projected to rise by 60% by 2020. Historically the country has been a net exporter of electricity, but after the transition from centrally planned economy to an open market in the late 1980s it has been dependent on import of energy. Due to this increased energy-demand, the Albanian government has in the recent years been focusing on strengthening its energy security. Hydropower is the largest energy resource in the country, where only 30-35% of the possible capacity has been harnessed this far, leaving a potential for further development. In its campaign for strengthening energy security the Albanian government has been focusing on constructing smaller projects (100MW or less), while giving incentives for private investors to invest in larger projects. This has led to several international companies devoting to projects, with one of these companies being the Norwegian utility company Statkraft. As a parent company for the Albanian company Devoll Hydropower in a joint venture with EVN AG, Statkraft has bought the rights to develop a cascade of hydropower plants in the Devoll river. Once finished, the project will have a total installed capacity consisting of 256 MW, with an estimated annual production of 729 GWh. This will improve the total electricity production in Albania with approximately 17% (International Hydropower Association, 2015).

3.1.3 Existing Data

Data for the Devoll project valuable in the estimation of sediment yield and erosion was available prior to this thesis. A DEM (Digital Elevation Model) based on a WGS 1984 spatial reference coordinate system, and a UTM Zone 34N projection. The model has a resolution of approximately 81x81 m, and is useful when determining i.e. slope, area, channel systems and flow lengths in the catchment.

The discharge at the Kokel measuring station is also assessed. The data set used in this thesis contains values of water level in the Kokel gauging station at intervals of 60 minutes that spans from January 2015 to December 2016. The relationship between discharge and water level is described by a rating curve derived by the velocity index method (VIM).

Land cover characteristics was determined by data from the European Environment Agency. Land cover coefficients were defined by a visual inspection of the 2006 CORINE land cover map at a resolution of 100x100m (European Environment Agency, 2006). The values used in this thesis are based on coefficients derived by Haan (1994), and the conversion between these coefficients and CORINE land cover data is described in 3.3.4 as well as in the appendix.

3.1.4 Sediment Situation in Devoll

The catchment of Devoll experiences extremely high rates of erosion. The soil characteristics and the lacking vegetation in large parts of the catchment are favourable for extensive rates of soil loss, and this is shown in the valley sides that show clear signs of weathering. Field observations of the slopes in the catchment suggest that the scars left behind after mass wasting will contribute heavily to production of eroded material and sediment at rainfall events. The river banks are also filled with deposited sediments after prolonged erosion of the catchment over many years, and at high flood events the water will rise and re-suspend the deposited sediments along the banks and transport them further down the catchment (Devoll Hydropower and Støle, 2010). This supports the theory that sediment yield will increase with rising water levels as discussed in 2.1.2. In fact, erosion in the catchment of the Devoll river is sufficient enough to ensure that the river is often referred to as the most turbid river in Europe (Pano and Frasheri, n.d.).

(a) (b)

Figure 3.3 (a) Alluvial plane downstream of Kokel gauging station. High levels of deposited sediments (b) Signs of heavy weathering of the valley sides downstream of Kokel gauging station (photos taken by Sigurd Sørås)

Because of this enormous sediment production, the Devoll river has been monitored for sediment concentrations for a long period of time. Historical data exists with daily measurements of suspended sediment concentration and discharge from as early as the 1950s. The validity of these measurements can however be discussed, as with most historical data sets. Feasibility studies performed prior to the start of construction was based on historical data from measuring stations at Kokel (1965-1995) and Kozare (1995-1983) (Devoll Hydropower and Støle, 2010). For this study, the information from the measuring station at Kokel is interesting to assess. This is because the sediment load from sub-catchments that is draining through the gauging-station is further investigated in the following chapters. The results from the feasibility studies show high sediment concentrations, and the annual sediment yield has been produced directly by calculation of daily average SSC values multiplied by the average daily discharge. The correlation between annual water discharge and Suspended sediment yield is low, with a R^2 value of 0.5995 as shown in Figure 3.4. Therefore it is important to be aware that sediment transport cannot be described by discharge alone. (Devoll Hydropower and Støle, 2010).

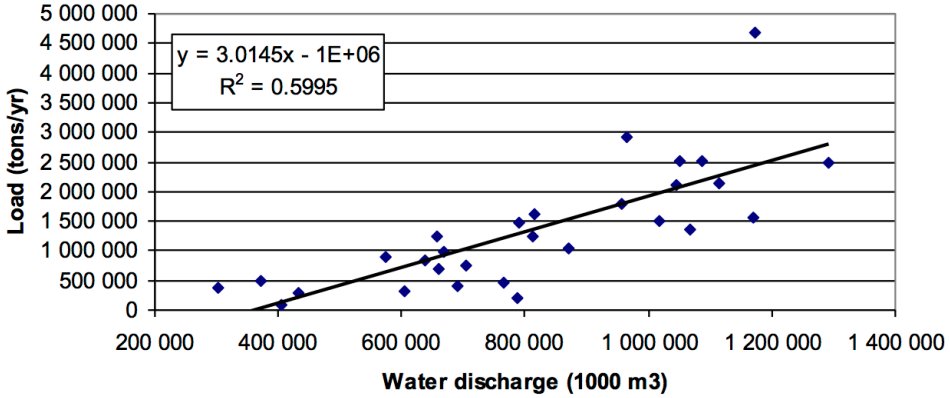

Figure 3.4 Correlation between annual load and annual water discharge at Kokel gauging station (1965-1996) (Devoll Hydropower and Støle, 2010)

Sediment yield is often described by the area specific load (tons/km^2). The average area specific sediment load was also calculated by the historical data from Kokel, as presented in Table 3-2 where the column # describes the sub-catchments in Figure 3.2. The higher value has been adjusted to include bed load and increased to reduce uncertainties in design of sediment handling devices.

Table 3-2 Results from feasibility studies (Devoll Hydropower and Støle, 2010, Devoll Hydropower et al., 2012)

#	Catchment area [km^2]	Average sediment yield [1000t/year]	Average area specific sediment yield [t/km^2*year]
1-6	1884	1 386 614	736
1-6	1884	2 704 000*	1 434*

*Adjusted for designing sediment handling devices

For a chosen 10-year period, data for concentration and discharge exists both for sub-catchments 1-4 (referred to as Gjinkas in the report) as well as the Kokel measuring station describing sub-catchments 1-6 (referred to as Kokel). The time series showed that the average area specific load for the whole Kokel catchment was insufficient to describe the sub-catchments below the Gjinkas measuring station, as calculations with an area specific load of 770 t/km^2*year resulted in an underestimation of the measured total load. A set of new assumed specific loads were assigned to the sub-catchments to better describe the measured load for the time period. The results are presented in Table 3-3. These values must be assessed with care,

as they contain even larger uncertainties than the estimations obtained for the catchment as a whole. They are also lacking bed-load estimations. (Devoll Hydropower and Støle, 2010).

Table 3-3 Estimated sediment yield for sub-catchments upstream Kokel (Devoll Hydropower and Støle, 2010)

#	Catchment	Catchment area [$km^{2]}$	Average assumed yield [t/year]	Average assumed area specific yield [t/km^2*year]	% of total load*
1-4	Gjinkas	1 354	415 421	307	29*
6	Malsise	300	585 600	1952	40*
6	Gjinkas-Kokel	155	302 715	1952	21*
5	Graboves	75	146 475	1952	10*
	Total	1884	1 450 211	770	100*

*Not given in report

Newer estimations for sediment and soil erosion in the Devoll catchment have also been carried out. One estimation is done through RUSLE, in an attempt to quantify both soil loss and sediment yield for each of the sub-catchment in the Devoll basin. The results for the catchments discussed in this thesis are presented in Table 3-4. The Kokel catchment (#6) is the largest contributor in terms of sediment yield, delivering approximately 42% of the load.

Table 3-4 RUSLE and sediment values for basins upstream Kokel (Omelan, 2015)

#	Catchment area [km^2]	Average Soil loss [t/year]	SDR [%]	Average sediment Yield [t/year]	Average specific Sediment Yield [t/km^2 *year]
6	459.37	8 829 514.02	19.8	1 750 892.63	3 811.50
1-6	1879.65*	21 114 180.23*	-	4 166 525.06*	2 216.65*

*Not specifically given in RUSLE-results in report.

The RUSLE estimation was significantly higher than the calculations based on historical data, proving the uncertainties in sediment yield estimations. The results from all estimations, although different, show exceptionally high values of sediment production in the upstream parts of the Devoll catchment.

3.2 ADCP Estimation of Sediment Concentration and Yield

3.2.1 ADCP in Devoll

As a part of the SEDIPASS (Sustainable design and operation of hydro power plants exposed to high sediment yield) project, two horizontal, 2D, ADCPs have been placed in the Devoll river as an attempt to quantify the sediment concentrations at different discharges. The devices are located one meter above the local reference point at the Kokel gauging station as shown in Figure 3.5. The ADCPs are transmitting pings at two frequencies (1200 kHz and 600 kHz), where the data from the ADCP transmitting at 600 kHz is further analysed in this thesis.

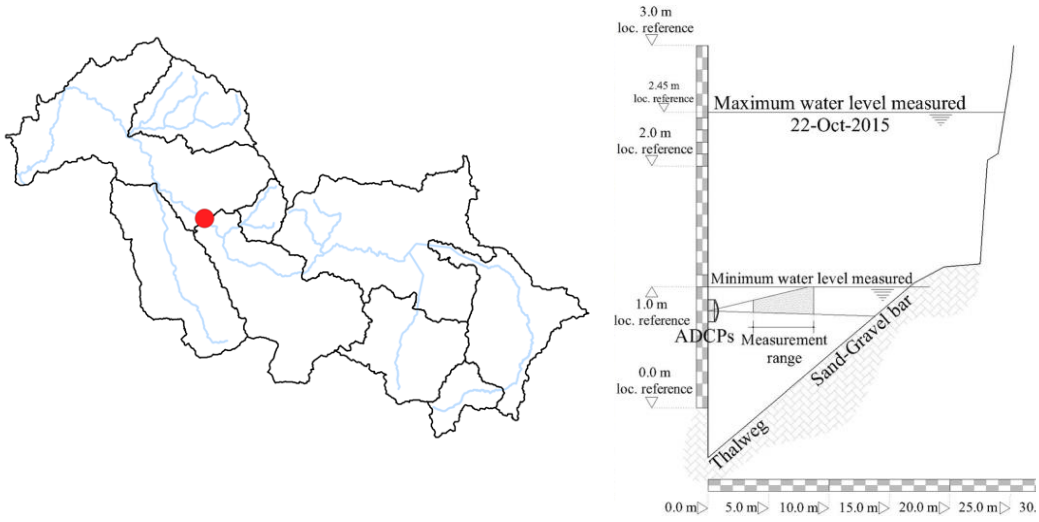

(a) (b)

Figure 3.5 (a) Location of ADCP at Kokel gauging station (b) cross section of measurement arrangement (Guerrero et al., 2016a)

The location of the ADCP is chosen because of its advantageous morphological geometry, with a rock wall on its left bank, leading to a V-shape of the cross-section. The sensors are placed on a platform facing perpendicular from the rock wall, horizontally towards the opposite bank. This ensures a relevant part of the streamflow width being monitored in terms of echo-intensity and velocity. The gauging station is located next to a bridge making it easier to access, as well as enabling sampling and other field surveys such as water velocity profiling with boat mounted ADCPs. The Kokel cross section is also situated at the end of a part of the river characterized with narrow passage between steep hills, just before the Devoll river flows into a wide alluvial

plane where deposition of sediments is bound to occur. The location is also propitious because of the historical data connected to the site, as presented in 3.1.4.

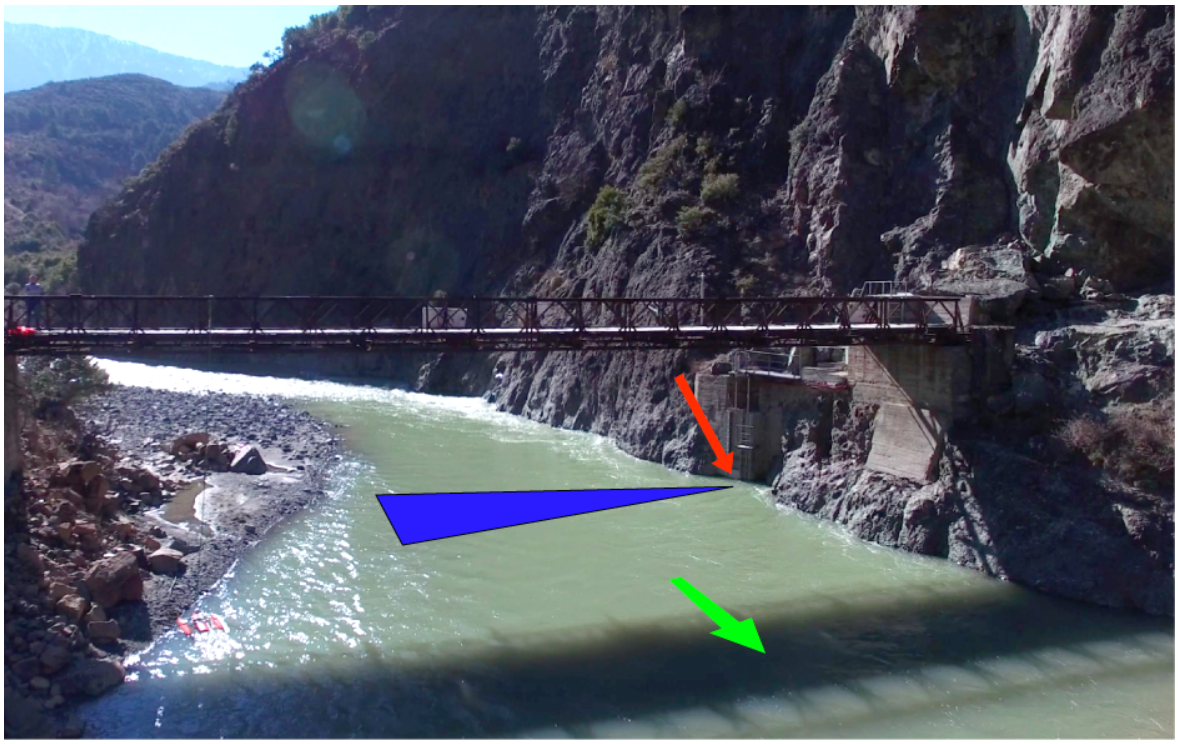

Figure 3.6 Kokel cross section. Red arrow marking location of ADCPs, green arrow indicating flow direction. Blue field representing acoustic beam (photo taken by Nils Ruther, edited by Sigurd Sørås)

3.2.1 MATLAB

In this thesis the data and equations for computing sediment concentrations in the Devoll river is processed by the MATLAB software. MATLAB (Matrix Laboratory) is a platform designed as a tool for numerical computation and visualization. It is a matrix based program that is widely used by engineers and scientists worldwide (The MathWorks, 2017). In this thesis the data used to determine sediment concentrations was delivered in combination with a processing script created as part of the SEDIPASS project. The script is at the time of writing still under development, but is treated as a finished product in this thesis.

3.2.2 Quantifying ADCP data

By an inverse approach the sediment concentration can be estimated through the acoustic parameters discussed in 2.2.3. From the backscattered intensity and the known constants, the MATLAB script uses a mean echo intensity derived for 60 minute intervals to calculate a ratio

between the attenuation coefficient (α_s) and the backscatter strength (k_s^2) by equation 8 in 2.2.1. The ratio is useful information when comparing values obtained by the ADCP with collected from sediment samples for calibration.

From samples, the ratio between attenuation (ζ_s) and backscatter intensity (k_s^2), as well as the viscous attenuation (ζ_{sv}), can be calculated from equations in 2.2.2. By a best fitting curve derived both from theoretical values for homogeneous PSD as well as samples from the Devoll river at Kokel, all ADCP ratio values (ζ_s/k_s^2) were converted into ζ_{sv}. Dividing ζ_{sv} with α_s from ADCP data gives the concentration (M_s) for the intervals recorded by the ADCP. A concentration time-series can be derived, as shown in 4.1.1 The largest parts of the ratio values are located within a range of three orders of magnitude. However, after conversion to ζ_{sv} values, the results spans over only one order of magnitude, leaving an indication of a correctly calibrated model with low levels of uncertainties.

To determine the suspended sediment yield by means of concentration values, discharge data is assessed. As mentioned in 3.1.3, the discharge for the given period is known with an interval of every whole hour. The ADCP derived concentrations are given at intervals that are not consistently 60 minutes, and an interpolation of the discharge data-series was done to find the discharge for the given time of the corresponding concentration value. By multiplying the discharge [m^3/s] with the sediment concentration [g/l] at a given point of time, an estimation for the suspended sediment yield [kg/s] for 2016 can be derived. Because the concentration curve has some discontinuities (further discussed in 5), the sediment yield time-series also experiences the same missing data. To calculate the total suspended sediment yield during the observed time period, the discontinuities in the sediment yield graph were filled by linear interpolation, which can lead to some uncertainties. The time period for the interpolation is however low compared to other interpolation procedures done in the field of sediment estimations. An estimate for the total suspended sediment yield was calculated by trapezoidal numerical integration performed on the sediment yield time-series. This was chosen to sufficiently describe the rapid change in the sediment attributes of the Devoll river.

3.3 InSAR Estimation of Sediment Yield

3.3.1 InSAR data coverage

The InSAR data further analysed in this thesis is produced by the SBAS processing. This method relies on giving a mean value of deformation to a pixel (in this thesis 40x40m) as described in 2.3. The data covers large areas of the Devoll catchment, with a focus around the Banja reservoir. This means that the sub-catchments above the Kokel gauging station is only partially covered. To describe the erosion that occurs for the non-covered sub-catchments, scaling techniques have been used. The coverage of InSAR data is described in Figure 3.7, where the sub-catchment marked by the colour red is further assessed with the method described in the following sub-chapters.

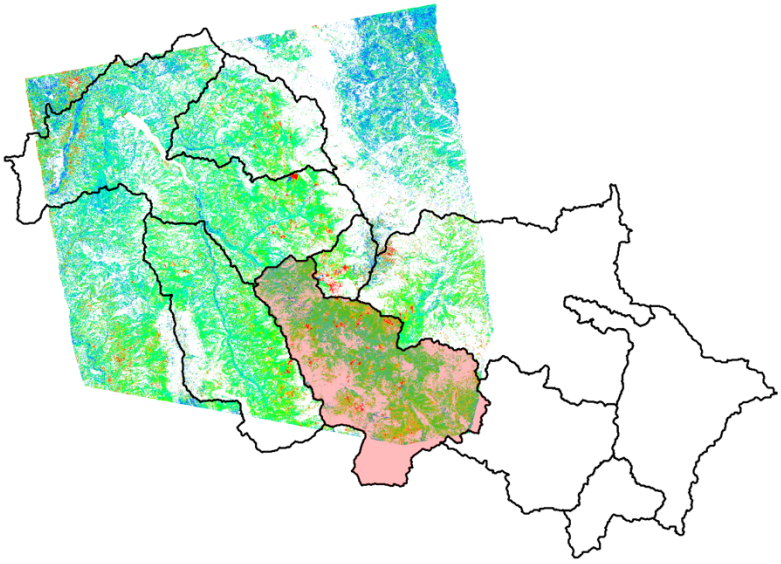

Figure 3.7 InSAR coverage of the Devoll catchment. Kokel sub-catchment in red

The produced data set consists of a time series of vertical cumulative deformation for every 90 days between the dates 16.10.2014 to 29.03.2017, covering approximately 407 km^2 of the Kokel sub-catchment.

3.3.2 QGIS

In this study the geospatial attributes of the Kokel catchment was observed. To do this, the GIS tool QGIS was applied. QGIS is a free and open source geographic information system that

gives the user the ability to analyse and visualize spatial data that is related to geographical coordinates. QGIS also includes valuable tools to compute various geological phenomena, such as locating channel systems, analyse slopes etc. GIS gives the user a tool to handle large data sets by assigning user input to cells in a grid (raster) (OSGeo, 2017). This advantage is the reason why GIS is frequently used in i.e. soil erosion models.

3.3.3 Quantification of Erosion from InSAR data

The data set assessed in this thesis consists of georeferenced points with cumulative deformation values. To assign the point an area, a Voronoi diagram is produced by processing methods in QGIS. This diagram assigns a set of centres a value based on the distance from other centres. The space between the points are divided according to "spheres of influence", meaning that the area will represent the space that is closest to the observed pixel (Ferenc and Néda, 2007).

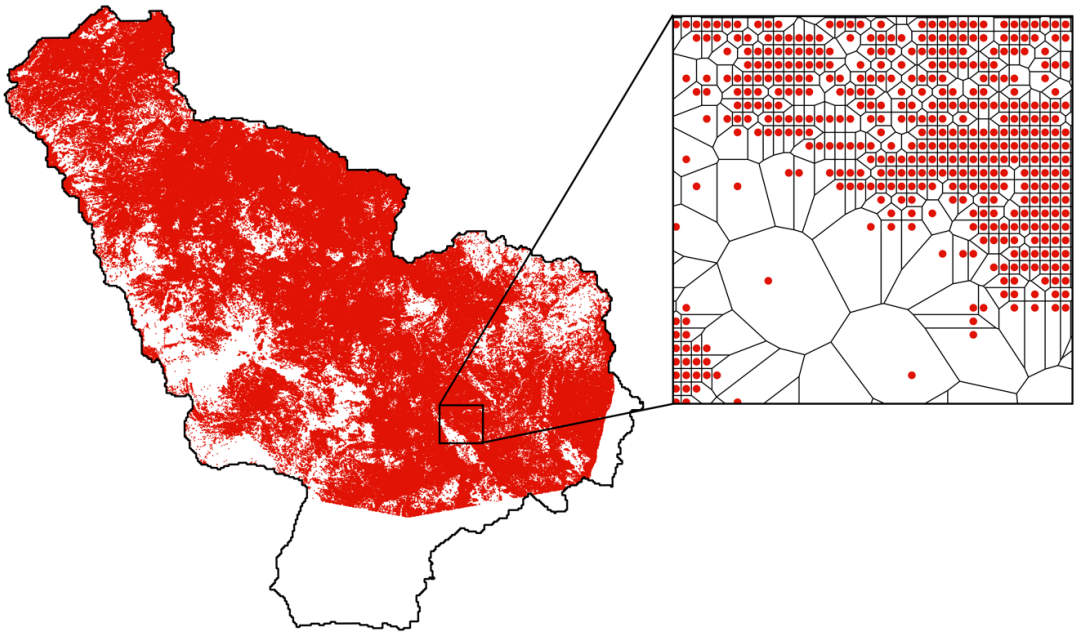

Figure 3.8 Voronoi diagram of fluctuating density of InSAR points

By dividing the cells in the fashion described by Figure 3.8, the point density will affect the area distribution, thus providing the high spatial density InSAR produces where possible, while areas with low coverage is represented by a lower resolution of cells. This is necessary when assessing the deformation, as an area for each point value must be given to calculate the occurring volume change. The point values are subsequently transferred to the corresponding

Voronoi polygon and later converted into a raster map with a resolution of 7.93x9.68m. The significantly higher resolution than in the DEM was chosen to sufficiently describe the Voronoi shapes, as many of them are not rectangular. The resulting raster layers were developed as shown in example by Figure 3.9.

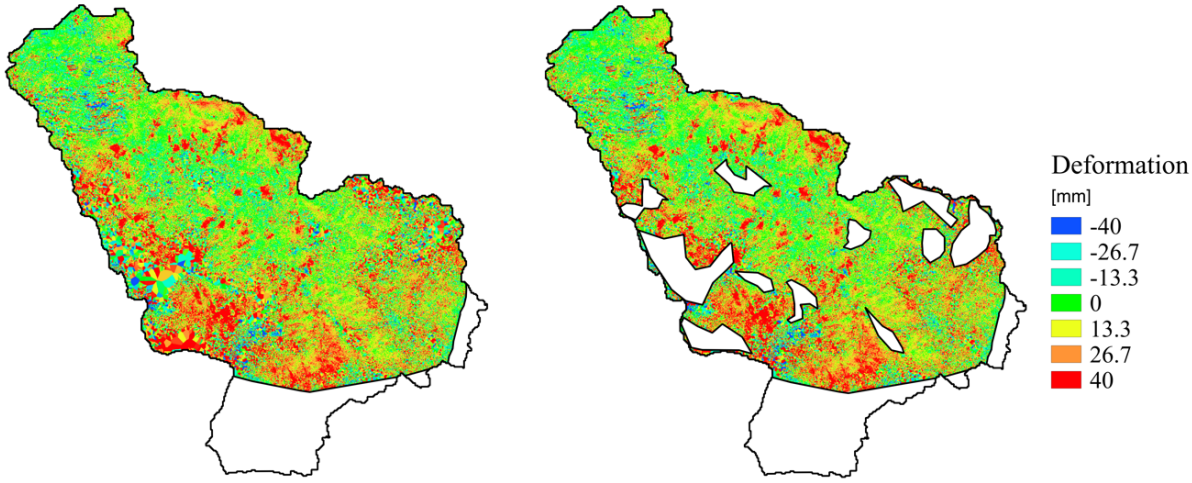

Figure 3.9 Example of raster describing deformation [mm] between 28.01.16 and 21.04.16. (a) unprocessed (b) areas with low InSAR coverage removed

A visual inspection was performed to remove cells with an exceedingly high area because of low InSAR point density. One InSAR point will insufficiently describe the surface deformation of an area that is too large. Figure 3.9 shows an example of a processed raster map. As described in chapter 2.3.3 the InSAR processing method will filter out measurements with low coherence, resulting in a low or inexistent density of InSAR points in areas unable to be measured by satellites. A general remark for the areas chosen to be removed to reduce uncertainties, is that these zones are clearly highly vegetated, thus proving filtering in InSAR processing.

The raster maps that were produced describes the deformation taking place between every interval of 90 days. To calculate the volume-change, the deformation of each pixel was multiplied with the raster cell size (7.93x9.68m), producing a new set of grids consisting of volumetric change for each pixel. The sum of N cells was assumed to describe the gross erosion $E_{catchment}$ as shown in the equation below, where Δd_i is the vertical deformation between intervals and a_i is the area for cell i:

$$E_{catchment} = \sum_{i=1}^{N} \Delta d_i a_i \qquad \text{Eq. (21)}$$

The volume difference between calculated intervals is described in Figure 3.10. The first raster working as a reference to the succeeding raster. The sum of volume change was assumed to be eroded mass.

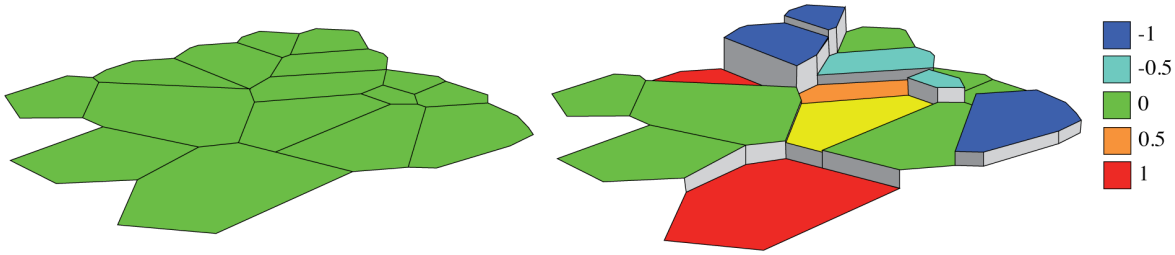

(a) (b)

Figure 3.10 Quantifying soil erosion by assigning voronoi cells with deformation values. (a) illustrating situation prior to occurrence of erosion (b) erosion and deposition has shifted cells in the vertical component resulting in volume change [m^3]

3.3.4 Quantification of Sediment Yield

To describe the total sediment yield for the sub-catchment by means of InSAR data, the rate between erosion and sediment production must be known. Because the occurrence of sediments is heavily affected by catchment characteristics, the erosion cannot be directly connected to the sediment yield. In this thesis the sediment yield from grid cells has been calculated by the sediment delivery distributed (SEDD) model as described in 2.1.4 by equations 3-6. With QGIS, the parameters necessary for the SEDD model can be obtained through the DEM for the Devoll catchment as well as the land cover map. The process of determining sediment yield by combination of InSAR and SDR is described in Figure 3.11.

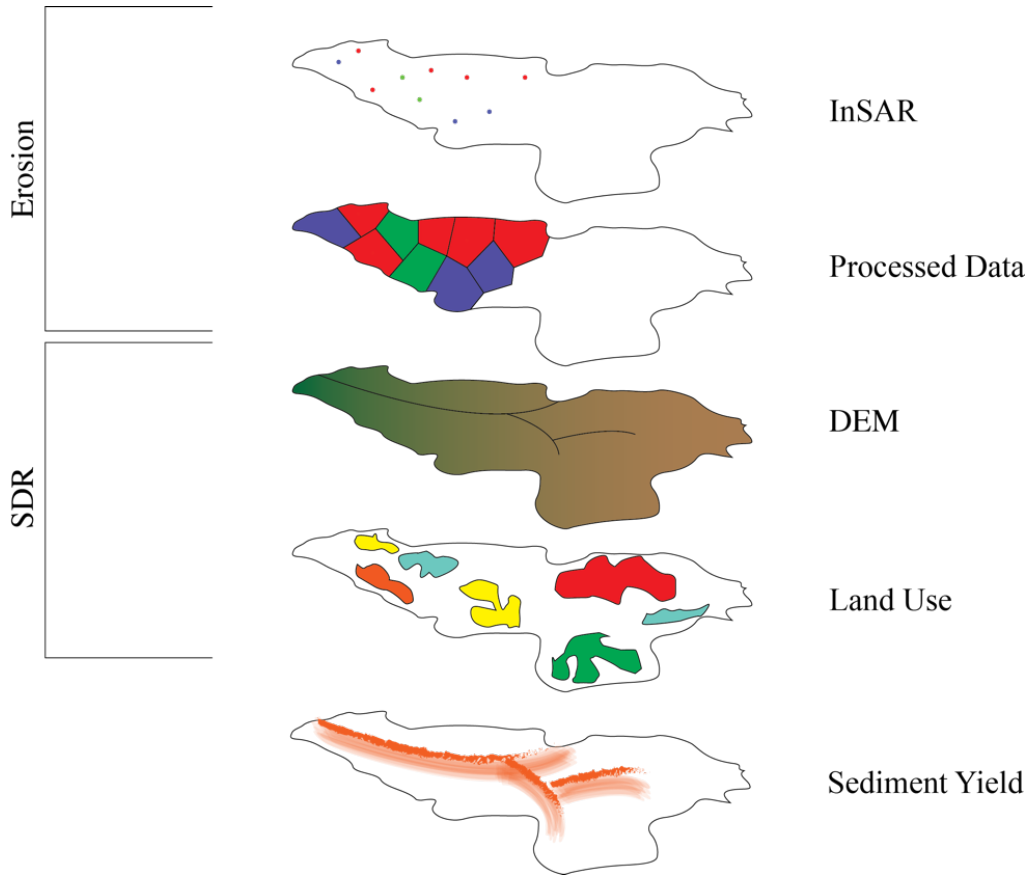

Figure 3.11 Step-wise illustration of quantifying sediment yield with InSAR and SEDD

To determine travel time in equation 3 (2.1.4), overland flow length l_i was found through the eight direction pour point algorithm plugin and a raster containing information around the channel system in the Kokel catchment. The eight direction pour point algorithm assigns a flow direction for each cell in a raster by determining the direction of the steepest descent out of eight permitted options for each cell (Holmgren, 1994). With an inspection of satellite images of Kokel, a threshold for the SAGA (System for Automated Geoscientific Analyses) channel system plugin in QGIS was chosen to determine the extent of the channel system. The SAGA overland flow distance plugin in QGIS creates a raster that states the number of cells, in effect the distance, from the individual cell to the nearest channel grid cell, illustrated in Figure 3.12.

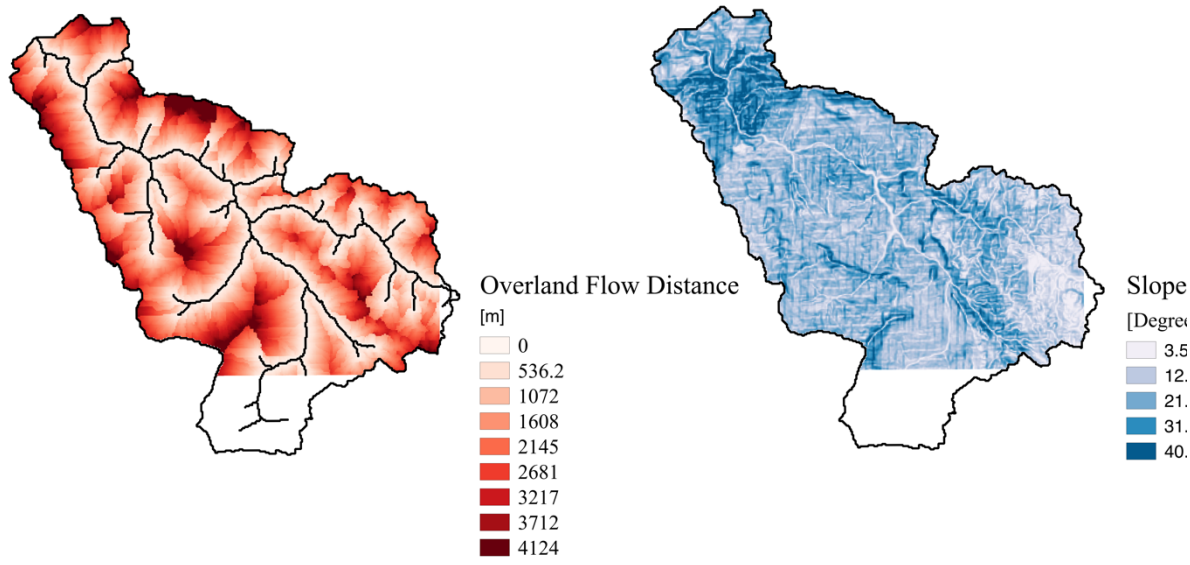

(a) (b)

Figure 3.12 (a) Overland flow distance of cells to nearest channel network. (b) slope in degrees for Kokel catchment

The velocity of the overland flow is a function of land use and slope in degrees. In this thesis values for land use and slope were assigned for every cell in the raster. The slope was computed through the SAGA slope plugin in QGIS, resulting in a raster map containing slope information for the Kokel catchment as shown in Figure 3.12.

Land use information was defined by visual inspection of the CORINE raster map, and assigning the CORINE Land Cover (CLC) labels with a value of *a,* given by Haan et al. (1994), shown in in Table 3-5 and the appendix. The conversion between CLC and *a* resulted in a raster describing the Kokel sub-catchment in terms of land use coefficient *a*.

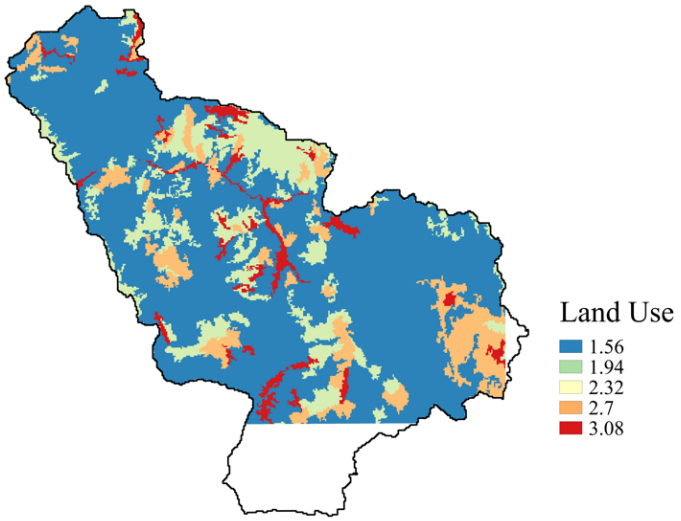

Figure 3.13 Land Use map for Kokel

Table 3-5 a values for different land cover types (Haan et al., 1994)

Surface	a
Overland flow	
Forest with heavy ground litter	0,76
Hay; meadow	0,76
Trash fallow; min. tillage	1,56
Contour; strip cropped	1,56
Woodland	1,56
Short grass	2,14
Straight row cultivation	2,62
Bare; untiled	3,08
Paved	6,19
Shallow concentrated flow	
Alluvial fans	3,08
Grassed waterways	4,91
Small upland gullies	6,19

With the three raster maps containing information for slope, land use and overland flow length, the raster calculator in QGIS was used to determine the basin specific parameter β, along with estimations for sediment yield for the Kokel basin. As mentioned in 2.1.4, β can be found through trial and error by estimations of the total watershed sediment delivery ratio. In this thesis, this was done by application of the inverse modelling approach as described by equation 6 in 2.1.4. The inverse modelling approach (eq. 6) was combined with the SDR_w equation introduced by Vanoni (1975) (eq. 2). The inverse modelling approach uses a weighted average of the grid based parameters in the SEDD model to describe SDR_w, where the combined equation is presented below. As the InSAR data covers large parts of the Kokel catchment (#6), the area chosen to calibrate β is the sub-catchment area (459 km^2). The calibration process is shown in Figure 3.14, where the SDR_w is decreasing with increasing β.

$$0.4724 \times A^{-0.125} = \frac{\sum_{i=1}^{N} \exp(-\beta t_i)\, {l_i}^{0.5} {s_i}^2 a_i}{\sum_{i=1}^{N} {l_i}^{0.5} {s_i}^2 a_i} \tag{22}$$

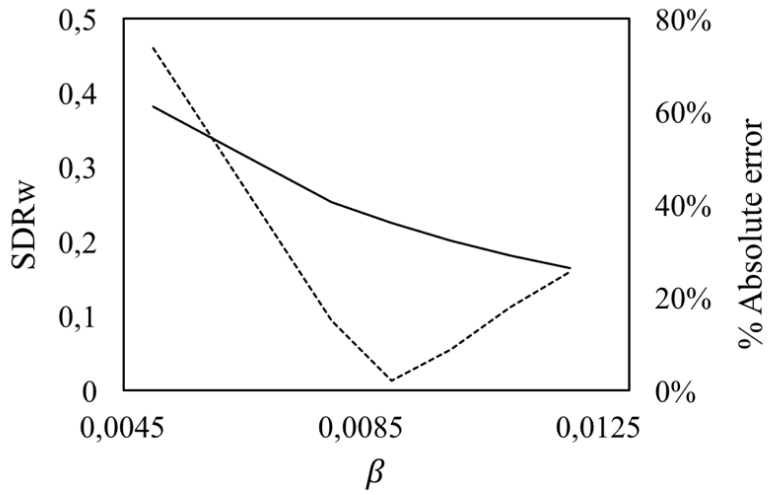

Table 3-6 Vanoni SDR_w

Area	SDR_w
459	0.22

Table 3-7 Calibration of β

β	SDR_w
0.004	0.38
0.008	0.25
0.009	0.22
0.012	0.16

Figure 3.14 Calibration of β for Kokel catchment through inverse modelling, dashed line representing % absolute error from SDR_w

Figure 3.15 shows the SDR_i grid system at the lowest and highest investigated value of β. Lower values of β results in a grid system that allows larger values of SDR_i, and thus resulting in a higher rate of erosion converted to sediment yield. The SDR_i value is as shown higher closer to the channel system, supporting the theory that the areas close to channel systems will produce significantly higher levels of sediments than the rest of the catchment.

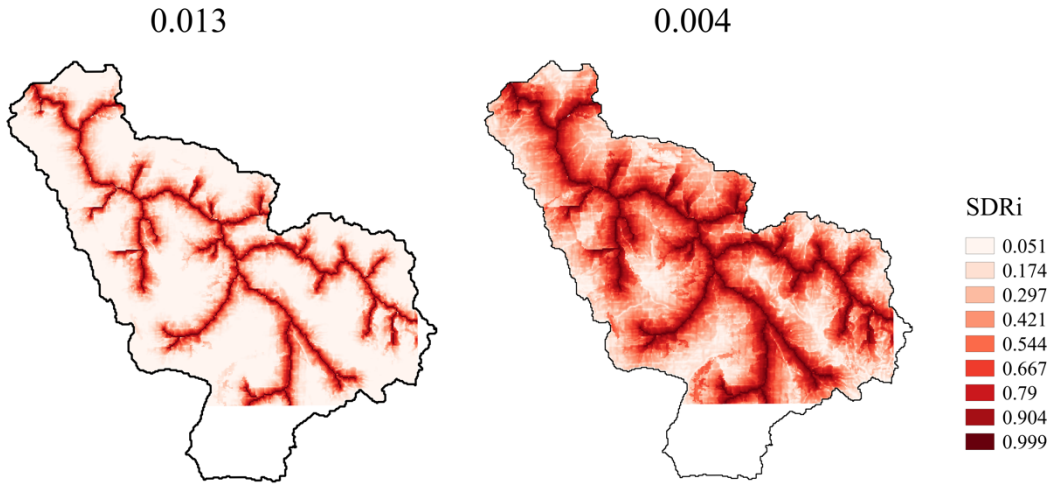

Figure 3.15 Lower values of β results in higher sediment yield for the same erosion rate

The calibration routine enabled the InSAR + SEDD model to be utilized for sediment yield estimations for the entire InSAR data set by β = 0.009. In this thesis the time period investigated by InSAR data to determine an annual value of sediment yield was 21.01.20115 to 28.01.2016.

4 Results

4.1 ADCP Results

4.1.1 Concentration

The sediment concentration in the Devoll river was derived for the period 27.01.2016 - 20.12.2016. The concentration is as expected, very fluctuating, and can vary by orders of magnitude within hours, which clearly illustrates the complexity of sediment transport and sediment gauging. There is also a large discontinuity in the concentration curve in the summer months, that can be explained by the water level falling below the ADCP sensor, leaving it unable to record echo intensities.

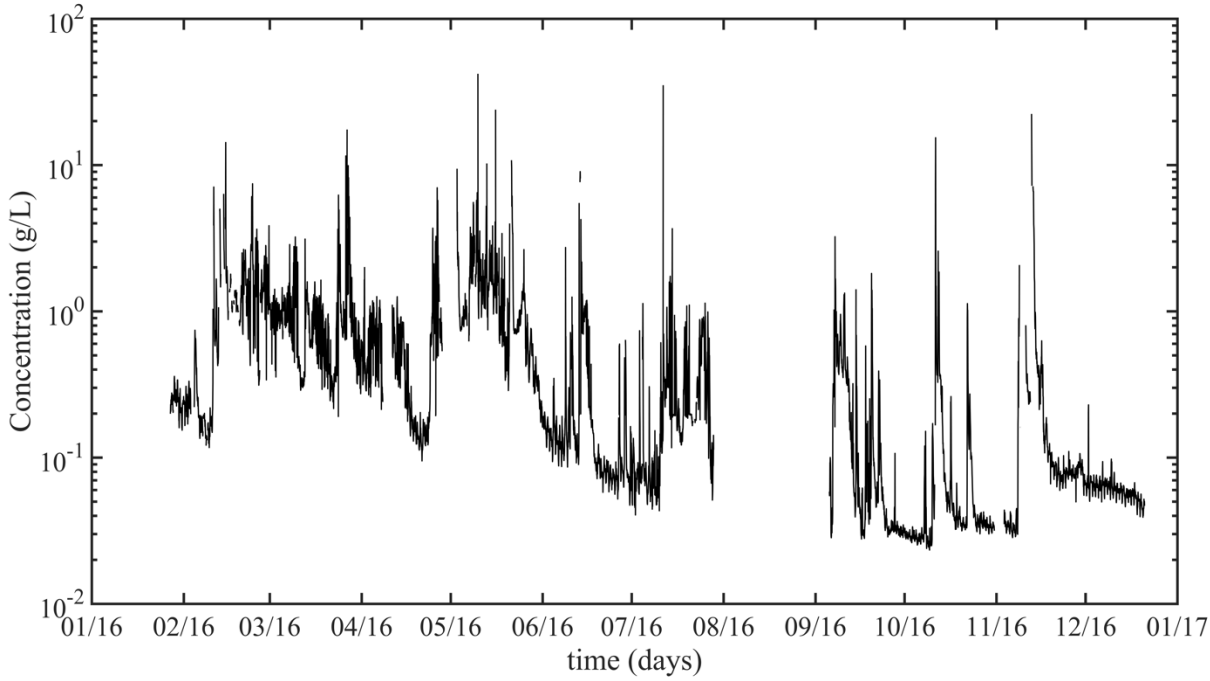

Figure 4.1 Concentration of suspended sediments for 2016

The recorded data oscillates heavily, proving one of the many challenges of sediment surveying. To sufficiently describe the annual fluctuation of sediment concentrations with traditional devices would require an immense number of samples. An indication of the sediment variation can be described by the minimal and maximum values obtained by the ADCP as presented in Table 4-1. The standard deviation and median for the data set describes a situation where the largest portion of sediment concentrations are situated around lower values.

Table 4-1 Statistical values for recorded and historical concentration values

	2016 [g/l]	historical [g/l]
Max	42.94	76
Min	0.02	-
Mean	0.57	0.83
Median	0.19	0.17
Standard deviation	1.40	2.97

It must be noted that the concentration curve also experiences some gaps at the highest flood peaks, meaning that the highest discharge levels are not represented by corresponding concentration values. The reason for these discontinuities are at the present unknown, where the working theory is a technical issue regarding the ADCP not measuring correctly at rapidly rising water levels. An example of such a discontinuance is shown for a flood in February 2016 in Figure 4.2.

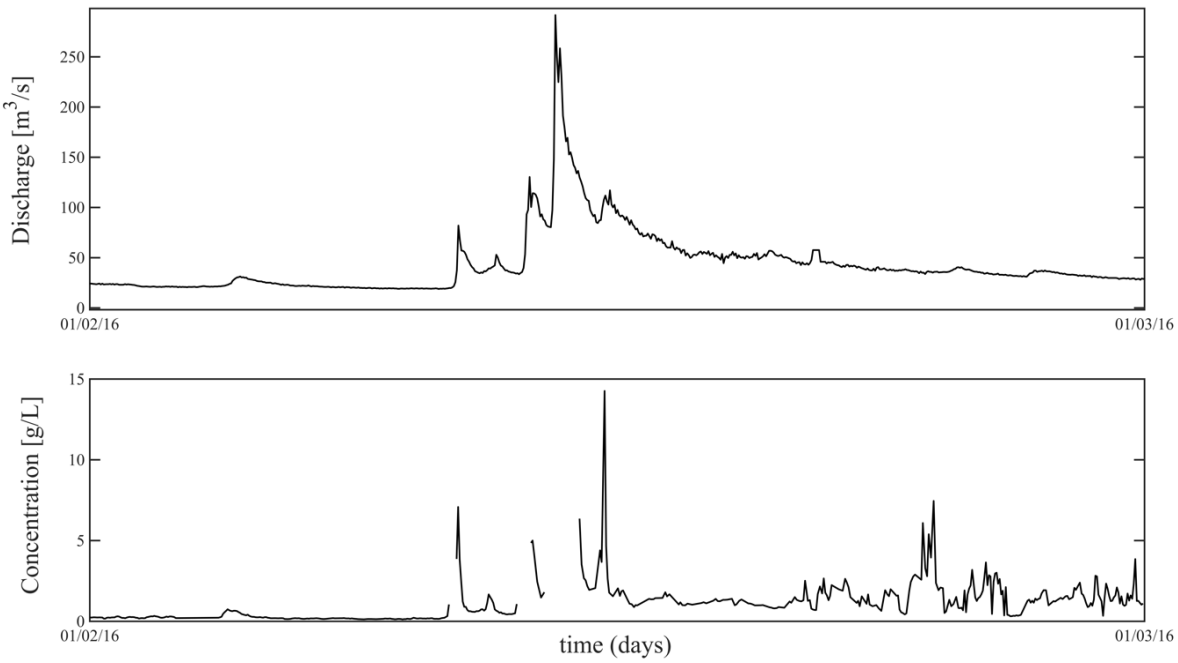

Figure 4.2 Discontinuity in concentration data for flood event in February 2016

The suspended sediment concentrations (SSC) recorded by the ADCP was further assessed in context with the discharge data to establish a sediment rating curve. A sediment rating curve can be of benefit for understanding the nature of sediment transport for the observed site, but is

often related to uncertainty. This is also the case for the rating curve derived for the sediment attributes in the Kokel-catchment. As illustrated in Figure 4.3, the sediment concentrations recorded by means of ADCP has weak correlation with recorded discharge. A linear regression results in a coefficient of determination (R^2) of only 0.18, indicating that the relationship cannot be sufficiently described by such modelling techniques.

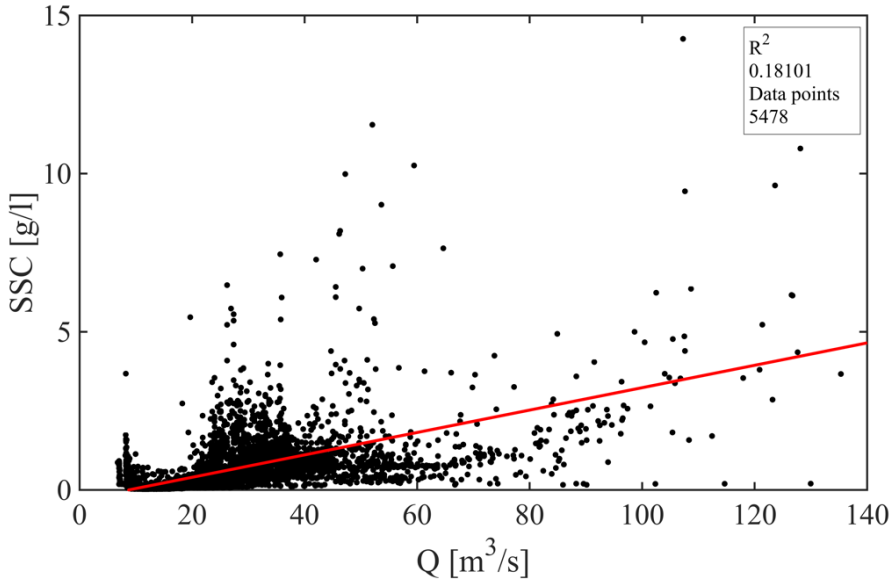

Figure 4.3 Rating curve for SSC

Interestingly, the main fluctuation in concentration relative to discharge can be found around lower discharges. Following this thought, the period of high concentrations at relative lower discharges would be interesting to locate to further understand the low correlation of the rating curve. To illustrate, a new rating curve for a flood event in march 2016 was derived as shown in Figure 4.4.

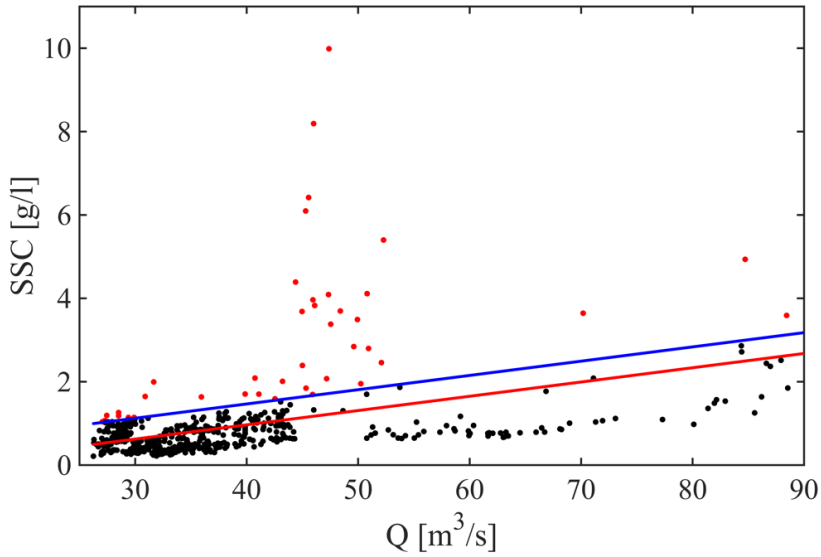

Figure 4.4 SSC rating curve for flood period in march 2016

The rating curve for the flood event also indicates low correlation between discharge and suspended sediment concentrations. As a tool to investigate the low correlation, a threshold line (blue colour) relative to the linear regression line (red) was chosen to determine data points to further investigate. Data points with a higher value than the threshold line was then located relative to the concentration/discharge curve as shown in Figure 4.5 where red circles represent concentrations not described by the linear regression.

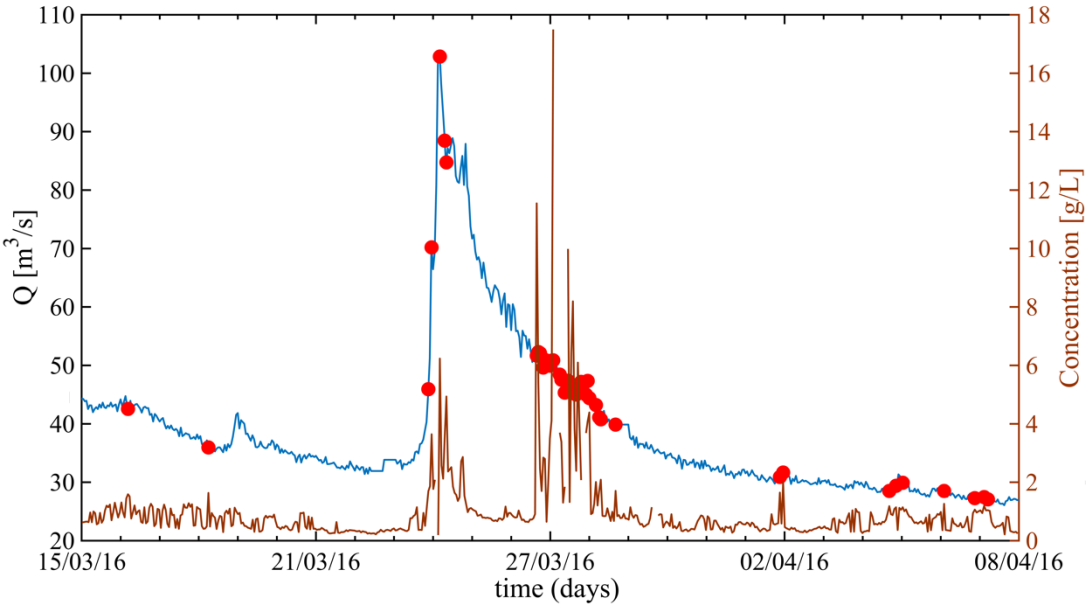

Figure 4.5 Recorded sediment concentrations for flood event in March 2016. Discharge on right y-axis, concentration on left y-axis

As observed in Figure 4.5, the sediment concentration will rise simultaneously as the discharge in the start of a flood period, showing correlation with the linear regression in the rating curve. As stated earlier, some data at the highest flood peaks are missing, leaving an uncertainty of this correlation, indicating that the form of the discharge and concentration curve should be even more alike if the data was existing. However, the highest recorded concentrations are not always occurring simultaneously to the discharge peak. Higher suspended sediment concentrations relative to discharge are generally located in the wake of the flood peak, showing a lag of higher concentrations of sediment particles compared to discharge. In this event, the flood peak is nearly three days prior to the highest concentration of sediment particles. As a trend, the highest sediment concentrations for large parts of 2016 set are located after or in a high flood peak supporting the theory of floods being the main driving force for sediment yield, even if high values of sediment concentrations does not necessarily occur as discharge rises.

4.1.2 Suspended sediment Yield

To determine the sediment yield derived from ADCP, the concentration values were combined with the discharge data, and a sediment yield plot was derived as shown in Figure 4.6. The result indicates lower values than previous estimations based on historical data (from 2010 and 2012, see 3.1.4). As a reference for the reader, estimations from historical data are presented in Figure 4.6 as dashed lines.

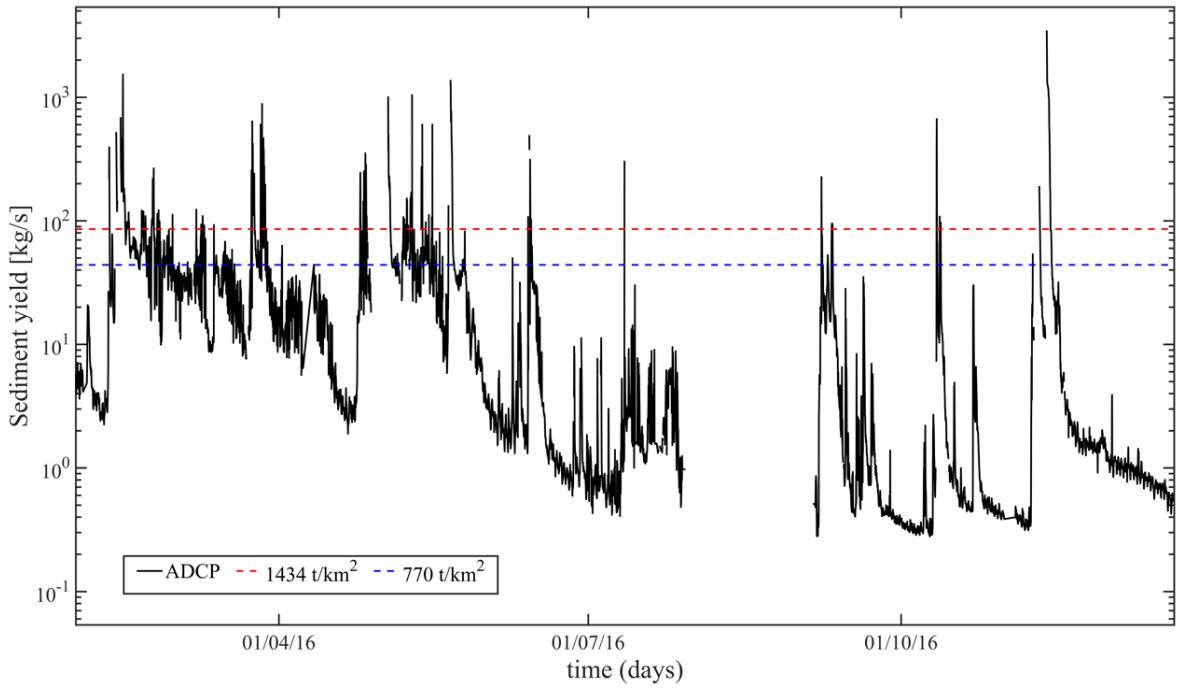

Figure 4.6 Sediment yield for 2016. Dashed lines representing historical data

Because of lower water level during the summer, the sediment yield time-series, as the concentration plot, experiences a discontinuity due to the ADCP not being submerged. Missing concentration data at discharge peaks also leads to a probable peaks of sediment transport being underestimated.

The relationship between sediment yield and discharge is expected to be higher than the correlation between concentration and discharge. This is because the increase of concentration occurring at the same time as rising water levels will be weighted by a higher discharge than the lagged concentration wave in the wake of a flood peak. For the same flood event as discussed in 4.1.1, the sediment yield and discharge were compared, as shown in Figure 4.7.

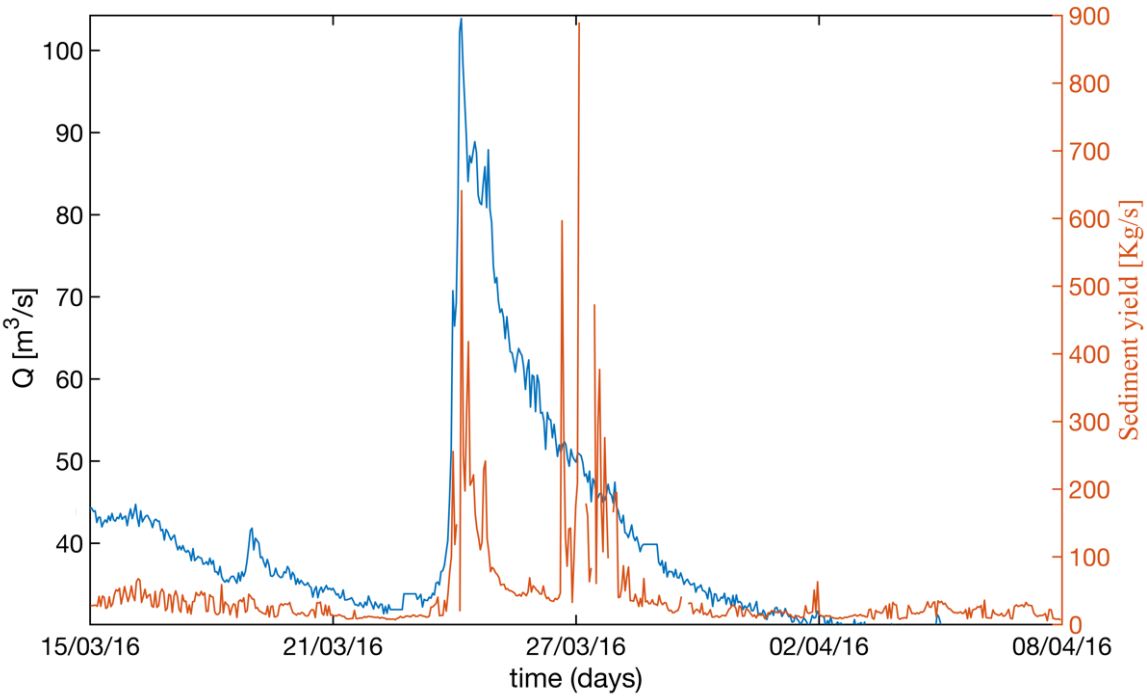

Figure 4.7 Discharge/sediment plot for flood period in march 2016. Discharge on left y-axis, sediment yield on right y-axis

Although higher than for the concentration, the correlation between sediment yield and discharge is low. This is because of the large concentrations that are occurring in the wake of high flood periods results in high rates of sediments being transported at lower discharges. As seen in Figure 4.7, rising flood levels results in momentarily high sediment yield levels that decreases as the flood level sinks. Equally, and even higher, levels of sediment are transported as the lagged wave of high concentration values passes the ADCP.

A short time-interval cannot describe the relationship between sediment yield and discharge because of the large rate of sediment transport taking place in the aftermath of floods. Following this thought, a suspended sediment yield rating curve was derived for monthly intervals of 2016, as shown in the appendix and in Figure 4.8. This time span was chosen to sufficiently describe the lag in sediment transport.

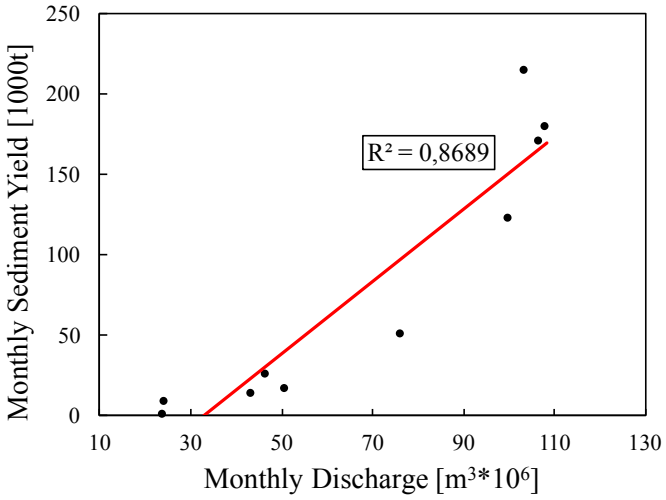

Figure 4.8 Suspended sediment yield rating curve based on monthly values from 2016

The monthly suspended sediment yield rises with increasing discharge, as seen in Figure 4.8. It is assumed that this method of describing the nature of sediment transport on the basis of discharge contains less errors than the concentration rating curve, because the lagged wave of high concentrations will be included. The rating curve should however contain more data points than presented in this thesis to reduce uncertainties, and a verification should be done whether the relationship is linear or can be better described by another regression method. The intervals in the development of the rating curve could have been chosen to be smaller, i.e. at weekly intervals, but the plot sufficiently describes the train of thought.

To establish an estimation of total suspended sediment yield for 2016, blank values in the data series of sediment transport were assigned a sediment yield value by a linear interpolation and the integral of the sediment yield variations for 2016 was calculated. The suspended sediment yield was derived for the period 01.02.2016-20.12.2016, resulting in an estimation for the annual load from the sub-catchments upstream Kokel presented in Table 4-2. An annual estimation for 2016 is also presented by an assumption that the ADCP time coverage is representative for the year. The assumption will contain uncertainties, as there are several flood peaks unaccounted for in January 2016 that probably carried large rates of sediment.

Table 4-2 Results from suspended sediment yield estimations by means of ADCP

Time period [days]	Area [km^2]	Estimated sediment yield [t]	Estimated specific sediment yield [t/km^2]	Annual discharge [mill m^3]
323	1880	852 516	453	-
365*	1880	963 369*	512*	855

*Assumed values

4.2 InSAR Results

4.2.1 Erosion

The determination of volume change was done for the period 16.10.2014 to 29.03.2017 by calculating the change of volume between InSAR measurement intervals as described in 3.3.3. The results are shown in more detail in the appendix. The volume change was assumed to represent the erosion occurring in the Kokel catchment, with a density of 1.4 t/m^3. The InSAR data produced deformation values for 333 126 points in the 407 km^2 coverage of the Kokel sub-catchment.

The raster maps produced showed as expected high rates of erosion in the Kokel catchment. The InSAR data covers large parts of the Kokel catchment, and is assumed to describe the majority of deformation taking place in the sub-catchment. Interestingly, the channel system is often clearly visible in the volume change maps, as shown in Figure 4.9, indicating that there are large deformations taking place in the slopes and banks of channels, as supported by previously discussed theory in chapter 2 and the survey of the site in 3.1.

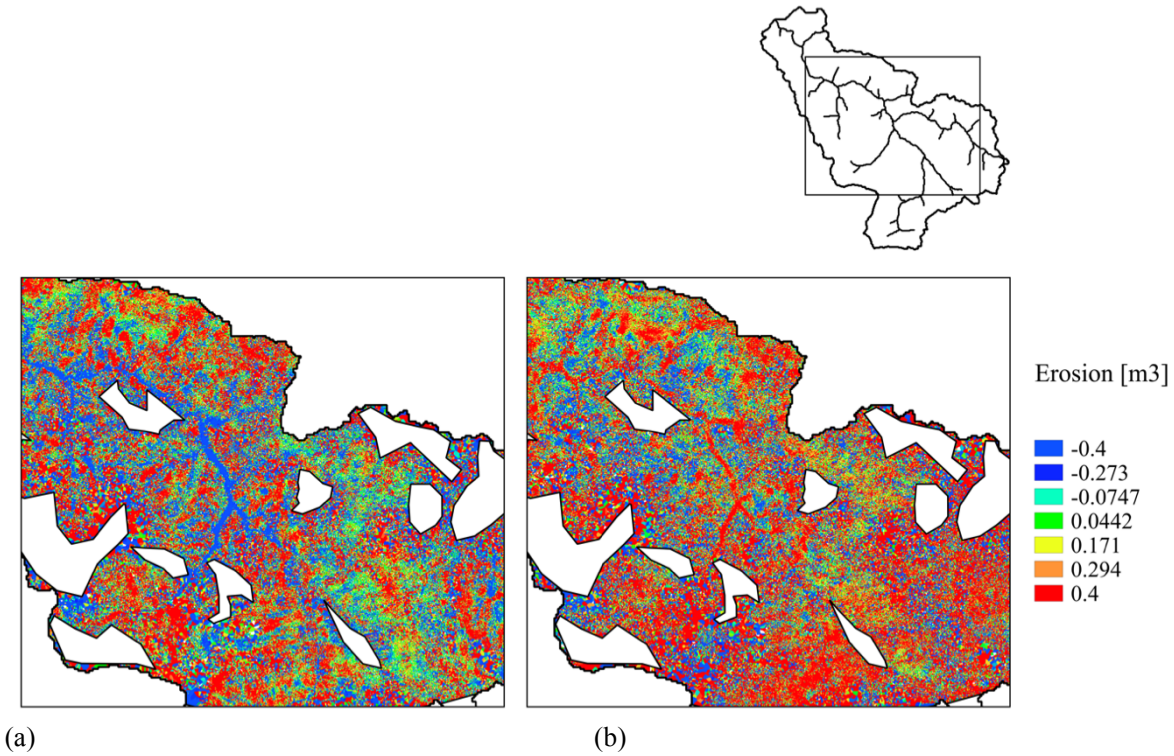

Figure 4.9 (a) Erosion raster for time period 27.04.15 – 20.07.15. Clearly visible accumulation of mass in channel system and erosion of slopes. (b) Erosion raster for time period 16.10.14 – 21.01.15. Visible erosion of channel system, indicating accumulated mass being transported away from catchment.

The pattern of the volume loss produced by post-processing of InSAR data also shows good similarity to expected zones in the catchment prone to erosion. As seen in Figure 4.10, the scars after landslides are clearly visible in the satellite image (a). The erosion in such scars will be expected much higher than other areas, and is proven by the processed InSAR data in (b), where the red zones describes loss of mass.

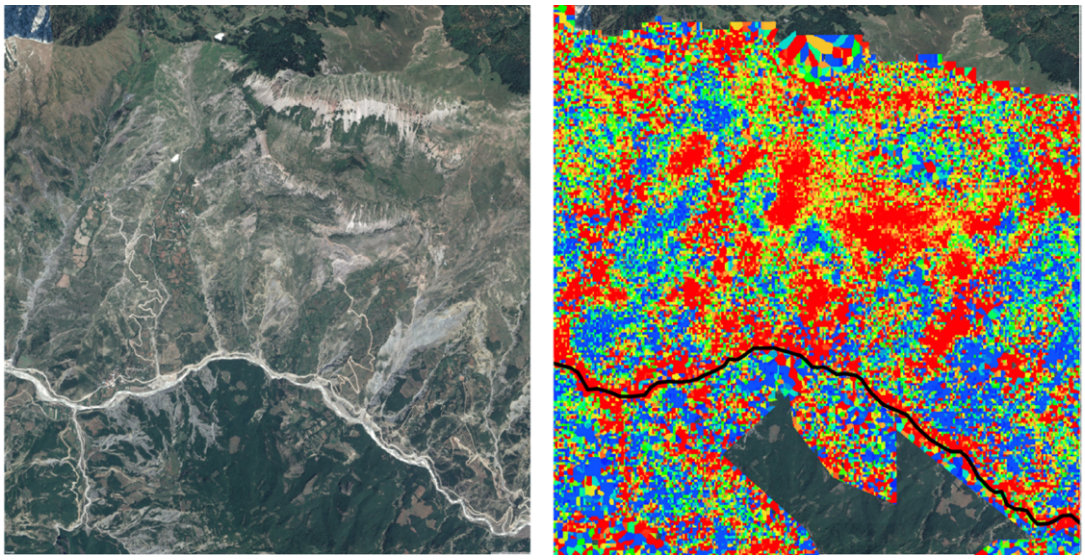

(a) (b)

Figure 4.10 (b) Erosion pattern for time period 16.10.14-21.01.15 compared to satelite images (a) (Google Earth, 2017)

By computing the total volume change from the intervals, the erosion from approximately 90-days was calculated and is presented in Figure 4.11. The volume change, hereafter referred to as erosion, is significant for the observed area of 407 km^2. The estimated erosion is however negative between July 2016 and march 2016, meaning that there is a supply of mass to the observed area, somewhat contradicting the assumption of volume change describing erosion. Different reasons for the occurrence of negative erosion is further discussed in chapter 5. The negative erosion rates for 2016 led to the year 2015 being further assessed in this thesis.

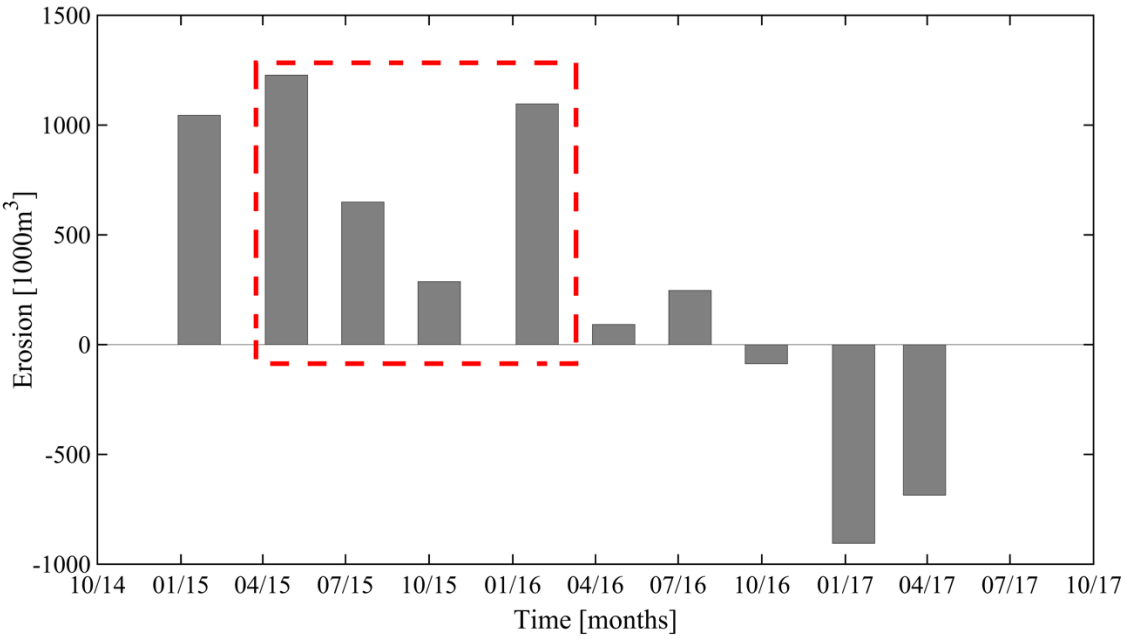

Figure 4.11 Erosion in the Kokel sub-catchment derived from InSAR intervals. Red dashed box represents further assessed values

The erosion taking place in 2015 is varying heavily, with the highest values in the period January-April and October-January, and the lowest rate in the summer months. The reason for this deviation in erosion would be interesting to assess. The assumption in this thesis is that the erosion rate derived from InSAR can be converted to sediment yield. If there is a relationship between precipitation and erosion, the assumption is further validated. As the recorded water levels for 2015 has large portions of lacking data due to both civil works at the gauging station and technical issues concerning the sensor, a comparison with average daily discharge from the historical data set was done.

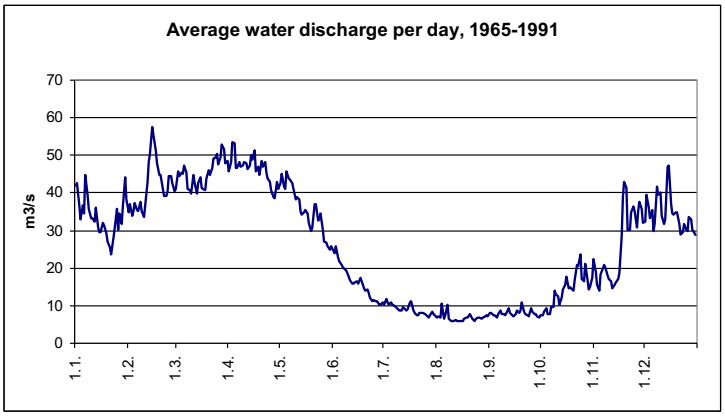

Figure 4.12 Average daily waster discharge for Kokel from 1965-1991 (Devoll Hydropower and Støle, 2010)

The historical values indicate higher discharge values in the time interval January-April and October-January than the rest of the year, indicating similarity with the rate of erosion found in InSAR estimations from 2015.

4.2.2 Sediment Yield

The calibration routine performed to find the basin specific parameter (β) led to the production of the raster map containing SDR_i values for every raster cell in the Kokel sub-catchment, shown in the appendix. As stated, total sediment yield is the product of erosion and SDR, enabling production of raster maps containing sediment yield values for each cell in the raster. As seen in Figure 4.13, the sediment contribution will increase significantly in the proximity of the channel system. In the presented example, the largest contributions of sediments (represented by red grid colour), are coming from areas in the south of the sub-catchment while there is some accumulation of mass (blue colour) in the channel system in the north and centre of the catchment.

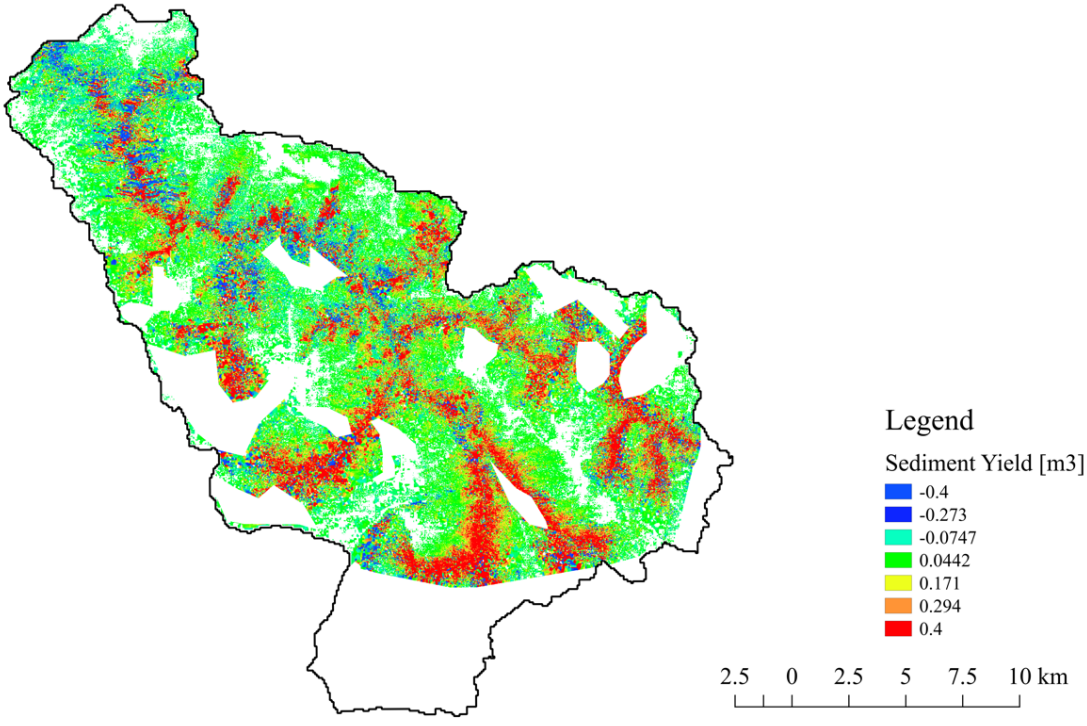

Figure 4.13 Sediment yield for time period Jan.15 - Apr.15

The corresponding sediment yield for each InSAR interval was calculated and is presented in Figure 4.14. As a comparison, the sediment yield was also calculated with InSAR and the SDR_w equation derived by Vanoni (1975), and is represented by the light-grey bars in Figure 4.14.

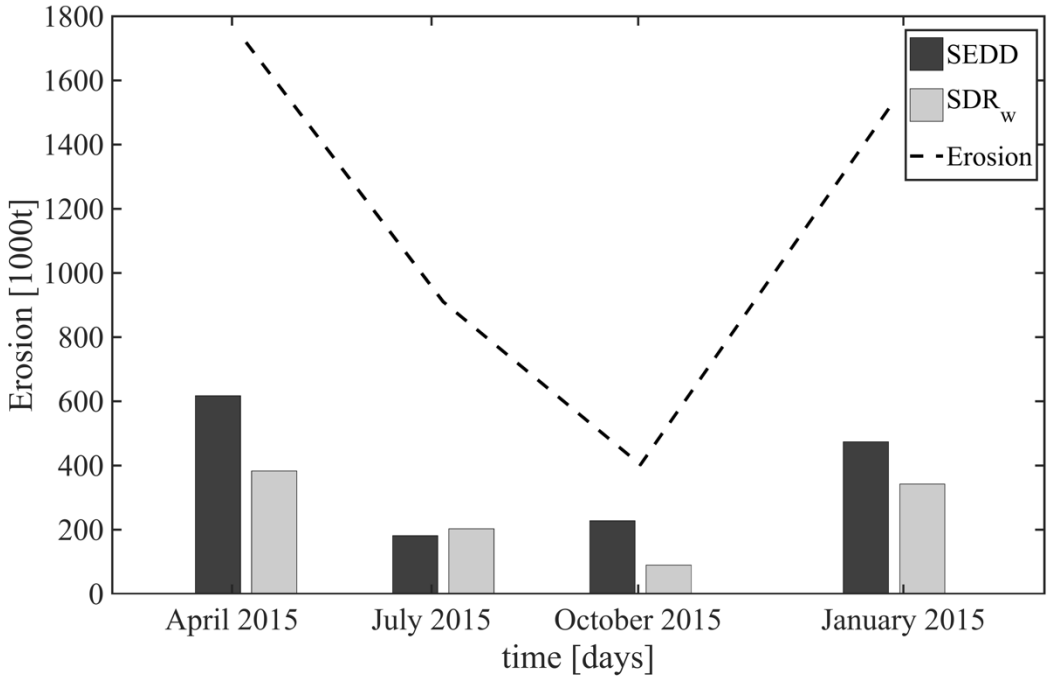

Figure 4.14 Sediment yield from the Kokel subcatchment calculated by two methods in combination with InSAR. Erosion represented by dashed line

As seen in Figure 4.14, the sediment yield derived from the SEDD model will be affected by the rise and fall of the erosion as expected. Worth noting is that the sediment yield calculated in April is lower than for October, although the erosion being larger for the July interval. This is because the different SDR_i cells in the model will weight erosion occurring close to the channel system higher than erosion taking place further away. When calculating georeferenced sediment yield from a relative limited time period, as is the case for InSAR estimations, this is important. Large rates of erosion close to the channel will be neglected if such weighting is not taken into account, as is shown with the SDR_w values that will not equally be affected by local area variations.

The annual sediment yield for 2015 derived from InSAR is also interesting in a further discussion of the technique, and for a comparison to other estimation methods. As mentioned the Kokel sub-catchment is highly erosive, and high rates of both erosion and sediment

production are expected. As shown in Table 4-3, the results from the processed data from 2015 also states high levels of sediment yield.

Table 4-3 Erosion and sediment yield from observed InSAR area (407 km^2)

		Erosion InSAR [1000t]	Sediment yield SEDD [1000t]	Sediment yield Vanoni [1000t]
Jan.15 - Apr.15		1 719	618	383
Apr.15 - Jul.15		910	182	202
Jul.15 - Oct.15		402	228	90
Oct.15 - Jan.16		1 536	474	342
Total	[1000t]	4 567	1 501	1 018
Total specific	[1000t/km^2]	11.22	3.69	2.50

As the Kokel sub-catchment is not representative for the total sediment yield transported through the Kokel gauging station, scaling has to be performed. It is expected that the InSAR coverage (459 km^2) of Kokel sub-catchment (407 km^2) is sufficient enough to describe the sediment production of the catchment, as the coverage is approximately 90%, where only the higher parts with expected lower contribution of sediments are not covered. From estimations done with historical data (presented in 3.1.4), it is shown that the Kokel sub-catchment will contribute to approximately 61% of the total sediment yield from the upstream catchment. With this assumption, the sediment yield from the whole watershed upstream Kokel was calculated. The result presented in Table 4-4 must be interpreted with care, as it contains uncertainties both due to limitations of the InSAR technique as well as shortcomings in estimations from historical data.

Table 4-4 Estimation of sediment yield from sub-catchments upstream Kokel by feasibility study

	Area [km^2]	Sediment contribution [%]	Estimated sediment yield [t]	Estimated specific sediment yield [t/km^2]
Kokel	459	61	1 501 000	3270
Remaining	1421	39	959 656	510
Total	1880	100	2 460 656	1309

The relationship between the different sub-catchments upstream Kokel were also found from the RUSLE estimations. RUSLE estimates that the Kokel sub-catchment contributes to approximately 42% of the total sediment yield observed in Kokel. This enabled the total sediment yield to be estimated from all the sub-catchments upstream Kokel with InSAR estimations, as shown in Table 4-5.

Table 4-5 Estimation of sediment yield from sub-catchments upstream Kokel by RUSLE

	Area [km^2]	Sediment contribution [%]	Estimated sediment yield [t]	Estimated specific sediment yield [t/km^2]
Kokel	459	42	1 501 000	3270
Remaining	1421	58	2 072809	1103
Total	1880	100	3 573 809	1901

5 Discussion

5.1 ADCP Estimation

There is little doubt that the continuous logging of sediment concentrations offered by an acoustic device is a great benefit for the understanding of the nature of sediments. Concentrations will vary by orders of magnitude within short time spans, and the possibility to instantaneously monitor this phenomenon can vastly improve sediment yield estimations. This chapter is given as a further discussion of the method and results derived from ADCP.

5.1.1 Discontinuities

The data used in this thesis was derived for major parts of 2016 at an attempt to quantify a time-series of sediment concentrations. The method produces continuous concentration values for every interval of approximately 60 minutes. At high flood peaks, however, concentration data will not be produced at this continuous rate, leaving probable high sediment transport rates undocumented. In the total sediment yield estimation, this can lead to uncertainties. Reasons surrounding the missing data are yet unknown, where the current working theory is a technical issue in the ADCP equipment occurring in rapidly rising water levels. A further use of ADCP to quantify sediment concentrations should address this shortcoming to sufficiently describe transports at high floods. The linear interpolation performed in the estimation carried out in this thesis leads to probable underestimations as shown in i.e. Figure 5.1.

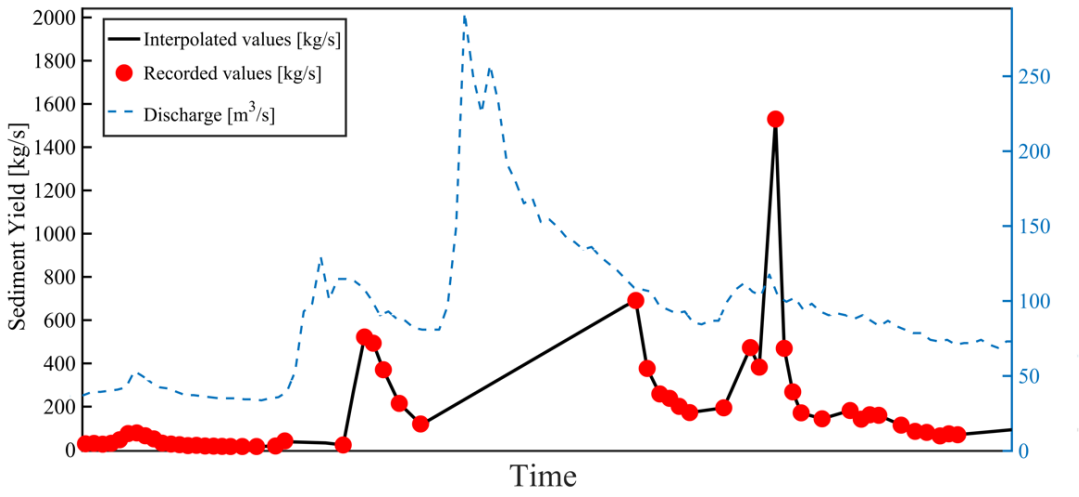

Figure 5.1 Linear interpolation of flood event in February 2016

The discontinuity shown for the February event is not necessarily representative for all floods in the data series, and the interpolation routine was not applied in such magnitude for most other events. The March event (discussed in Figure 4.7) contained more data regarding SSC. The largest time period of missing SSC values was for the summer months where the water level was too low to sufficiently submerge the ADCP. This time period was also assigned values based in the interpolation routine, where the concentration data produced for this period was low compared to the rest of the year. Historical data suggests that the daily average concentration values for the summer months also are significant and although the discharge recorded in the period is low, the sediment transport is probably higher than estimated.

Altogether, the lack of values for SSC in peak events and during the summer most likely causes an underestimation in regards of sediment yield estimations for 2016, but the magnitude of this underestimation is unknown.

5.1.1 Calibration Routine

The calibration of the curve derived to assess the relationship between echo intensity and concentration values was done prior to this thesis, as a part of the development of the script used to convert ADCP data to concentration values. The calibration procedure was based on both theoretical values derived from homogeneous PSDs by equations presented in 2.2, as well as samples collected in the Devoll river. The process was done by transferring the curve derived from theoretical values to sufficiently describe the ratio (ζ_s/k_s^2) and attenuation (ζ_s) calculated from samples. This enabled the quantification of values from the ADCP. The relationship between values retrieved by the ADCP and the actual concentration in the water column should be further investigated to verify the calibration. Examples of such verification can be comparing manually obtained samples of SSC with data produced by the calibrated script.

There is little doubt that the qualitative assessment of the ADCP data is an excellent tool for understanding the variation of suspended sediment concentrations in the Devoll river. The results produced from suspended sediment yield calculations on grounds of ADCP data in this thesis, nonetheless, indicate a lower estimation than previously attempted quantifications of the annual sediment yield based on historical data. The historical data contains several shortcomings, and does not necessarily reflect reality. However, it is most likely the most representative data-set to compare ADCP values with. As discussed in the previous sub-chapter,

it is assumed that the underestimation is partly because of missing data, but the calculation can also give low results due to the calibration process. An indication can be made that the fitting curve between ratio (ζ_s/k_s^2) and attenuation (ζ_s) should be further shifted compared to the curve derived from theoretical estimations, resulting in generally higher concentration values. Since the calibration routine was done prior to this thesis, the concentration plot was treated as a finished product. However, the script gives the ability to produce two concentration graphs (one from simply theoretical values, and one fitted to values obtained by samples as well as theoretical), and as a comparison, the suspended sediment yield for 2016 was calculated for both instances as shown in Table 5-3.

Table 5-1 Sediment yield for different calibration routines.

Calibration routine	Sediment yield [t]	Specific sediment yield [t/km^2]
Theoretical	504 472	268
Theoretical + samples	852 516	453

As shown in the table above, the calibration can greatly affect the predicted sediment yield, and should be further verified.

5.1.2 Relationship for Q and SSC

The absent concentration values relative to high discharges probably also causes some inaccuracy for the SSC rating curve. Additional SSC values at higher discharge rates would probably cause a better fit for the regression line, and the determination could be done if the relationship would be better described by i.e. non-linear regression. However, as previously discussed, the largest variations in the relationship between discharge and SSC can be found around the mean discharge of 2016. This indicates that the concentration also varies greatly at lower discharges, leading to the low correlation.

The general trend in the data from 2016 shows that the high sediment concentrations can be found in the aftermath of hydrological peak events, suggesting lagged waves of high concentrations being transported through Kokel. As discussed by Heidel (1956), the

relationship between the peak discharge and peak sediment concentration seldom appears instantaneously. The relationship can also be different within the reach of the river, depending on transport length and nature of the observed cross section. Therefore, the lagged concentration wave occurring in the Devoll river will not be described by a rating curve with values based on simultaneously occurring sediment concentrations and discharge. As presented in 4.1.2, a suspended sediment yield and discharge curve derived for time intervals would probably more sufficiently describe the nature of sediment transport the Devoll river. The time intervals should be large enough to cover both discharge and SSC peaks. The retrieval of the data required to produce such a rating curve would need to span over a longer time period than a year, or at shorter time intervals than done in this thesis.

A further determination of the particle size of the suspended sediments would be useful information to determine the origin of the sediments for the different concentration waves related to a discharge peak. Previous studies have shown that the instantaneously occurring concentration peak compared to flood events often consists of a larger portion of sandy particles, suggesting that their source is from the river bed or banks. The lagged wave is assumed to have larger portions of smaller particles (clay-silt), indicating that they are a product of external erosion in the catchment This is assumed to also be the case also for the Devoll river, as the catchment upstream of Kokel is highly erosive and will produce large rates of sediments at a rainfall event by both sheet erosion and mass wasting. The information regarding sediment size can be important in i.e. running of mechanical components in the hydraulic structure linked to the river. As this thesis only is based on data only from one ADCP, the differentiation of sediment grain size could not be determined. When the second ADCP (1200 kHz) is further implemented in coming studies, the PSD of the lagged wave of sediment transport can be estimated.

5.2 InSAR Estimations

Remote sensing of the surface of the Earth through InSAR methods is a widely accepted method to assess deformation. The method is used for observations of unstable slopes, and quantification of movement of man-made structures such as dams and other large buildings. In this thesis, however, the deformation values were assumed to describe the erosion in the highly active catchment of the Devoll river. This chapter will further discuss the method and the achieved results.

5.2.1 Erosion

Determining gross erosion over a large area is a difficult task, and is often done by empirical models that carry large uncertainties. The possibility of monitoring entire catchments with the accuracy that state of the art remote sensing techniques provide, is a great tool to understand the attributes of the catchment. Previous studies have performed erosion estimates with i.e. laser technology and photogrammetry, implying that the same also should be possible for other remote sensing methods such as InSAR . For the estimations of erosion performed this thesis, the assumption was made that the deformation recorded by the InSAR was in large parts due to the massive erosion in the catchment upstream Kokel.

The InSAR produced deformation data that with high resolution in most of the catchment, giving insight of the deformation attributes in the basin. Surprisingly, this was also the case for locations close to the river and channel system assumed prone to mass wasting. As mentioned in 2.3, the correlation between two SAR images has to be sufficient when using InSAR processing methods. This probably leads to areas that experience high rates of erosion between two measurements being filtered out. For the case of InSAR delivered for the Devoll basin, the largest deformation between two passes of the SAR satellite can be 25 mm (1/2 the wavelength of the Sentinel I and II satellites) (Cetinic, 2016). The high resolution indicated that the InSAR technique also sufficiently measures deformation in the proximity of the channel system, leading to the expected large rates of erosion happening in these areas being quantified. In a matter of fact, the erosion estimates presented for the Kokel sub-catchment indicate a pattern somewhat similar to the nature of erosion and sediment production. Accumulation and erosion occurs in the entire catchment, but there is a tendency towards higher activity in the areas surrounding the channel system, correlating with the high sediment yield related to the Devoll

river. In the slopes, the same areas are often responsible for the highest rates of erosion in the different intervals, indicating that the satellite is recording correctly.

The resolution of the InSAR derived deformation data is somewhat low compared to methods, such as LiDAR. This is a shortcoming, as a mean value from a 40x40m grid cell will give an uncertainty. By expanding this area of insecurity with a Voronoi-diagram will further increase the uncertainty. In coming use of this method, alternative ways of assigning deformation to a catchment should also be investigated, to determine if a data set with higher resolution will produce different results.

As discussed in 4.2.1, the total erosion for 2016 was negative, implying supply of mass to the catchment. This information somewhat contradicts the presented method and assumption of deformation in the catchment solely describing erosion. A gross accumulation in the catchment seems highly unlikely, and an examination of the data set was performed. The InSAR data set was delivered as cumulative values, where the deformation between every single measurement interval was described. To illustrate the displacement of the catchment in the observed time period, the mean cumulative deformation from all InSAR points (positive values indicating movement away from the satellite) was calculated for every interval as shown in Figure 5.2. The mean deformation is clearly indicating movement away from the satellite in the time span 16.10.2014-14.07.2015, and an advancement towards the satellite can be seen from 06.10.2016.

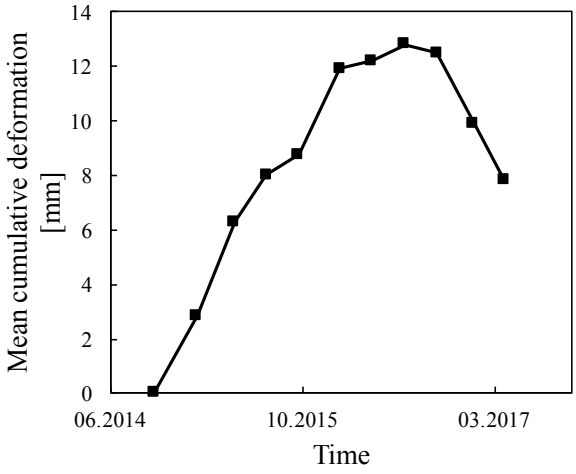

Figure 5.2 Mean cumulative deformation for every time interval of InSAR data

Reasons for why the given deformation values were contradicting the hypothesis of InSAR data describing erosion in 2016 and 2017 has to be further addressed, but some explanations

regarding this can be made by interpreting the data-set and the erosion estimations. The first reason can be errors in the assessed vertical deformation values. A general rise of the Kokel-catchment seems implausible. One possible explanation for such gross accumulation could be the delivery of sediments from upstream catchments. If the Devoll river carries sediments from higher parts of the watershed that accumulates on the banks of the river in the observed sub-catchment, this could potentially lead to an accumulation of mass if the erosion in the observed catchment was sufficiently low. To validate this assumption a visual interpretation of the erosion raster maps developed for this period was performed. The hypothesis of accumulation along the banks was falsified, as the accumulation was generally spread throughout the catchment, as shown in example by Figure 5.3.

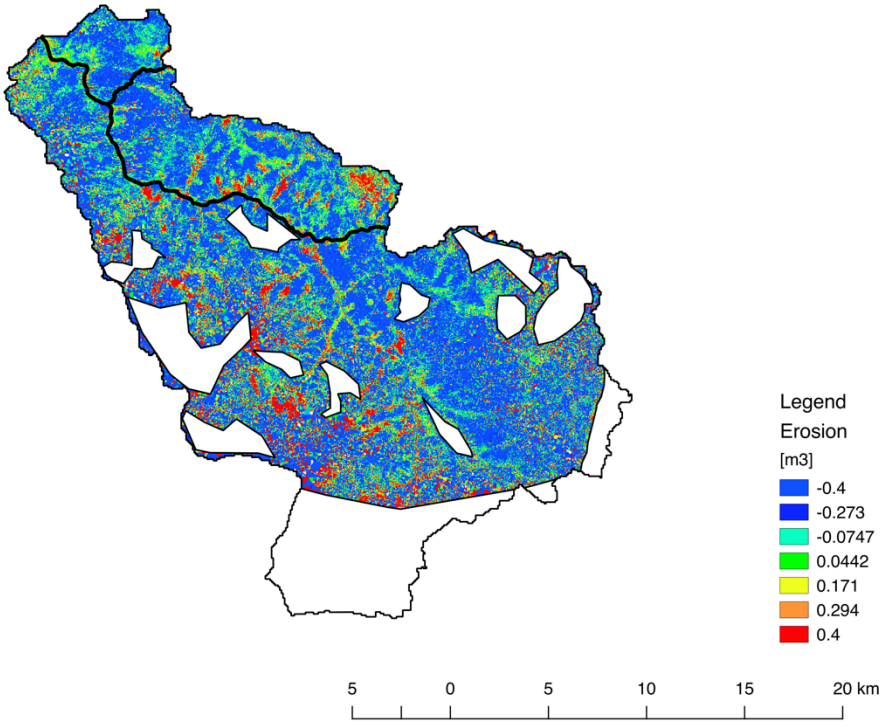

Figure 5.3 Erosion for interval 06.10.16-10.01.17

Another reason for why the data does not sufficiently describe expected erosion, is that there might be other factors affecting the deformation. To point out such factors, a further assessment of the relationship between deformation and erosion values should be performed for the continued use of the presented method. The verification should be done i.e. by field surveying of a relatively large plot, and comparing the obtained erosion volume with the calculated volume from basis on InSAR data. This field survey should also determine the density of eroded

material, as the method presented in this thesis calculates volume change that is later converted to mass by a density of 1.4 t/m^3.

The peculiar values for the time period 06.10.2016-29.03.2017 led to the data being neglected from the erosion estimates performed in this thesis. Despite these shortcomings, the results for 2015 showed promising results for erosion estimates, and the intervals show some correlation with higher expected erosion in intervals with higher total discharge volume based on historical data. Further analysis of the relationship between discharge and InSAR derived erosion rates would be interesting to perform, but was not possible with the discharge data used in this thesis. The erosion estimated for 2015 also correlates to previous studies concerning monthly variation of erosion in Albania. It is estimated that the soil erosion potential for Albania is largest in October, November, February and December while lowest for the summer months June and July (Grazhdani and Shumka, 2007), also indicated by the four intervals containing soil loss obtained for 2015 by InSAR.

5.2.2 Sediment Yield

By combining the sediment delivery distributed (SEDD) model with erosion rates obtained by InSAR, the sediment yield from the Kokel sub-catchment (459km^2) was calculated. The results showed large rates of sediment production occurring in the catchment, as is expected with the extensive erosion derived from deformation values. The catchment is assumed to be the largest contributor of sediment among the basins upstream Kokel, but this is not further validated as the satellite coverage was not sufficient to describe all parts of the total catchment.

The sediment delivery ratio for each grid cell was calculated with the SEDD model. This was done to weight erosion taking place in the proximity of the channel system higher than the erosion taking place in areas less likely to be transported by water. The SEDD model is originally developed in the use with USLE erosion estimates, and is not designed to take into account the negative erosion (accumulation) that occurs in post processing of InSAR data. However, this method of determining sediment yield is most likely more reliable than estimations done with a SDR describing the whole catchment. This is because the InSAR data varies between intervals, and also predicts large rates of erosion and accumulation in the areas far from the channel system that will be accounted for in a larger scale by viewing the catchment as a whole. The SEDD model is also designed to estimate sediment yield for hydrological

events, whereas the SDR equation presented by Vanoni (1975) is developed to calculate annual sediment yield.

Calibration of the basin specific parameter (β) is an important step that can result in significantly different estimations for sediment yield. In this thesis, this was done with an inverse method with a weighted average of the grid based parameters, where the sum of all cells resulted in SDR_w. Increasing or decreasing β will result in different weighting of the areas around a channel system. This calibration will be very important in the assessment of InSAR derived erosion values, as they are heavily varying throughout the catchment. As a comparison, three annual estimations of the sediment yield was done with increasing β as shown in Table 5-2.

Table 5-2 Estimated sediment yield with increasing β (407km^2)

β	Estimated annual sediment yield [t]	Estimated specific sediment yield [t/km^2]
0.005	2 407 692	5 915
0.009	1 501 000	3 688
0.011	1 305 202	3 207

As mentioned in 2.1.4, β can also be calibrated through field surveys, by finding a relationship between erosion and sediment yield. For the catchments upstream Kokel, this would probably result in a more accurate prediction, as the empirical basis for the SDR_w equation used in this thesis most likely does not sufficiently represent the attributes of the observed watershed. One method of obtaining such a relationship would be the combination of previously presented sediment yield estimations with a calibrated ADCP approach and erosion values obtained with InSAR. This relationship would give valuable insight of the catchment attributes, and possibly also explain the lagged concentration waves in the aftermath of heavy precipitation events.

The sediment yield estimation for this thesis does not describe the sediment yield of the whole upstream area of Kokel (1880 km^2) because of lacking InSAR coverage. This makes comparisons with other methods challenging. Further work should be based on an entire catchment that has no contribution of sediments that are not recorded by InSAR deformation values. With the data obtained for this thesis, sub-catchment # 5 (Poshtme) would represent

such a catchment because it does not have sediments coming from upstream areas and is sufficiently covered by InSAR data. There is also InSAR coverage of large parts of the catchment downstream the Kokel catchment. Previous estimations have shown that these areas are equally or even more erosive than the areas assessed in this thesis. Estimation of erosion and sediment yield by means of InSAR would be interesting to obtain for these locations.

Quantification of soil loss and sediment yield with a georeferenced data set, as possible by InSAR techniques and SDR derived by SEDD, is a great tool to design counter measures. Locating problem-areas in the catchment can be challenging and time-consuming through field work. With the presented method, vast surfaces can be monitored both to locate areas with high levels of erosion, but also which of these erosion-areas will contribute most to sediment production.

5.3 Comparison of Results

As an attempt to validate results from the two previously presented methods, Table 5-3 is given as a comparison between prior estimations and results from this thesis. The comparison must be assessed with care, as there are no definite ways of determining sediment yield, and all the estimations contain uncertainties.

Table 5-3 Comparison between estimation methods

	Area [km^2]	Estimated annual sediment yield [t]	Estimated specific sediment yield [t/km^2]	Year
Sediment transport report*	1884	2 704 000	1 434	-
Feasibility study**	1884	1 386 614	734	-
Feasibility study**	455	888 160	1 950	-
RUSLE***	1880	4 166 526	2 217	-
RUSLE***	459	1 750 893	3 812	-
ADCP	1880	963 369	512	2016
InSAR	459	1 501 000	3 270	2015
InSAR****	1880	2 460 656	1309	2015
InSAR****	1880	3 573 809	1901	2015

*(Devoll Hydropower et al., 2012)

**(Devoll Hydropower and Støle, 2010)

***(Omelan, 2015)

****Scaled values, shown in Table 4-4 and Table 4-5

This thesis will not go into detail for the shortcomings of other estimation methods. As seen the results obtained from the different methods are very fluctuating, illustrating the uncertainty related to quantifying sediment yield. The estimations are also performed for different time periods, where this thesis has calculated the sediment yield for two specific years, and the historical data and RUSLE method are based on mean values. The annual sediment yield can vary greatly, and there can be a significant difference between two succeeding years that will not be described by mean values. ADCP and InSAR computations will also give different results, as ADCP describes the suspended sediment yield, whereas the InSAR calculations are assumed to quantify the total sediment yield. A common factor for all estimation methods is the exceedingly large predicted sediment yield, not only in a European scale, but also globally.

Sediment yield estimations have been performed for many other catchments, and as a comparison, the specific sediment yield for the highly erosive Middle Mountain Zone in the Nepalese Himalayas range from 3000 to 8000 t/km^2*year. For the Higher Zones in the Nepalese Himalayas, the expectancy for specific sediment yield can be 1000-4000 t/km^2*year (Devoll Hydropower et al., 2012).

The presented methods in this thesis will provide far better understanding of the sediment situation in Devoll than previous methods, as the produced data contains a much higher amount of information than previous data sets. The historical data consisted of daily concentration measurements with questionable preciseness. With the ADCP the concentration can be given every 60 minutes, giving the possibility to unveil the variability of concentration during single events previously much harder to determine. In the determination of annual sediment yield this is valuable information, as the daily concentration can fluctuate considerable enough not to be adequately described by a single value. The InSAR technique also produces a far higher and more precise data set for deformation and in effect erosion than i.e. the RUSLE model does. The discussed RUSLE estimation for Devoll has been carried out with a relatively low resolution DEM and parameter raster maps that contain large uncertainties. This will not be the case for InSAR data, which will produce high georeferenced resolution hindered only by processing methods. However, the chosen method to determine sediment yield from erosion by SDR is, as other erosion estimates with GIS, held back by DEM resolution.

6 Conclusion

As the Earth is experiencing climate change, the weather patterns are drastically changing, leading to more extreme climate. Storing water will be more important than ever before, while erosion and sediment accumulation will cause even greater challenges. The introduction of improved gauging methods will be essential to uphold sustainability for both coming and existing projects. The determination of both soil loss and sediment yield will contribute to the proper design of countermeasures, leading to both economical and sociologic values being upheld.

In this thesis, an attempt to assess sediment yield from parts of the Devoll river in Albania was carried out. The quantification was done by two methods based on state of the art technologies: continuous concentration gauging by ADCP and ground deformational surveys with InSAR techniques. The results showed promising results, and both methods implied high erosion and sediment contribution from the upstream parts of the Devoll catchment.

Firstly, the application of continuous measuring of concentrations in a river can give great insight of the nature of sediment transportation. As observed for the upstream catchment of the Kokel gauging station, the highest concentrations were often measured in the wake of a discharge peak event, indicating that there is a lag in the highest concentrations compared to discharge. The high concentrations at lower discharges resulted in a rating curve that did not correctly describe the sediment transport in Devoll. A proposition was made to describe sediment transport in intervals, i.e. monthly, by creating a rating curve based on periodical discharge and sediment yield, to correctly describe both events with high flood peaks as well as formidable sediment concentrations. The sediment yield was calculated by combining sediment concentrations with the corresponding discharge, and the annual area specific suspended sediment yield for the upstream catchment of Kokel in 2016 was estimated to 512 tons/km^2. Although significantly high, this is a lower estimation than previous estimations for the catchment.

The ADCP gives great insight to information that previously only was possible to obtain with large amounts of manual field work, at a far lower cost. Stationing one or several ADCPs at a gauging station can also result in the surveying of other important attributes of the observed river. By simultaneously utilizing the originally intended features of the device (measuring of

velocity and pressure, i.e.), a quantification can be done both for sediment concentrations, as well as development of a stage-discharge rating curve for the cross section.

Traditional soil loss estimations often carry large uncertainties. With remote sensing, such as InSAR, the deformation of large areas can be calculated, proving a valuable tool for understanding the topographic displacement in the observed catchment. In this thesis, vertical deformation of parts of the catchment of the Devoll river was investigated to define erosion and sediment yield. The soil loss in the catchment was high, although correlating well with both the expected monthly erosion pattern and previous soil loss estimates performed by the RUSLE method. The sediment yield was also calculated on the basis of grid based SDR values derived from the DEM of the Devoll catchment. Estimates for sediment yield showed a high area specific sediment yield for 2015 of 3270 tons/km^2. The area investigated is previously defined as one of the main contributors to the total sediment yield of the Devoll catchment, and the results are, although high, reasonable for the site-specific characteristics.

The further verification of both ADCP and InSAR methods in erosion and sediment studies will contribute important value to the field of hydrology and geomorphology. The methods discussed in this thesis will reduce the amount of manual field surveying often required to perform estimations for both soil loss in a catchment, as well as sediment transport in a river. To ensure this, the methods have to be further developed and the results should be verified by subsequent field work. Securing continuity in the ADCP data should be a main focus, to correctly calculate sediment yield in flood periods. The calibration of the device should also be documented, as it is an important part of the quantification of the qualitative data produced by echo-intensity conversion. As for the InSAR method, the relationship between deformation and erosion should be further established. If this is done, the method will provide important information for many projects experiencing high rates of erosion. The InSAR technology will produce a dense georeferenced data set containing deformation values for areas with low vegetation, as is the case for most areas prone to large rates of soil loss and sediment yield. The method will also indicate locations in the catchment where the soil erosion and sediment yield are high, making it a great tool to design counter-measures.

References

BROZ, B., PFOST, D. & THOMPSON, A. 2003. Controlling Runoff and Erosion at Urban Construction Sites. Biological Engineering Department and MU Outreach and Extension: University of Missouri-Columbia.

BRUNDTLAND, G. H. 1987. *Report of the World Commission on environment and development:" our common future."*, United Nations.

CETINIC, F. 2016. *RE: E-mail correspondence.* Type to SØRÅS, S.

CETINIC, F. & LAUKNES, T. R. 2016. Sluttrapport for FoU prosjekt –" Verifisering av et satellittbasert system for kartlegging og overvåking av svakheter på jernbane, infrastruktur og naturlig terreng.". Oslo.

CORSINI, A., BORGATTI, L., CERVI, F., DAHNE, A., RONCHETTI, F. & STERZAI, P. 2009. Estimating mass-wasting processes in active earth slides – earth flows with time-series of High-Resolution DEMs from photogrammetry and airborne LiDAR. *Nat. Hazards Earth Syst. Sci.,* 9**,** 433-439.

DE VENTE, J., POESEN, J., ARABKHEDRI, M. & VERSTRAETEN, G. 2007. The sediment delivery problem revisited. *Progress in Physical Geography,* 31**,** 155-178.

DEVOLL HYDROPOWER & NORCONSULT 2011. ESIA Final Report - Executive Summary. *Devoll Hydropower Project, Engineering Services - Development Phase.*

DEVOLL HYDROPOWER, SKARBØRVIK, E. & STØLE, H. 2012. Sediment Transport and Sediment Handling. Devoll Hydropower.

DEVOLL HYDROPOWER & STØLE, H. 2010. Feasibility Study Report - Chapter 4: Geomorphology. Norconsult.

EDWARDS, T. K., GLYSSON, G. D., GUY, H. P. & NORMAN, V. W. 1988. *Field methods for measurement of fluvial sediment*, Department of the Interior, US Geological Survey.

EUROPEAN ENVIRONMENT AGENCY. 2006. *Corine Land Cover 2006 raster data*. European Environment Agency.

FERENC, J.-S. & NÉDA, Z. 2007. On the size distribution of Poisson Voronoi cells. *Physica A: Statistical Mechanics and its Applications,* 385**,** 518-526.

FERNANDEZ, C., WU, J., MCCOOL, D. & STÖCKLE, C. 2003. Estimating water erosion and sediment yield with GIS, RUSLE, and SEDD. *Journal of Soil and Water Conservation,* 58**,** 128-136.

FERRO, V. 1997. Further remarks on a distributed approach to sediment delivery. *Hydrological Sciences Journal,* 42**,** 633-647.

FERRO, V. & MINACAPILLI, M. 1995. Sediment delivery processes at basin scale. *Hydrological Sciences Journal,* 40**,** 703-717.

FERRO, V. & PORTO, P. 2000. Sediment delivery distributed (SEDD) model. *Journal of hydrologic engineering,* 5**,** 411-422.

GOOGLE EARTH. 2017. *Kokel sub-catchment 40°42'16.78"N, 20°26'11.50"Ø, elevation 750M, Picture Date 7/3/2014* [Online]. [Accessed 03.07.16 2017].

GRAZHDANI, S. & SHUMKA, S. 2007. An approach to mapping soil erosion by water with application to Albania. *Desalination,* 213**,** 263-272.

GUERRERO, M., ANTONINI, A., RÜTHER, N. & STOKSETH, S. Suspended load monitoring for sustainable hydropower development. River Sedimentation: Proceedings of the 13th International Symposium on River Sedimentation (Stuttgart, Germany, 19-22 September, 2016), 2016a. CRC Press, 57.

GUERRERO, M., RÜTHER, N., HAUN, S. & BARANYA, S. 2017. A combined use of acoustic and optical devices to investigate suspended sediment in rivers. *Advances in Water Resources,* 102**,** 1-12.

GUERRERO, M., RÜTHER, N., SZUPIANY, R., HAUN, S., BARANYA, S. & LATOSINSKI, F. 2016b. The acoustic properties of suspended sediment in large rivers: consequences on ADCP methods applicability. *Water,* 8**,** 13.

HANES, D. M. 2012. On the possibility of single-frequency acoustic measurement of sand and clay concentrations in uniform suspensions. *Continental Shelf Research,* 46**,** 64-66.

HEIDEL, S. G. 1956. The progressive lag of sediment concentration with flood waves. *Eos, Transactions American Geophysical Union,* 37**,** 56-66.

HOLMGREN, P. 1994. Multiple flow direction algorithms for runoff modelling in grid based elevation models: an empirical evaluation. *Hydrological processes,* 8**,** 327-334.

HAAN, C. T., BARFIELD, B. J. & HAYES, J. C. 1994. *Design hydrology and sedimentology for small catchments*, Elsevier.

INTERNATIONAL HYDROPOWER ASSOCIATION. 2015. *Albania Country Profile* [Online]. http://www.hydropower.org/country-profiles/albania. [Accessed 05.11.16 2016].

JACOBSEN, T. 1997. Sediment Problems in Reservoirs - Control of Sediment Deposits. Trondheim.

JAIN, M. K. & KOTHYARI, U. C. 2000. Estimation of soil erosion and sediment yield using GIS. *Hydrological Sciences Journal,* 45**,** 771-786.

KOSTASCHUK, R., BEST, J., VILLARD, P., PEAKALL, J. & FRANKLIN, M. 2005. Measuring flow velocity and sediment transport with an acoustic Doppler current profiler. *Geomorphology,* 68**,** 25-37.

KOTHYARI, U. C. & JAIN, S. K. 1997. Sediment yield estimation using GIS. *Hydrological sciences journal,* 42**,** 833-843.

LYSNE, D., GLOVER, B., STØLE, H. & TESAKER, E. 2003. Hydraulic Design. *Hydropower Development.* Trondheim: Norwegian University of Science and Technology.

MAHMOOD, K. 1987. Reservoir sedimentation: Impact, Extent and Mitigation. Washington D.C.: World Bank Technical Paper Number 71.

MORRIS, G. L. & JIAHUA, F. 1998. *Reservoir Sedimentation Handbook,* New York, USA, McGraw-Hill Book Co.

OMELAN, M. 2015. *Sediment management for sustainable hydro power development.* Master, Gottfried Wilhelm Leibniz Universität Hannover.

OSGEO. 2017. *About QGIS* [Online]. http://www.qgis.org/en/site/about/index.html: Open Source Geospatial Foundation. [Accessed 25.05.2017 2017].

PACHECO-MARTÍNEZ, J., CABRAL-CANO, E., WDOWINSKI, S., HERNÁNDEZ-MARÍN, M., ORTIZ-LOZANO, J. Á. & ZERMEÑO-DE-LEÓN, M. E. 2015. Application of InSAR and Gravimetry for Land Subsidence Hazard Zoning in Aguascalientes, Mexico. *Remote Sensing,* 7**,** 17035-17050.

PANO, N. & FRASHERI, A. n.d. The coastal geomorphology of the Semani River mouth – Karavsta Lagoon in the Southern Adriatic Sea. *Journal of the Balkan Geophysical Society.* Tirana, Albania.

SHUNDI, A. 2006. Country Pasture/Forage Resource Profiles. Durham, USA: Food and Agriculture Organization of the United Nations.

SMITH, L. C. 2002. Emerging applications of interferometric synthetic aperture radar (InSAR) in geomorphology and hydrology. *Annals of the Association of American Geographers,* 92**,** 385-398.

SØRÅS, S. 2016. The Use of Satellite Data to Quantify Sediment Yield from Vulnerable Catchments. Trondheim: Norwegian University of Science and Technology, NTNU.

THE MATHWORKS. 2017. *MATLAB Overview* [Online]. https://se.mathworks.com/products/matlab.html. [Accessed 25.05.2017 2017].

THORNE, P. D. & HANES, D. M. 2002. A review of acoustic measurement of small-scale sediment processes. *Continental shelf research,* 22**,** 603-632.

THORNE, P. D. & MERAL, R. 2008. Formulations for the scattering properties of suspended sandy sediments for use in the application of acoustics to sediment transport processes. *Continental Shelf Research,* 28**,** 309-317.

TIGREK, S. & ARAS, T. 2012. *Reservoir sediment management*, CRC Press/Balkema.

UN GENERAL ASSEMBLY 2015. Transforming our world, the 2030 Agenda for sustainable development. UN General Assembly.

URICK, R. 1948. The absorption of sound in suspensions of irregular particles. *The Journal of the acoustical society of America,* 20**,** 283-289.

VANONI, V. A. 1975. *Sedimentation Engineering: Classic Edition*, American Society of Civil Engineers.

WALLING, D. E. 1983. The sediment delivery problem. *Journal of Hydrology,* 65**,** 209-237.

WALLING, D. E. & WEBB, B. W. 1996. Erosion and Sediment Yield: A Global Overview. Department of Geography, University of Exeter, Exeter EX4 4RJ, UK.

WHITE, W. R. 2010. World Water: Resources, Usage and the Role of Man-Made Reservoirs. Foundation for Water Research.

WISCHMEIER, W. H. & SMITH, D. D. 1958. Rainfall energy and its relationship to soil loss. *Eos, Transactions American Geophysical Union,* 39**,** 285-291.

Appendix

DEM

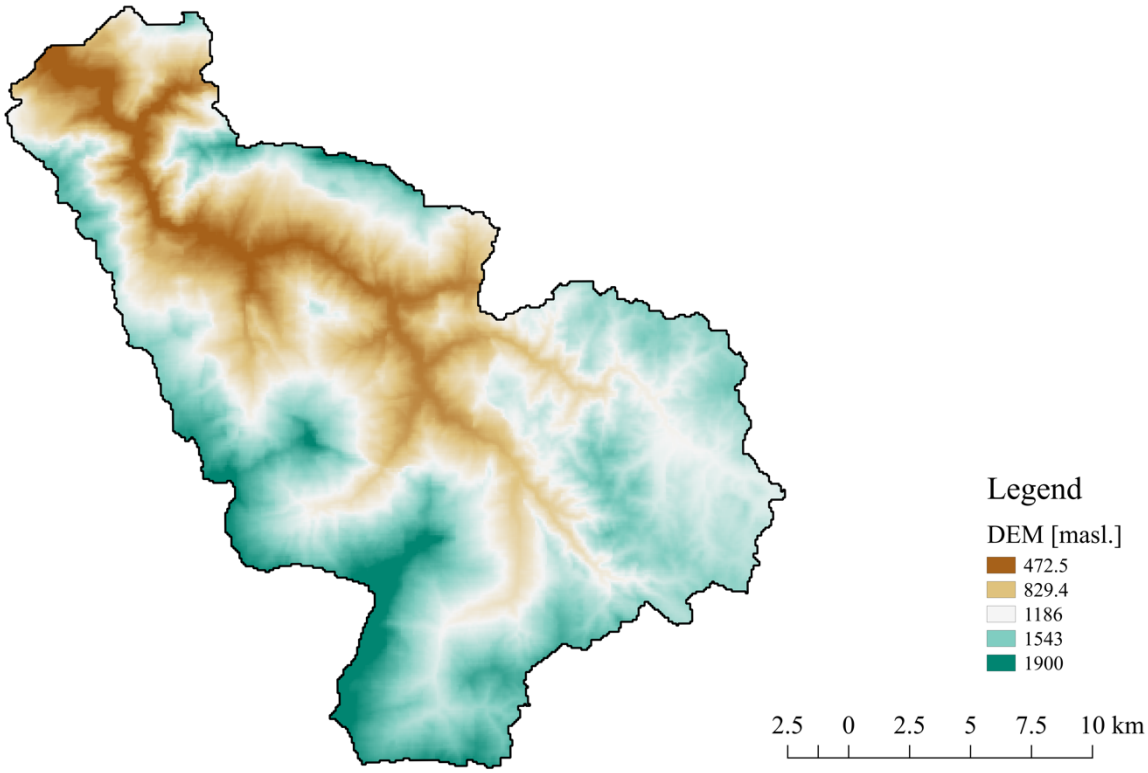

Land Use CORINE

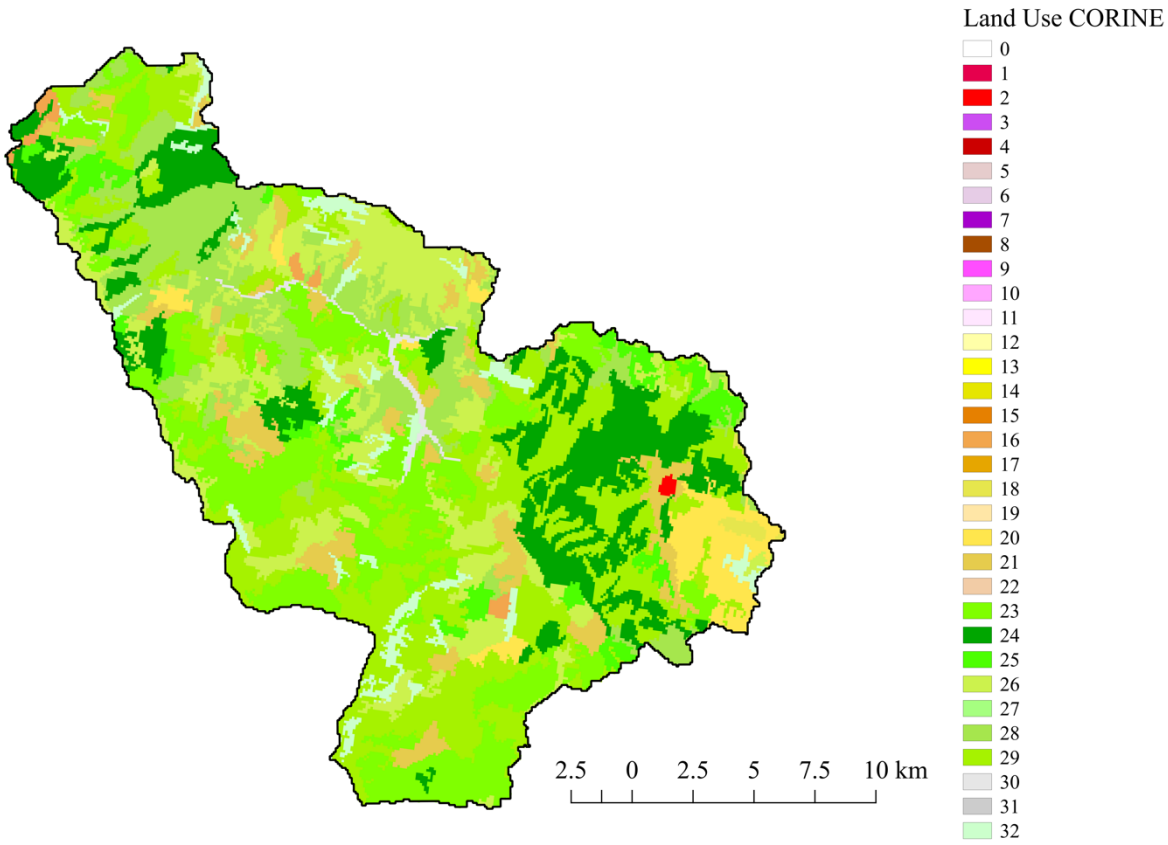

Land Use Conversion

	CLC label	a [fps]	a [m/s]
2	Discontinuous urban fabric	20,3	6,19
16	Fruit trees and berry plantations	8,6	2,62
18	Pastures	7	2,14
20	Complex cultivation patterns	8,6	2,62
21	Land principally occupied by agriculture with significant areas of natural vegetation	8,6	2,62
23	Broad-leaved forest	5,1	1,56
24	Coniferous forest	5,1	1,56
25	Mixed forest	5,1	1,56
26	Natural grasslands	7	2,14
28	Sclerophyllous vegetation	5,1	1,56
29	Transitional woodland-shrub	5,1	1,56
30	Beaches - dunes - sands	10,1	3,08
32	Sparsely vegetated areas	10,1	3,08

Land Use *a*

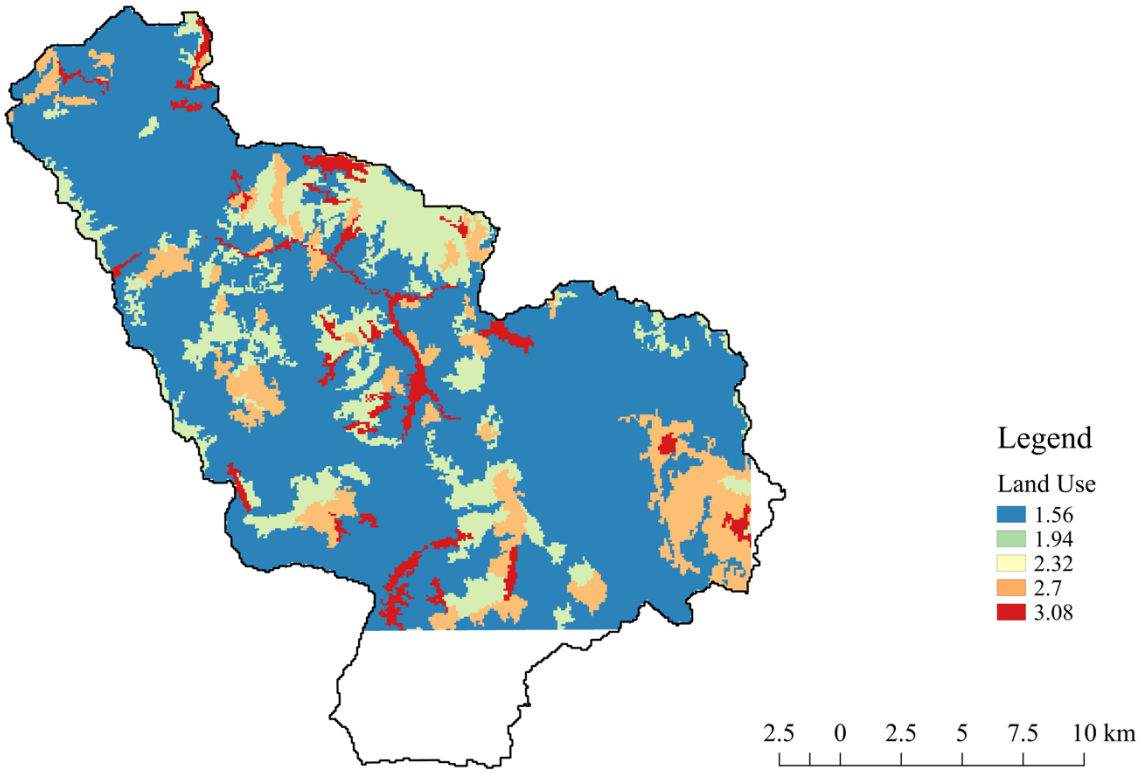

Slope

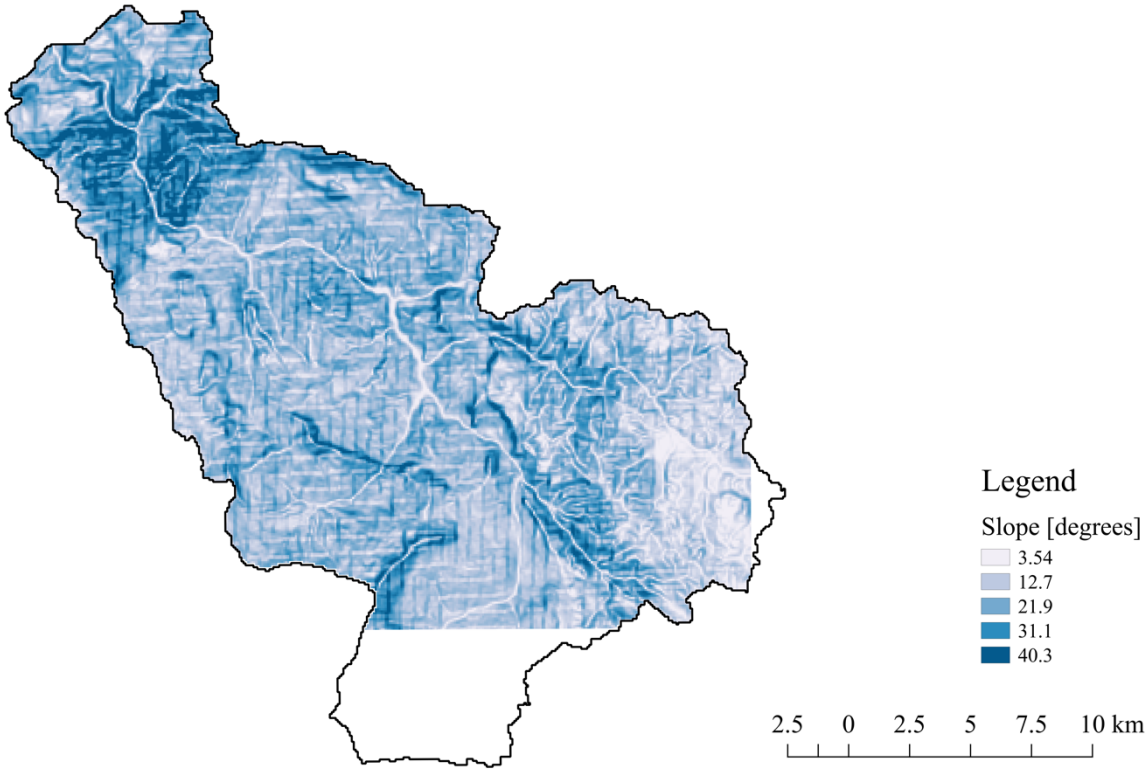

Overland Flow Distance and Channel System

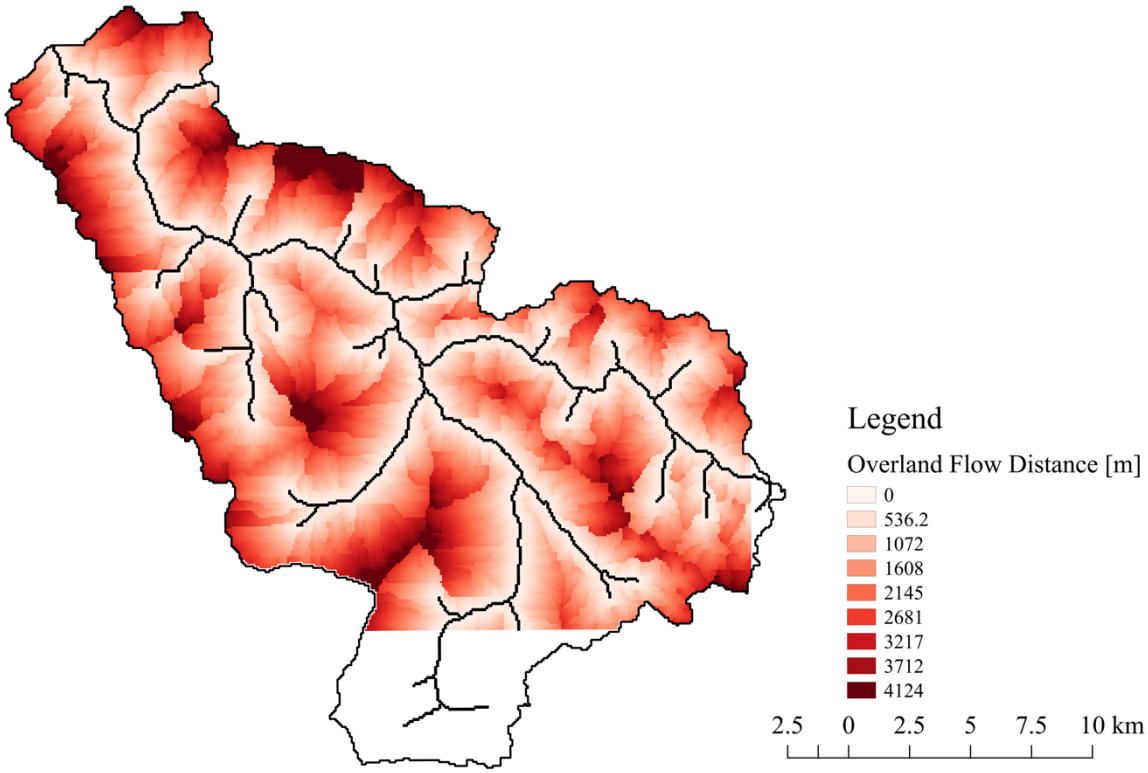

Sediment Delivery Ratio (β = 0.009)

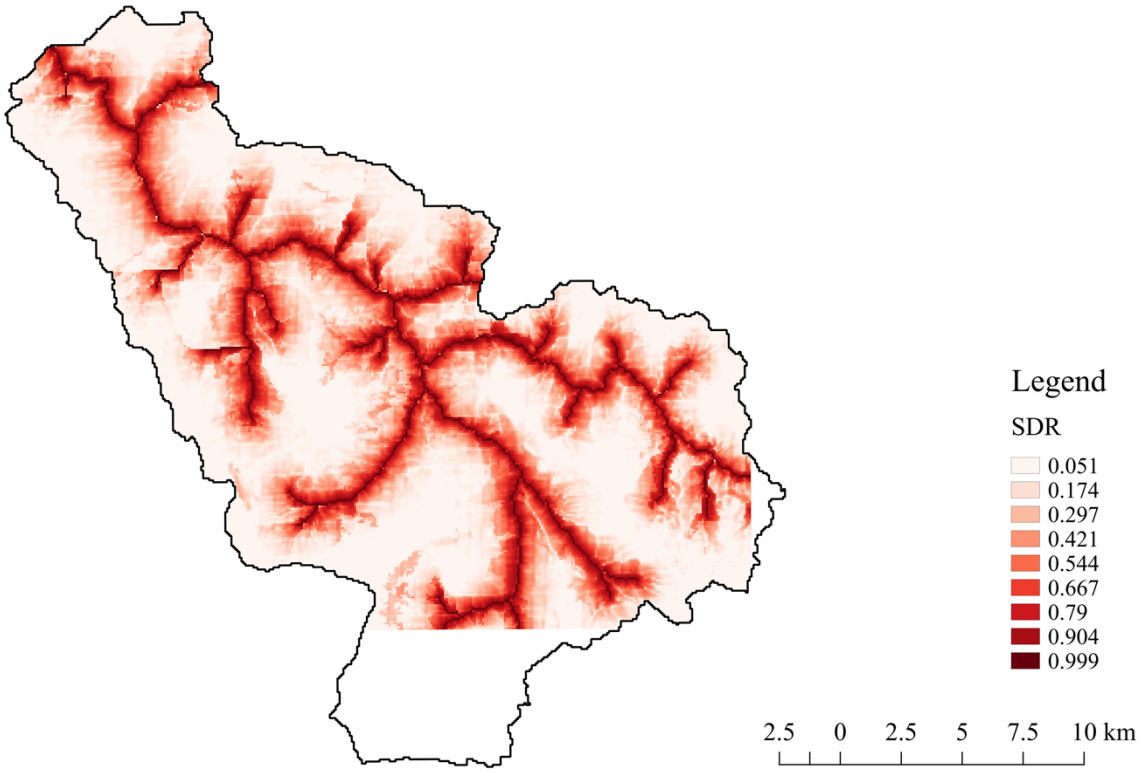

Erosion 21.01.2015 – 21.01.2015

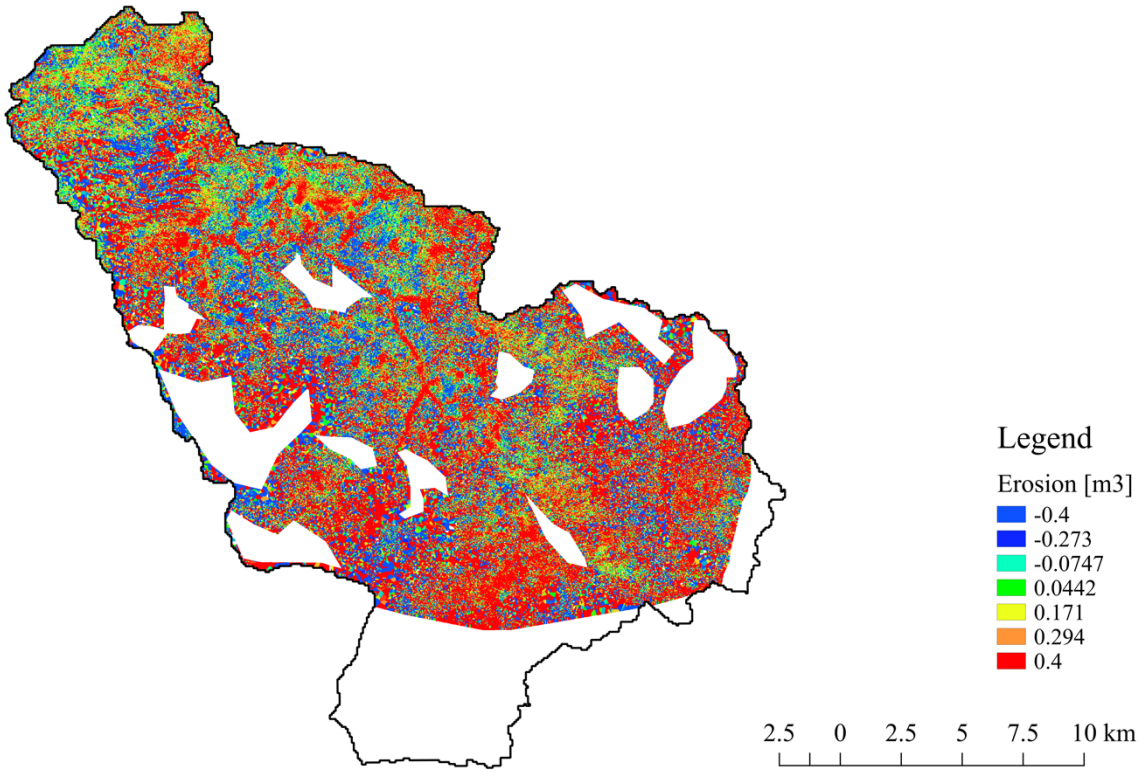

Erosion 21.01.2015 – 27.04.2015

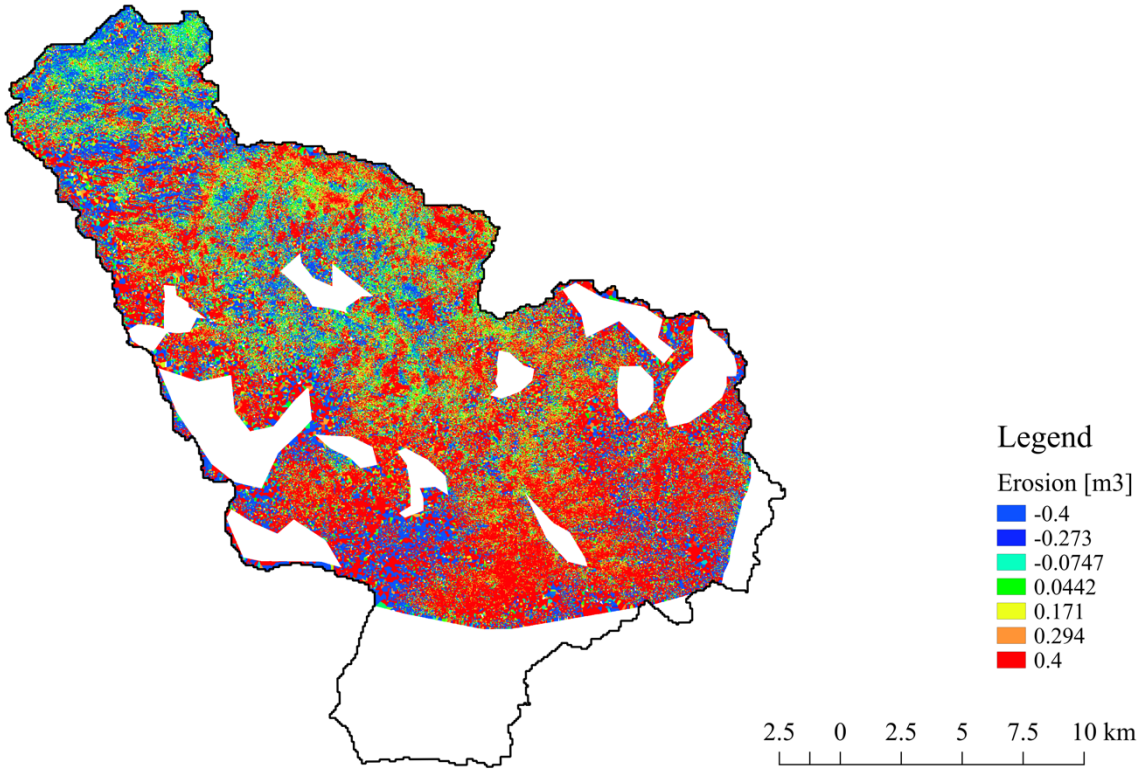

Erosion 27.04.2015 – 20.07.2015

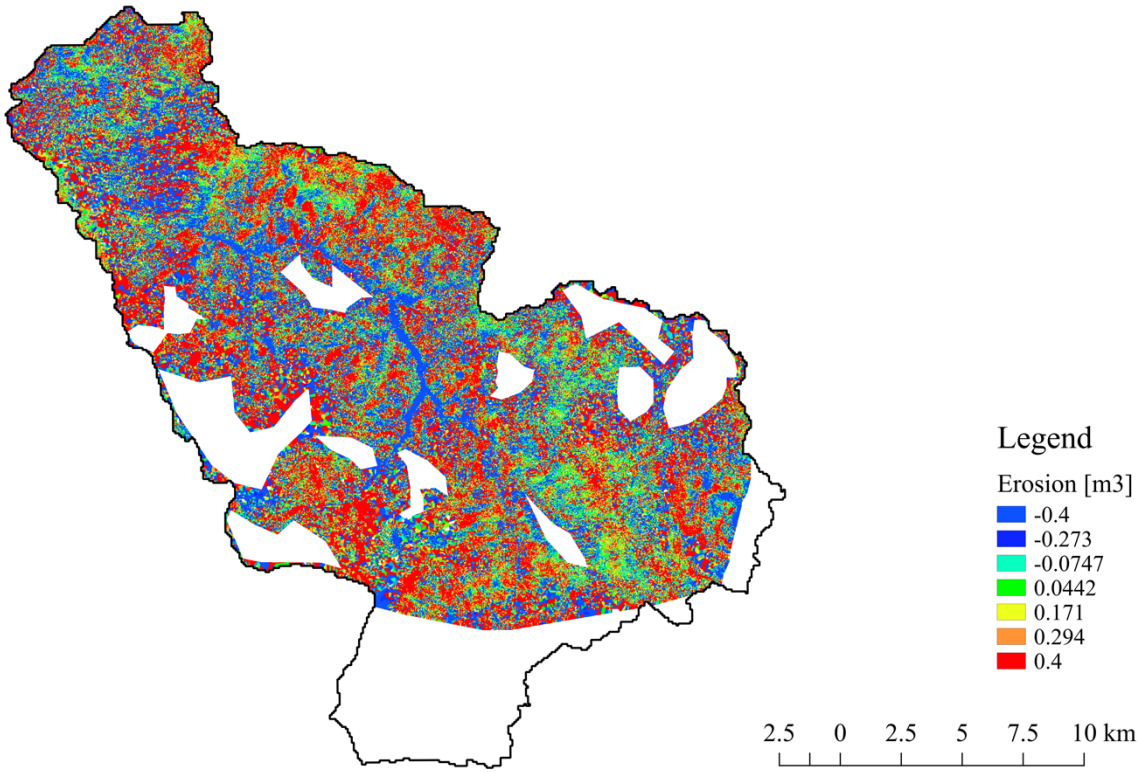

Erosion 20.07.2015 – 12.10.2015

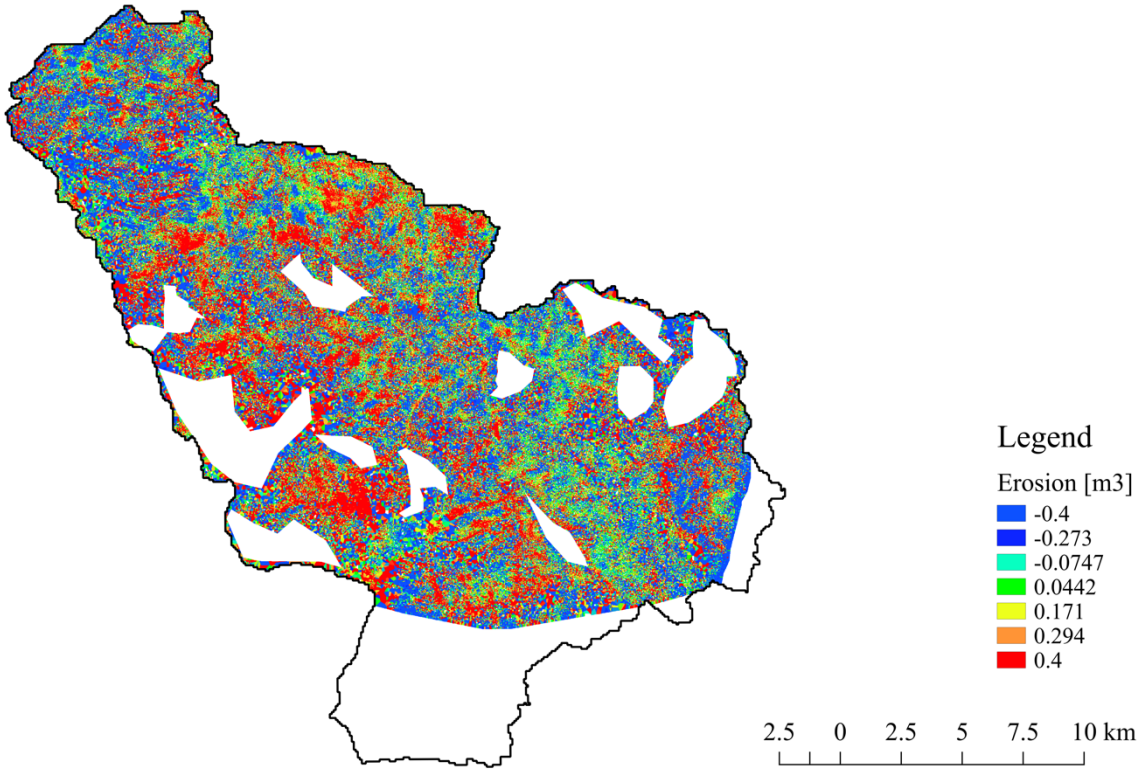

Erosion 12.10.2015 – 28.01.2016

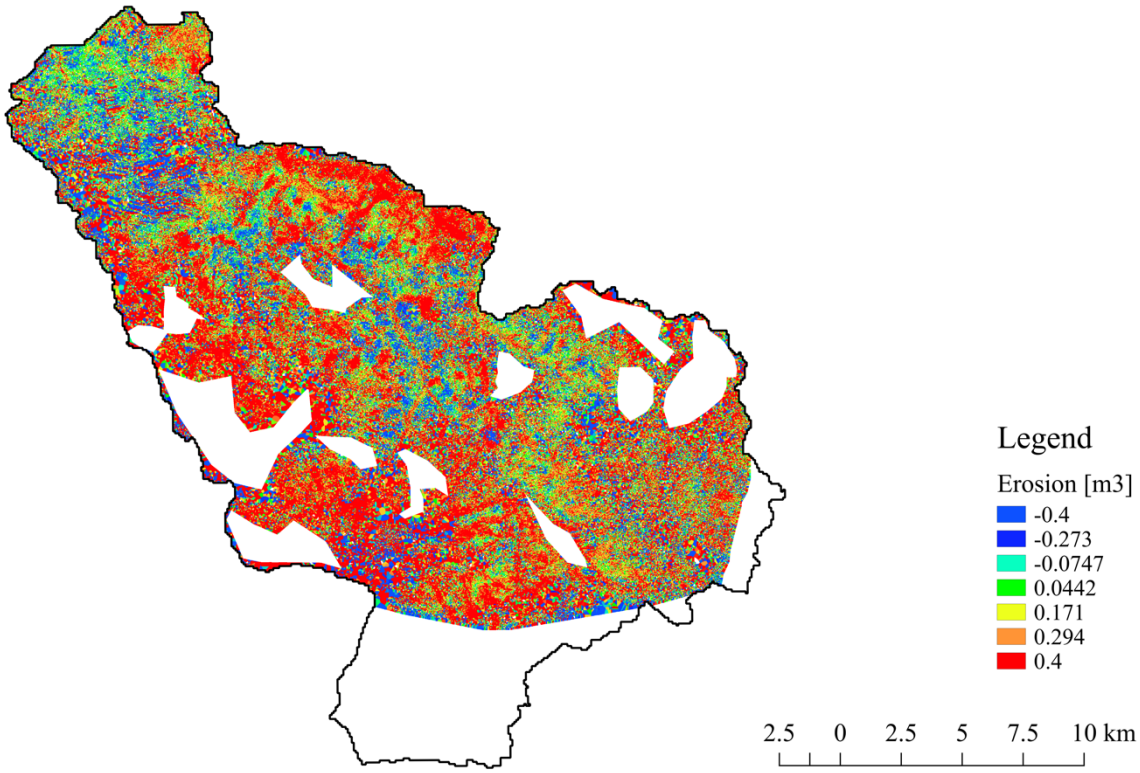

Erosion 28.01.2016 – 21.04.2016

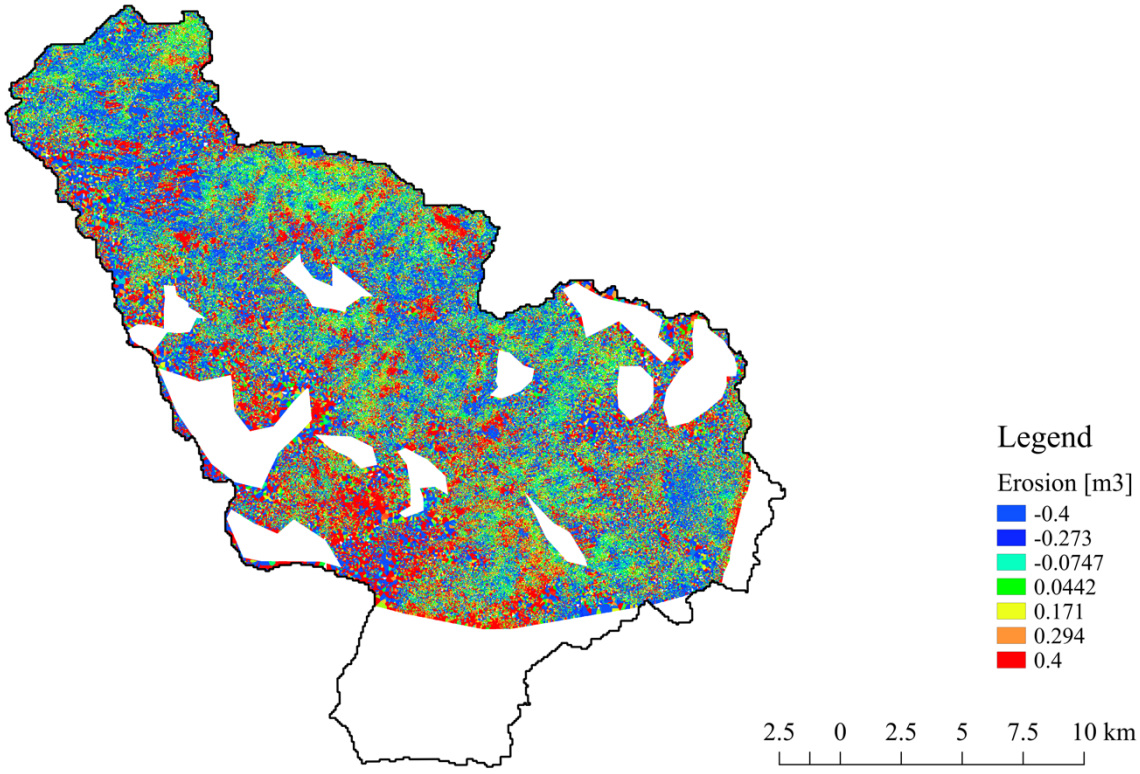

Erosion 21.04.2016 – 14.07.2016

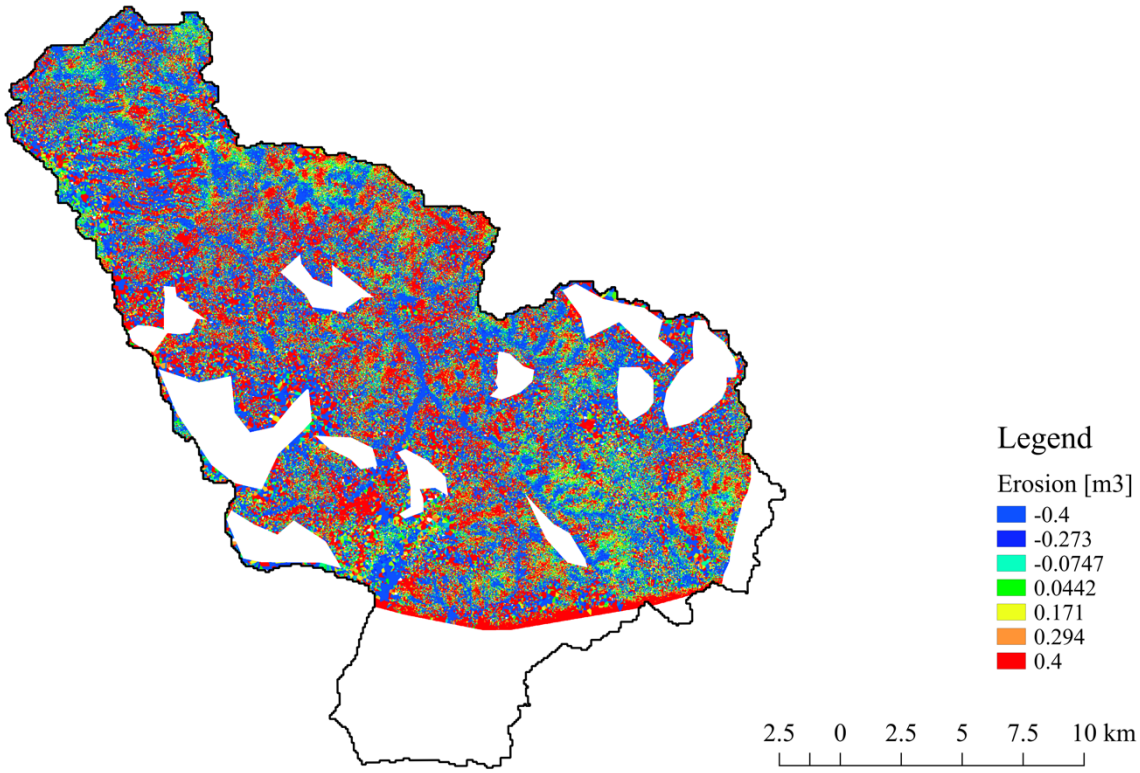

Erosion 14.07.2016 – 06.10.2016

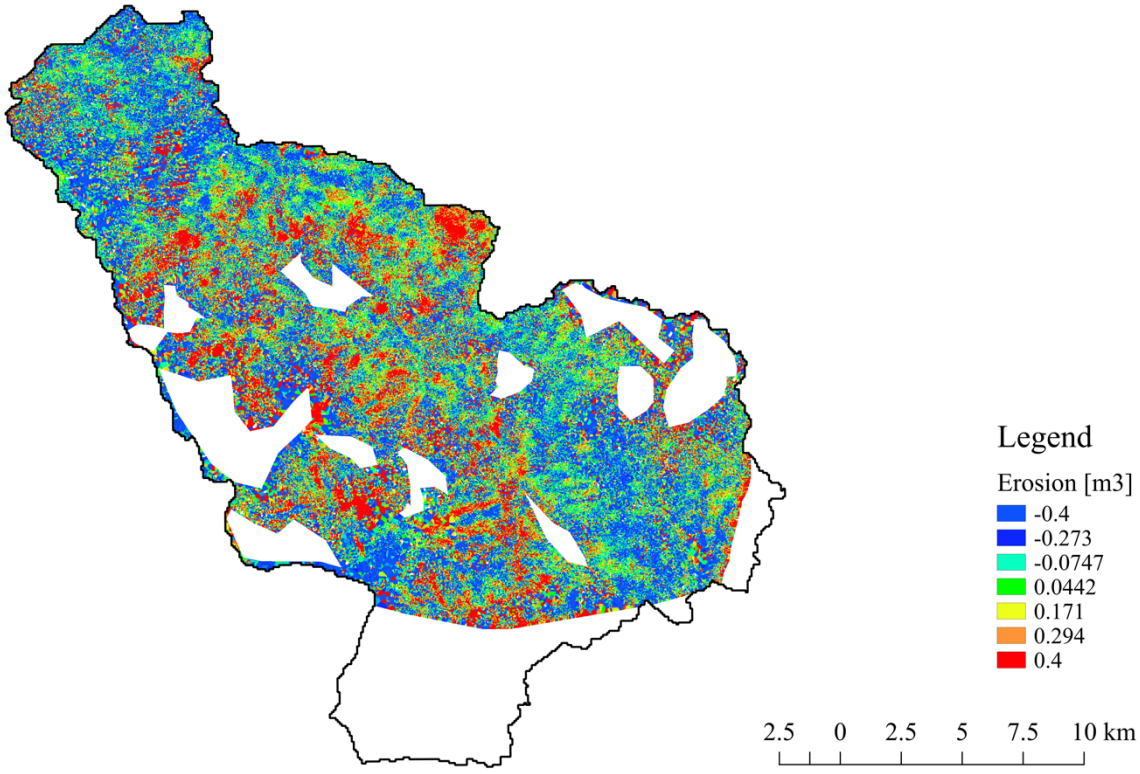

Erosion 06.10.2016 – 10.01.2017

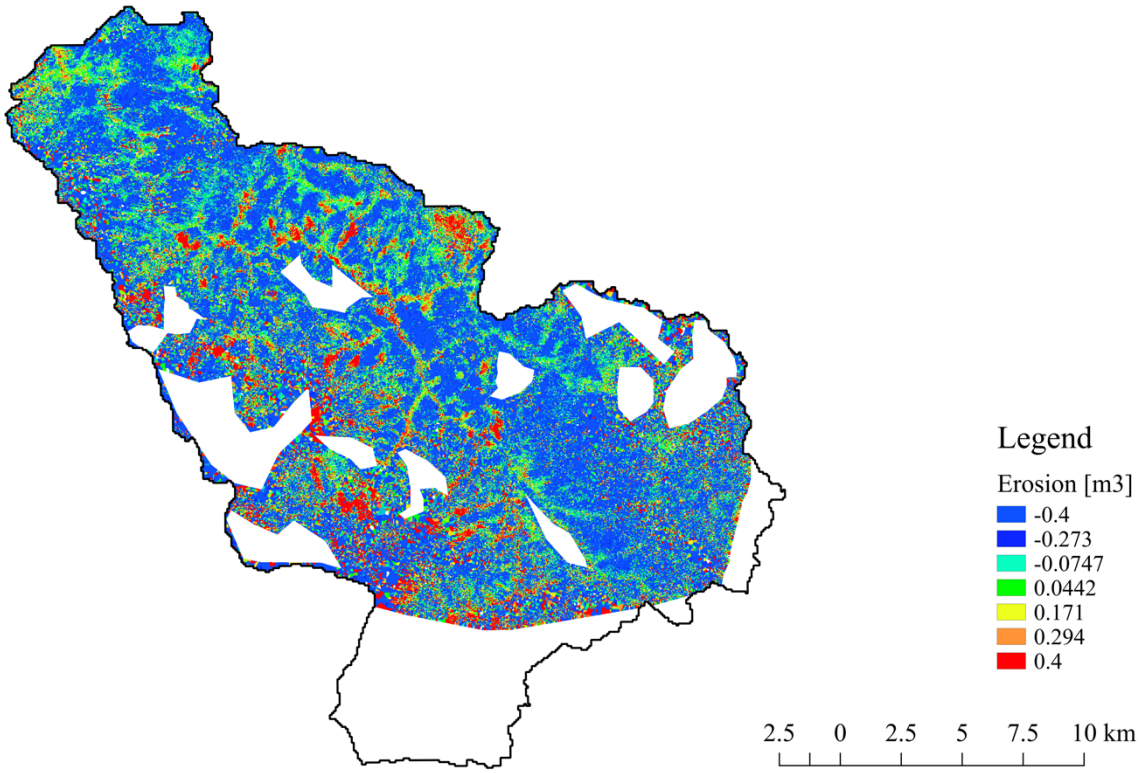

Erosion 10.01.2017 – 29.03.2017

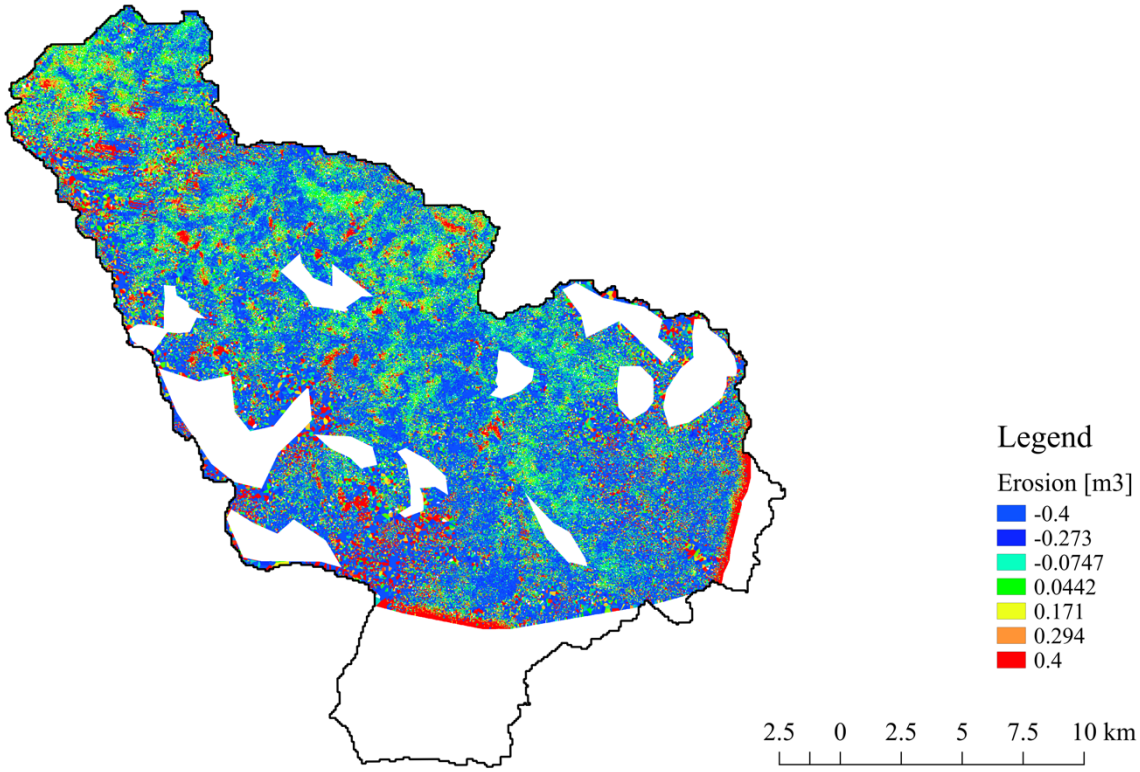

Sediment Yield 21.01.2015 – 27.04.2015

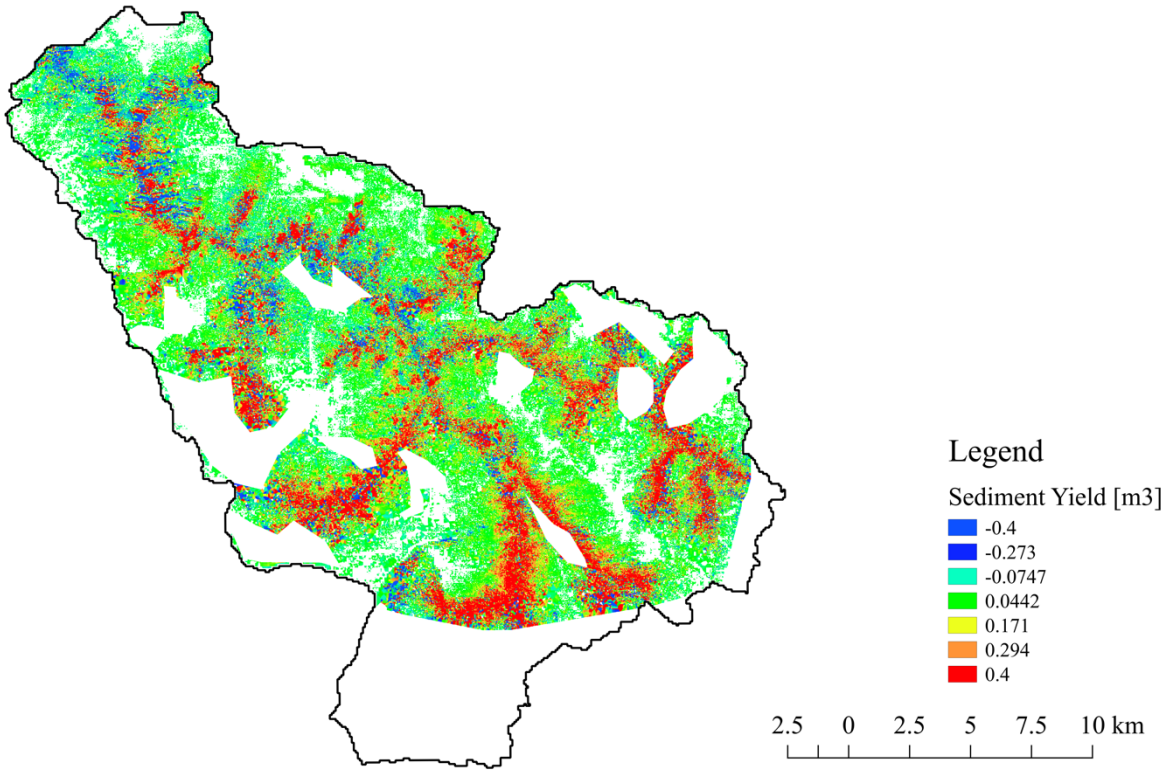

Sediment Yield 27.04.2015 – 20.07.2015

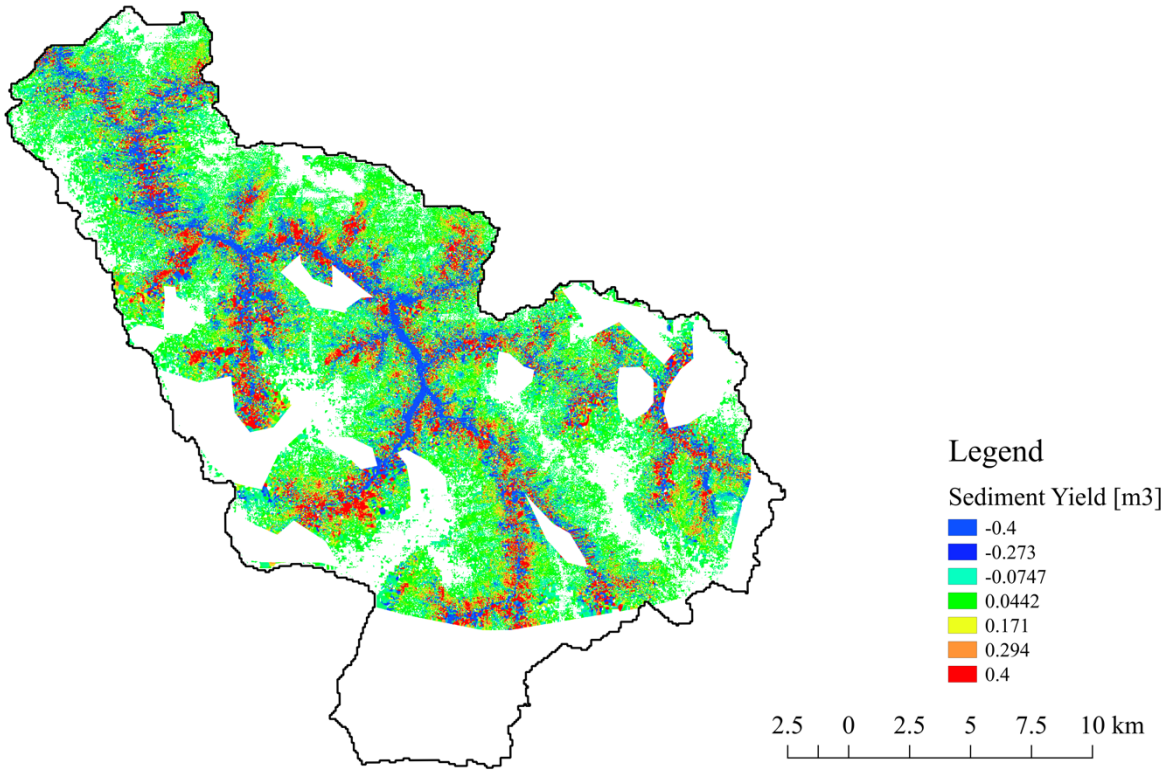

Sediment Yield 20.07.2015 – 12.10.2015

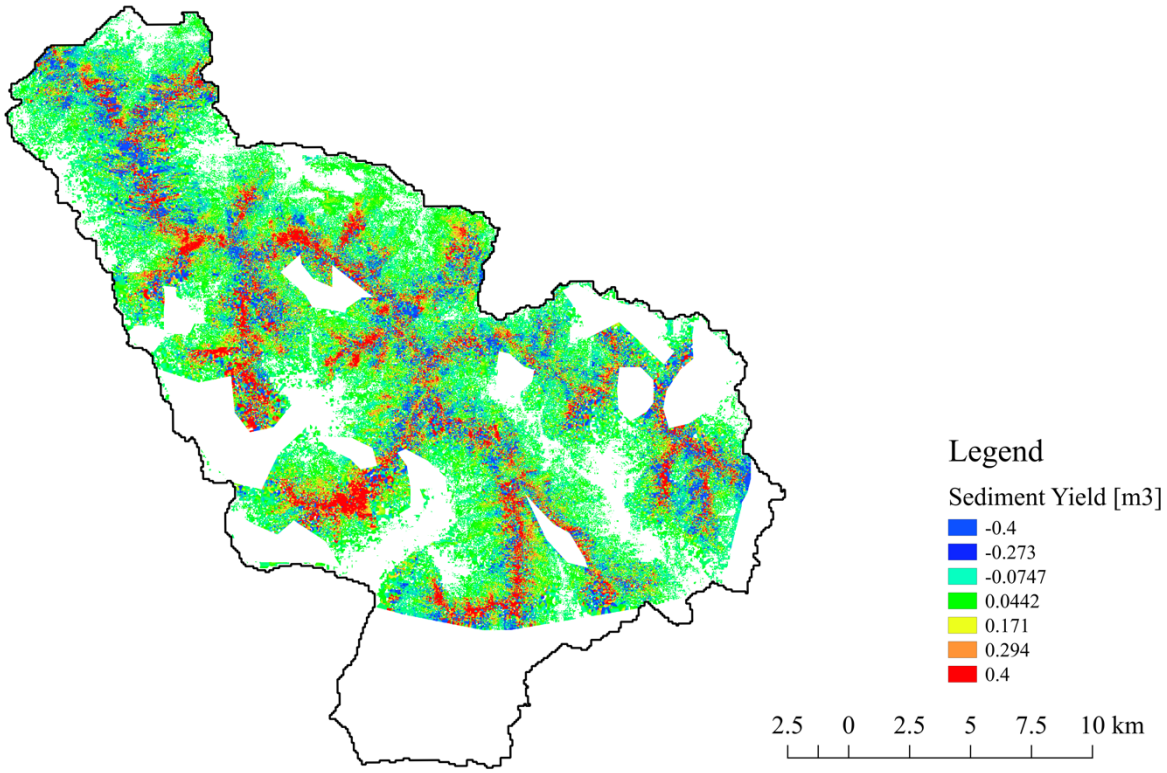

Sediment Yield 12.10.2015 – 28.01.2016

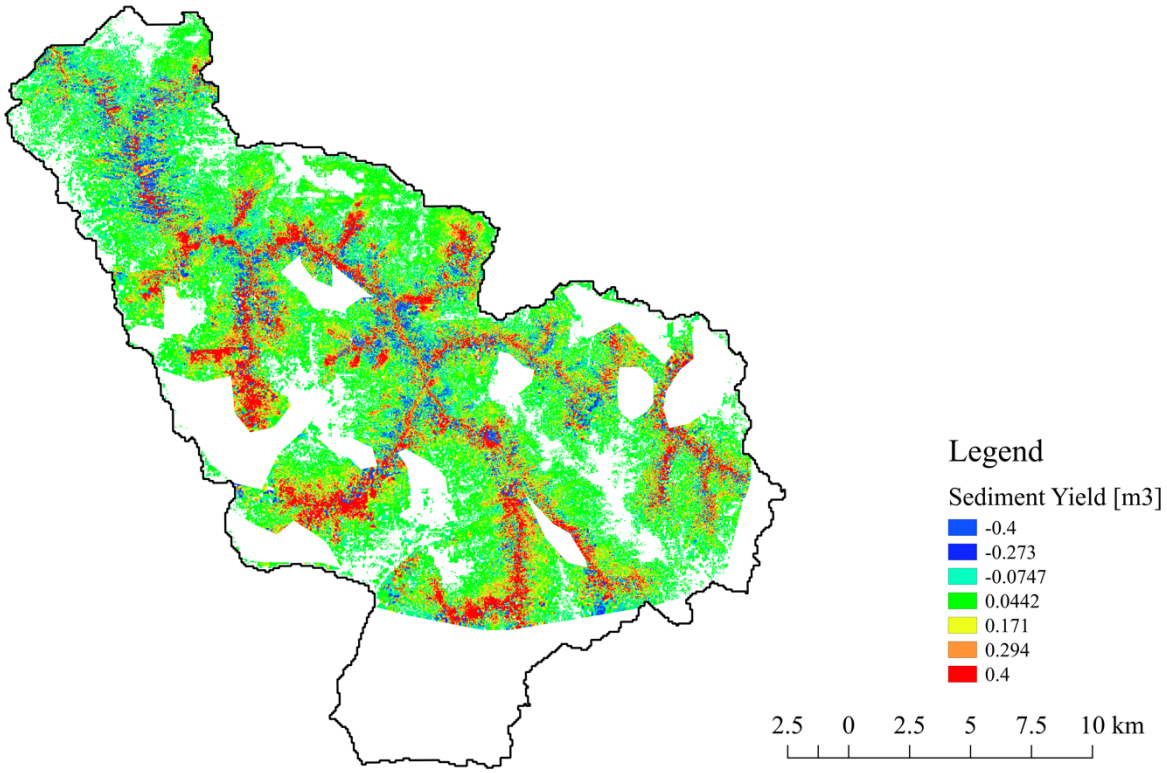

Erosion and Sediment Summary

From	To	Erosion [m^3]	Erosion [t]	Sediment Yield [m^3]	Sediment Yield [t]
16.10.2014	21.01.2015	1 045 056	1 463 078	-	-
21.01.2015	27.04.2015	1 227 820	1 718 948	441 039	617 455
27.04.2015	20.07.2015	649 911	909 876	129 664	181 530
20.07.2015	12.10.2015	287 328	402 259	162 808	227 931
12.10.2015	28.01.2016	1 096 817	1 535 544	338 531	473 943
28.01.2016	21.04.2016	91 889	128 644	-	-
21.04.2016	14.07.2016	247 065	345 891	-	-
14.07.2016	06.10.2016	-87 240	-122 136	-	-
06.10.2016	10.01.2017	-905 250	-1 267 350	-	-
10.01.2017	29.03.2017	-686 021	-960 430	-	-

Monthly Sediment Yield and Discharge (Rating Curve)

	Discharge [m3]	Discharge [mill m3]	Sediment Yield [t]	Sediment Yield [1000t]
jan.16				
feb.16	106 780 000,00	106,78	169 777,00	169,78
mar.16	99 790 000,00	99,79	122 142,00	122,14
apr.16	76 364 000,00	76,36	50 311,60	50,31
mai.16	103 500 000,00	103,50	213 594,00	213,59
jun.16	46 468 000,00	46,47	24 776,40	24,78
jul.16	24 294 000,00	24,29	8 007,00	8,01
aug.16	23 863 000,00	23,86	-	-
sep.16	50 916 000,00	50,92	16 199,00	16,20
okt.16	43 466 000,00	43,47	12 726,70	12,73
nov.16	108 120 000,00	108,12	179 072,00	179,07
des.16	-	-	-	-